

©Copyright 2012

Ingrid Swanson Pultz

The cyclic-di-GMP receptors of *S. Typhimurium*: testing their signaling specificity through
second messenger affinity and their use as biosensors

Ingrid Swanson Pultz

A dissertation

submitted in partial fulfillment of the
requirements for the degree of

Doctor of Philosophy

University of Washington

2012

Reading Committee:

Samuel I. Miller, Chair

Caroline S. Harwood

Joseph D. Mougous

Program Authorized to Offer Degree:

Microbiology

University of Washington

ABSTRACT

The cyclic-di-GMP receptors of *S. Typhmuri*um: testing their signaling specificity through second messenger affinity and their use as biosensors

Ingrid Swanson Pultz

Chair of the Supervisory Committee:

Professor Samuel I. Miller

Department of Microbiology

c-di-GMP is a second messenger that regulates motility and the production of adhesive factors in many bacterial species. Enzymes containing specific c-di-GMP metabolizing domains integrate information about the environment into an intracellular level of c-di-GMP that then binds to specific downstream receptors, including proteins that contain the PilZ domain. Many bacterial species encode dozens of c-di-GMP metabolizing enzymes in their genomes. Although each of these enzymes metabolizes the same small, diffusible second messenger molecule, many of these proteins can be specifically linked to downstream c-di-GMP-regulated processes. The mechanisms involved in achieving this signaling specificity between c-di-GMP metabolizing enzymes and their downstream receptors are not known. Here, we provide evidence that c-di-GMP signaling specificity is achieved through differences in the binding affinities of downstream receptors. *Salmonella* Typhimurium harbors two PilZ domain proteins: YcgR, which controls flagellar-based motility, and BcsA, an enzyme that produces cellulose. Using a Forster resonance energy transfer (FRET)-based method, we measured the binding affinities of

these PilZ domain proteins and found that they span a 43-fold range. Increasing the binding affinity of BcsA for c-di-GMP increased the amount of cellulose that this enzyme produced at lower levels of c-di-GMP. Decreasing the affinity of YcgR for c-di-GMP increased the amount of this second messenger needed for YcgR to inhibit motility. In addition, we found that mutation in *yhjH*, which encodes a predicted c-di-GMP-degrading enzyme, increased the fraction of the cellular population that demonstrated c-di-GMP levels high enough to bind to the higher-affinity YcgR protein, but did not enough to bind to the lower-affinity BcsA protein and stimulate cellulose production. Thus, the specific affinities of these proteins for c-di-GMP are important for their biological functions. Additionally, the binding affinities of the eight PilZ domain proteins in *Pseudomonas aeruginosa* were measured and found to span a 145-fold range, implying that regulation by binding affinity of downstream receptors for c-di-GMP may be a common theme in c-di-GMP signaling. Finally, we generated a panel of FRET-based c-di-GMP biosensors which will allow for the accurate measurement of the free c-di-GMP level in individual cells from the nanomolar to the micromolar range.

TABLE OF CONTENTS

	Page
List of Figures.....	iv
List of Tables.....	v
Chapter 1: c-di-GMP Signaling Networks in Bacteria.....	1
The second messenger c-di-GMP regulates many important biological processes.....	1
Synthesis and degradation of c-di-GMP is performed by defined enzymatic domains.....	5
c-di-GMP binds to diverse downstream receptor molecules in order to exert its effects..	11
Methods used to analyze intracellular c-di-GMP concentrations.....	18
The c-di-GMP signaling network in <i>Salmonella</i> Typhimurium: a model system.....	23
Conclusions.....	32
Figures.....	34
Chapter 2. Materials and Methods.....	39
Bacterial strains.....	39
Plasmids.....	40
Growth conditions.....	43
Protein purification.....	43
Protein identification using mass spectrometry.....	44
Fluorescence spectra and kinetic measurements.....	45
Analysis of BcsA protein expression.....	46
Analysis of cellulose production.....	47
Soft-agar motility plate assays.....	49
Measurement of <i>in vivo</i> FRET/CFP ratios in individual cells.....	50
Mouse virulence assays.....	53
Tables.....	54

Chapter 3. The Binding Affinities of PilZ Domain Proteins Span a Large Range of c-di-GMP Concentrations	56
Summary.....	56
Introduction.....	57
A FRET-based method to measure PilZ domain protein binding affinities for c-di-GMP.....	59
The binding affinities of <i>S. Typhimurium</i> PilZ domain proteins differ by 43-fold.....	59
The binding affinities of <i>P. aeruginosa</i> PilZ domain proteins differ by 145-fold.....	61
Discussion.....	63
Tables and Figures.....	67
Chapter 4. The Binding Affinities of <i>Salmonella</i> Typhimurium PilZ Domain Proteins Affect their Biological Functions.....	74
Summary.....	74
Introduction.....	74
Cellulose synthesis by BcsA is predominantly regulated at a post-translational level by c-di-GMP.....	76
Mutation of the amino acid immediately N-terminal to the RxxxR motif alters the affinities of <i>S. Typhimurium</i> PilZ proteins for c-di-GMP.....	79
A <i>S. Typhimurium</i> strain harboring a BcsA protein with a lower c-di-GMP binding affinity demonstrates an increase in cellulose production at low levels of c-di-GMP.....	80
A <i>S. Typhimurium</i> strain harboring YcgR with a lower c-di-GMP binding affinity requires higher levels of c-di-GMP to demonstrate motility inhibition.....	81
Mutation in <i>yhjH</i> results in an increase in the fraction of <i>S. Typhimurium</i> cells that demonstrate c-di-GMP levels that are high enough to bind YcgR.....	83
A <i>S. Typhimurium</i> strain harboring the lower-affinity <i>ycgR-R113A</i> mutation does not demonstrate YcgR-dependent motility inhibition in a Δ <i>yhjH</i> mutant.....	85
Mutation in <i>yhjH</i> does not result in cellulose production in soft-agar motility plates.....	86
<i>S. Typhimurium</i> PilZ domain proteins are not essential for virulence.....	87

Discussion.....	88
Tables and Figures.....	92
Chapter 5. Biosensors with Altered Affinities for c-di-GMP Expand the Measurable Range of c-di-GMP <i>in vivo</i>	105
Summary.....	105
Introduction.....	105
FRET-based biosensors that demonstrate different binding affinities for c-di-GMP expand the measurable concentration range of c-di-GMP <i>in vitro</i>	108
FRET-based biosensors with different binding affinities for c-di-GMP distinguish between populations of cells with high and low c-di-GMP levels <i>in vivo</i>	109
Discussion.....	111
Tables and Figures.....	113
Chapter 6. Conclusions and Future Directions.....	120
Does c-di-GMP signaling specificity also occur by the generation of local c-di-GMP pools?.....	122
Do the enzymatic activities of c-di-GMP metabolizing enzymes determine their abilities to affect different downstream receptors?.....	124
What is the significance of heterogeneity of c-di-GMP concentrations within a population?.....	125
References.....	127

LIST OF FIGURES

	Page
Figure 1.1: c-di-GMP is responsible for the switch between the motile and sessile lifestyle.....	34
Figure 1.2: The minimal functional module in c-di-GMP signaling.....	35
Figure 1.3: The binding pocket of the PilZ domain protein PP4397 bound to c-di-GMP.....	36
Figure 1.4: A genetically-encoded c-di-GMP biosensor.....	37
Figure 1.5: c-di-GMP controls motility and rdar morphotype formation.....	38
Figure 3.1: The FRET-based biosensor method.....	67
Figure 3.2: YcgR- and BcsA PilZ-based biosensors.....	68
Figure 3.3: The effect of temperature on the binding affinity of the BcsA PilZ domain.....	69
Figure 3.4: The binding affinities of YcgR and the BcsA PilZ domain differ by 43-fold.....	70
Figure 3.5: Binding curves of PA3353 for c-di-GMP suggest two binding sites.....	71
Figure 4.1: <i>S. Typhimurium</i> makes cellulose at 24°C, but not at 37°C.....	92
Figure 4.2: Cellulose is predominantly regulated at a post-translational level.....	93
Figure 4.3: The <i>S. Typhimurium</i> YcgR protein contains an arginine in “Position-X”.....	94
Figure 4.4: Mutation of the “Position-X” residues in <i>S. Typhimurium</i> PilZ domain proteins.....	95
Figure 4.5: A <i>S. Typhimurium</i> strain harboring a chromosomal arabinose-inducible DGC.....	96
Figure 4.6: A <i>S. Typhimurium</i> strain harboring the <i>bcsA-V695R</i> mutation.....	97
Figure 4.7: The YcgR R113A mutation increases the amount of c-di-GMP to inhibit motility...98	98
Figure 4.8: A <i>S. Typhimurium</i> <i>yhjH</i> mutant demonstrates an increase in c-di-GMP levels.....	99
Figure 4.9: The YcgR R113A mutation does not inhibit motility in a Δ <i>yhjH</i> background.....	100
Figure 4.10: A <i>S. Typhimurium</i> Δ <i>yhjH</i> mutant does not show c-di-GMP bound to BcsA.....	101
Figure 4.11: A <i>S. Typhimurium</i> Δ <i>yhjH</i> mutant strain does not produce cellulose.....	102
Figure 4.12: Binding affinities of YcgR and BcsA for c-di-GMP determine phenotypes.....	103
Figure 5.1: c-di-GMP binding curves of FRET-based biosensors used in this study.....	113
Figure 5.2: Fluorescence emission spectra of the YcgR S147A biosensor.....	114
Figure 5.3: The YcgR biosensor separates cells based on c-di-GMP levels.....	115
Figure 5.4: The YcgR R113A biosensor separates cells based on c-di-GMP levels.....	116
Figure 5.5: The BcsA PilZ biosensor separates cells based on c-di-GMP levels.....	117
Figure 5.6: FRET/CFP ratios of purified biosensors immobilized on Ni-NTA silica beads.....	118

LIST OF TABLES

	Page
Table 2.1: Description of the strains used in this study.....	54
Table 2.2: Description of the plasmids used in this study.....	55
Table 3.1: Affinities of c-di-GMP-binding molecules in selected bacteria.....	72
Table 3.2: Affinities and Hill coefficients of YcgR and BcsA at various temperatures.....	73
Table 4.1: Survival of mice inoculated with PilZ deletion mutant strains of <i>S. Typhimurium</i> ...	104
Table 5.1: Measurement range of c-di-GMP concentrations for biosensors used in this study..	119

ACKNOWLEDGEMENTS

This work was overseen by Dr. Samuel I. Miller, M.D., who provided direction and advising during the course of this project. John Leigh, Ph.D.; Caroline Harwood, Ph.D.; Joseph Mougous, Ph.D.; Colin Manoil, Ph.D.; and Carleen Collins, Ph.D. acted as committee members to this Ph.D. thesis work and provided guidance throughout. Dr. Matthias Christen, Ph.D., and Dr. Hemantha Kulasekara, Ph.D were involved in the conception of this project. Dr. Christen and Dr. Kulasekara developed the genetically-encoded FRET-based YcgR biosensor used in this work. Dr. Christen assisted in measuring binding affinities of PilZ domain proteins, and has been invaluable for this work due to his extensive knowledge of biochemistry. Dr. Kulasekara has provided a tremendous amount of assistance and direction in the generation of the different constructs used in this study, equipment use, experimental design, and data analysis. Dr. Richard Pfuetzner, Ph.D, provided much assistance and expertise in purifying the various proteins that were produced during the course of this project. Dr. Erez Mills, Ph.D., has provided considerable knowledge in c-di-GMP signaling in *S. Typhimurium* and has acted as a sounding board for experiments and data interpretation. Bridget Kulasekara developed the analysis used in determining the FRET/CFP ratios in all experiments that involved *in vivo* FRET-based c-di-GMP biosensors. In addition, Mrs. Kulasekara provided hours of guidance and instruction on fluorescence microscopy. Andrew Kennard assisted in generating the *S. Typhimurium* binding affinity mutants used in this study. This work was funded in part by a National Science Foundation Graduate Research Fellowship, by an Achievement Awards for College Scientists Scholarship, and by the National Institute of Allergy and Infectious Diseases.

DEDICATION

My thesis is dedicated to my husband, Scott Pultz, who makes my life special and every day an adventure. Scott's writing in an attempt to emulate this thesis: *Then we cross vectored the Pr13 gene with the polarized version of Sec9(a) resulting in dialecting decreases of vector x/y movement without affecting the anterior cellular wall membrane FGhT. The y/r plane rotated around a secondary axis based on the thermodynamic resistance of the radial quadrant, not factoring in the quaternion vector subB which interpolated bi-linear x/y between 0.3 and 4.6. The histogram chart had DMA readouts of 2.45 joules per microgram which notes that pvR is the likely location for high taCo infinity.*

This work is also dedicated to my parents, who took every opportunity to encourage me to pursue what I loved, molecular biology. They fostered a love of science and engineering within me at a very young age, and have selflessly supported me in all of my endeavors.

This thesis is also dedicated to two fantastic mentors under whose tutelage I have learned a considerable amount regarding molecular biology, ethics of science, and life in general. Dr. Tanya V. Golovkina taught me that expecting the best from other people causes them to fulfill this expectation and become the best. Dr. Samuel I. Miller taught me that you have to love what you do in order to be successful at it. I have been fortunate to have both of you as advisors.

Finally, this work is also dedicated to the UW iGEM team. May you always discover new things about the natural world, engineer new biological systems that no one thought possible, and push the limits of what society thinks that young people are capable of doing.

CHAPTER 1: C-DI-GMP SIGNALING NETWORKS IN BACTERIA

The second messenger c-di-GMP regulates many important biological processes

There is no environment in the natural world that exists without change. In order to survive and thrive, all organisms must be able to sense and respond to changes in their environment and between environments. In the past few decades, genetic and biochemical experiments have elucidated the sophisticated mechanisms by which bacteria sense and respond to their environments. These mechanisms include the use of second messenger signaling systems, in which the sensing of an environmental signal (the “first messenger”) results in the production of a small molecule (the “second messenger”) inside of the cytoplasm, which then regulates cellular behavior. In bacteria, no second messenger is as versatile as cyclic diguanosine monophosphate (c-di-GMP). In response to environmental or intracellular changes, cytoplasmic enzymes generate a c-di-GMP signal that is transduced to effector proteins, thus coordinating a response to the original message. c-di-GMP was first discovered in 1987 as an allosteric regulator of cellulose production in *Gluconacetobacter xylinus* (105). Later, the advent of genome sequencing resulted in the discovery of many c-di-GMP signaling components in the genomes of diverse bacterial species, though these components were not found in archaea or eukarya (36). These discoveries have triggered an explosion in c-di-GMP signaling research in the past decade, identifying functions for many of these components. It is now well established that c-di-GMP is an important global regulator that controls diverse cellular processes.

c-di-GMP is a master regulator of the lifestyle switch between motility and sessility

A major function of c-di-GMP signaling is to regulate the transition between the motile and sessile lifestyle (Figure 1.1). Generally, low levels of c-di-GMP are associated with motile, free-living cells, while high levels are associated with sessile cells that form biofilms and bacterial communities. This has been demonstrated by comparing the phenotypes of different strains of bacteria that overexpress exogenous c-di-GMP-metabolizing enzymes, for many bacterial species (113). The presence of high levels of c-di-GMP results in a wrinkly and rough colony phenotype on agar plates, or the formation of a clumping or of a pellicle in standing liquid culture, both of which involve cells embedded in an extracellular matrix of adhesive factors and exopolysaccharide (37, 62, 121, 151). Conversely, c-di-GMP has also been shown to directly inhibit motility in many bacteria (21, 59, 71, 108). Analysis of the transcriptome of c-di-GMP signaling demonstrates its role as a global regulator of surface-associated components. Transcriptional profiling of c-di-GMP-regulated genes in *Escherichia coli* found that 4% of genes in this organism are regulated by c-di-GMP, and that 35% of these genes encode membrane-associated factors, illustrating c-di-GMP's role in cell surface-associated structures (74). In *Pseudomonas aeruginosa*, c-di-GMP was found to affect the expression of several hundred genes, including those involved in motility (inhibited by c-di-GMP) or exopolysaccharide biosynthesis (induced by c-di-GMP) (47). In some organisms, c-di-GMP signaling is linked to cell-cell communication and quorum sensing, which allows density-dependent control over c-di-GMP-regulated processes (120, 129, 149). In others, c-di-GMP signaling is involved in the cell cycle, and allows for the differentiation of daughter cells into motile or sessile cells, depending on their intracellular c-di-GMP levels (23, 28). Finally, although the general paradigm for c-di-GMP signaling states that c-di-GMP induces the

production of adhesive factors and inhibits motility, there are nevertheless some cases in which the opposite is true. In *P. aeruginosa*, for example, exposure to a low level of aminoglycoside antibiotics results in biofilm production in a manner that is dependent on an enzyme that acts to degrade, not produce, c-di-GMP (49). Thus, although generalities exist in c-di-GMP signaling, the signaling systems in individual organisms may vary.

Benefits of regulating cellular behavior by small-molecule second messengers

In addition to c-di-GMP, bacteria also regulate cellular processes using other small, diffusible nucleotide-based second messenger signaling systems, which mediate signals from the cell surface to target receptors inside of the cell. These include cAMP, which regulates carbon utilization (91); ppGpp, a master regulator of the stringent response (17); cGMP, which regulates cyst formation in *Rhodospirillum centenum* (70); c-di-AMP, required for cell viability in *Listeria monocytogenes* (144); and the hybrid molecule cAMP-GMP, which is involved in colonization of the human intestine by *Vibrio cholerae* (26). Although similarities exist between all these signaling systems, most second messenger systems exhibit only one synthesis enzyme, one degradation enzyme, and one receptor molecule that controls a single cellular process. This is in contrast to the large numbers of processes and components involved in regulation of cellular behaviors by c-di-GMP signaling.

Signal transduction using small-molecule second messengers has several advantages. First, separating the original message from an intracellular response allows protection of the cytoplasm from potentially toxic signals such as antibiotics or pH change. Second, large macromolecular complexes are energy-intensive to produce compared to the production of a

small molecule, so allosteric regulation of these complexes via small molecules is more energetically favorable than regulation by their construction and destruction. Finally, enzymatic production and degradation of nucleotide-based second messengers can be very rapid, allowing for a quick response to changes in environmental conditions. Regulation by c-di-GMP signaling also has another advantage compared to regulation by other bacterial second messengers. The use of many different c-di-GMP-metabolizing enzymes in a single organism allows for signal integration of many different inputs into a precise second messenger concentration, which then affects many diverse outputs. This allows for the simultaneous control of many different bacterial processes by one second messenger.

c-di-GMP plays a role in the virulence of many pathogens

The colonization of an animal host requires adaptation to different niches, so it is not surprising that c-di-GMP has been implicated in the ability of many bacterial pathogens to cause disease. In general, low levels of c-di-GMP are required for motility and acute virulence, and high levels of c-di-GMP are associated with persistent, chronic infection. In the intracellular pathogen *Salmonella* Typhimurium, inappropriate production of high levels of c-di-GMP abolishes virulence, implying that the level of c-di-GMP must be kept low for this organism to cause disease (63). Likewise, in *V. cholerae*, low levels of c-di-GMP result in the production of cholera toxin (120, 128). On the other hand, in *P. aeruginosa*, a pathogen that colonizes the lungs of cystic fibrosis patients, the appearance of small colony variants and the production of alginate, both factors that are strongly linked to elevated c-di-GMP levels, are associated with antibiotic resistance and persistence (32, 75, 121). Mutant strains of *P. aeruginosa* that lack

certain c-di-GMP producing or c-di-GMP degrading enzymes have a virulence defect in a mouse model of infection, highlighting the need to precisely regulate the level of c-di-GMP during infection (49, 62). c-di-GMP signaling components also play important roles in the pathogenesis of *Xanthomonas campestris*, *Yersinia pestis*, *Aeromonas hydrophila*, *Borrelia burgdorferi*, as well as in many other pathogens (9, 60, 93, 149). Because of its ubiquity in the bacterial kingdom, c-di-GMP has also been utilized by mammalian cells as an important indicator of bacterial infection when detected inside of the host. Indeed, pretreatment of mice with c-di-GMP has been shown to protect against challenge with *Staphylococcus aureus* or *Klebsiella pneumoniae*, indicating that c-di-GMP stimulates an immune response (56, 57). The basis for the c-di-GMP-specific immune response is the subject of much current research. One host factor that has been implicated in this response is the mammalian sensor protein STING, which has been shown to sense the presence of c-di-GMP inside of the host cell, and to mount a Type I interferon response (16). These studies on the role of c-di-GMP in pathogenesis highlight the importance of researching c-di-GMP signaling in bacteria.

Synthesis and degradation of c-di-GMP is performed by defined enzymatic domains

The mechanisms by which c-di-GMP is produced and degraded have been the subject of much study (4, 45, 54, 113). It is now well established that c-di-GMP is generated by diguanylate cyclases (DGCs) that contain GGDEF domains, and is degraded by c-di-GMP-specific phosphodiesterases (PDEs) that contain EAL or HD-GYP domains. GGDEF, EAL, and HD-GYP domains are named for conserved active site residues that are involved in catalysis. Mutation of any one of these residues, with the exception of D to E in GGDEF domains, or of A

to any hydrophobic residue in EAL domains, abolishes catalysis. Many bacterial species encode dozens of predicted c-di-GMP-metabolizing enzymes containing these domains in their genomes. For example, *Caulobacter crescentus* encodes 14, *S. Typhimurium* encodes 20, *E. coli* encodes 29, *Clostridium difficile* encodes 37, *P. aeruginosa* encodes 41, and *V. cholerae* encodes 72 proteins containing GGDEF, EAL, and/or HD-GYP domains (13, 36, 37, 62, 138). GGDEF, EAL, or HD-GYP domain proteins constitute approximately 4.5% of all response regulators, earning them the designation as some of the most abundant protein families known (36). The abundance of potential c-di-GMP-metabolizing enzymes encoded in the genomes of these bacteria, combined with the fact that the majority of predicted DGCs and PDEs also contain known sensory domains, implies that the level of c-di-GMP in the cell is very precisely regulated in response to environmental conditions.

Diguanylate cyclases produce c-di-GMP from two molecules of GTP

c-di-GMP is synthesized by DGCs harboring an intact GG(D/E)EF motif from two molecules of GTP in a Mg^{2+} -dependent manner. During catalysis, one molecule of GTP binds to the GGDEF domain, which then dimerizes with the GTP-loaded GGDEF domain of a second DGC (18). Structural studies of the DGC PleD from *C. crescentus* have shown that the GGDEF motif is located in a β -hairpin, and have illustrated specific roles for many of the conserved residues of this domain in catalysis (137). The enzymatic synthesis of c-di-GMP has been shown to occur on biologically relevant timescales. The c-di-GMP biosynthetic reaction rate of DgcA from *C. crescentus*, for example, has been measured at $43 \mu\text{mol product} * \mu\text{mol enzyme}^{-1} * \text{minute}^{-1}$ (20). In addition, many DGCs display strong product inhibition by binding of c-di-

GMP to an inhibitory I-site. This binding then alters the conformation of the enzyme in such a way that catalysis is prevented (20). The I-site consists of an RxxD motif typically 5 amino acids N-terminal of the GGDEF motif that makes direct contact with c-di-GMP. Product inhibition occurs at a c-di-GMP concentration that is defined by the affinity of the I-site for this molecule. PleD and DgcA are both feedback-inhibited by the binding of c-di-GMP to the I-site, though their affinities for binding are different: 960 nM for PleD and 5.8 μ M for DgcA (20). Thus, these DGCs would be expected to generate different concentrations of c-di-GMP inside of the cell. Mutation of these I-sites resulted in overactive DGCs that produced more c-di-GMP, and also inhibited growth, potentially due to GTP depletion (20). The presence of an I-site presumably allows the levels of c-di-GMP to be precisely maintained in the cell cytoplasm. Other DGCs do not harbor an I-site; it is therefore assumed that these DGCs do not experience product inhibition.

Phosphodiesterases degrade c-di-GMP by breaking the phosphodiester bond

The phosphodiester bond in c-di-GMP is broken by the hydrolytic actions of EAL or HD-GYP domains of phosphodiesterases (PDEs). These enzymes degrade c-di-GMP to pGpG (for EAL-domain proteins), to be further degraded by cellular hydrolases, or directly to two molecules of GMP (for HD-GYP domains). This reaction involves monomeric PDEs, requires the presence of Mg^{2+} or Mn^{2+} , and is inhibited by Ca^{2+} (22). Like DGCs, PDEs have demonstrated biologically relevant reaction rates. For example, the PDE CC3396 from *C. crescentus* degrades c-di-GMP at a rate of $107 \mu\text{mol} * \mu\text{mol enzyme}^{-1} \text{ minute}^{-1}$ in the presence of its activator GTP (22). The affinity (K_m) for c-di-GMP of several PDEs range from 60 nM to 25

μM (22, 110, 125), indicating that there is a range of c-di-GMP concentrations that activate c-di-GMP degradation via PDEs.

Proteins that harbor both GGDEF and EAL domains

About a third of all GGDEF or EAL domain proteins harbor both of these domains. Some GGDEF-EAL domain proteins have demonstrated both DGC and PDE activity and to conditionally switch between the two, as the case for BphG1 from *Rhodobacter sphaeroides*. BphG1 demonstrates PDE activity unless the C-terminal EAL domain is proteolytically cleaved. Removal of this domain allows DGC activity to become dominant, and c-di-GMP is produced (127). In other proteins that contain both GGDEF and EAL domains, one of these domains is degenerate and is thus not predicted to perform its catalytic reaction, but instead is thought to allosterically regulate the activity of the other, intact domain. Inactive GGDEF domains may still retain the ability to bind c-di-GMP (through the I-site) or GTP (in the active site). Inactive EAL domains may bind c-di-GMP or GTP. The GGDEF/EAL domain protein CC3396 in *C. crescentus* has a degenerate, inactive GEDEF motif and so cannot function as a DGC. Instead, this domain acts to allosterically induce the activity of the EAL domain by binding GTP (22).

Regulation of diguanylate cyclase and phosphodiesterase activity

The activities of DGCs and PDEs are regulated based on environmental cues. Some DGCs and PDEs demonstrate regulation at the level of transcription. For example, many GGDEF and EAL domain protein encoding genes in *E. coli* are under the control of the sigma

factor RpoS (118). However, post-translational regulation of DGCs and PDEs is thought to be a major mechanism of enzymatic control in c-di-GMP signaling. GGDEF, EAL, and HD-GYP domains are highly modular, and most proteins encoding these c-di-GMP output domains are composite proteins that contain other modular signal input domains (35). Input domains include PAS, PAC, REC, HAMP, MASE1, MASE2, and GAF domains (13, 37, 62). These environmental sensing domains have been linked to the detection of small molecules, light, redox potential, voltage, oxygen, nutrients, osmolarity, homoserine lactones, and other signals. Many GGDEF, EAL, and HD-GYP-containing enzymes also contain transmembrane helices, which in Gram-negative bacteria would place the sensing domain in the periplasm, a prime location for sensing environmental changes that are restricted from accessing the cell cytoplasm. Although the majority of activating signals for DGCs and PDEs remain unknown, in some cases the direct signal that stimulates enzymatic activity has been identified. In the case of the DGC DosC and the PDE DosP from *E. coli*, the signal that stimulates both DGC and PDE activity is oxygen, which regulates their activities through their haem-containing sensing domains (132). DosC and DosP proteins interact with each other, and net DGC or PDE activity is preferred based on the level of oxygen to which the cell is exposed (131). Thus DosC and DosP likely form a macromolecular complex that generates a c-di-GMP output in response to changes in oxygen concentration. BphG1 from *R. sphaeroides* contains a light-sensing module in addition to the GGDEF and EAL domains (127). The level of c-di-GMP in *R. sphaeroides* may therefore be coupled to the sensing of light in this organism. Due to the variability of sensory inputs of DGCs and PDEs, and the abundance of these components encoded in the genomes of many bacteria species, the potential for complex signal integration of environmental conditions to a c-di-GMP concentration output is great.

Signaling specificity in c-di-GMP networks

The minimal functional module in second messenger signaling includes an enzyme to create the second messenger molecule, and enzyme to destroy it, a receptor to detect the second messenger, and a target protein with which the receptor interacts to control cellular behavior (Figure 1.2) (45, 94). This is best exemplified by the cAMP signaling system in bacteria, which consists of one adenylate cyclase, one phosphodiesterase, one receptor protein (CRP), and a specific set of downstream targets (specific DNA promoters) (14). c-di-GMP signaling is much more complex than cAMP signaling, yet there is still sequestration of c-di-GMP signaling components into individual modules. Although every DGC produces the same small molecule, many c-di-GMP-metabolizing enzymes can be linked to a specific c-di-GMP-binding receptor (37, 55, 62, 138). This is in apparent contrast to the fact that this second messenger should be freely diffusible throughout the cell. Thus, functional compartmentalization occurs in c-di-GMP signaling, since certain DGCs and PDEs are associated with particular downstream behaviors. Since many of these c-di-GMP components appear to be constitutively expressed, differences in expression levels alone cannot account for the observed signaling specificity (116). A major question in the field of c-di-GMP signaling is how this signaling specificity is achieved despite the multiplicity of c-di-GMP components present in the genomes of many organisms. For example, in *P. aeruginosa*, inactivation of PA2870 and PA3343, which demonstrate DGC activity, does not affect biofilm formation, while inactivation of PA1120, which also demonstrates DGC activity, abolishes biofilm formation in this organism (62). This specific

targeting in c-di-GMP signaling, in which enzymes that contribute to a common c-di-GMP concentration participate in different regulatory pathways, is the subject of current research.

c-di-GMP binds to diverse downstream receptor molecules in order to exert its effects

In order to exert its downstream effects, c-di-GMP must bind to receptor macromolecules and alter their conformations. These binding partners thus “sense” c-di-GMP and transduce this signal through their altered conformation by interacting with target molecules. A number of c-di-GMP-binding receptors have been identified through bioinformatics analysis or by direct binding. These receptors have been shown to control cellular behavior at the transcriptional, translational, and post-translational levels. Like DGCs and PDEs, c-di-GMP-binding receptors frequently demonstrate multidomain architectures, in which a c-di-GMP-binding domain resides in the same macromolecule as an output domain. Output domains are remarkably diverse and include enzymatic domains, protein-protein interaction domains, and regions involved in controlling protein expression from DNA or RNA. Given the large number of cellular processes affected by c-di-GMP, it is likely that many more c-di-GMP receptors will be identified in the years to come.

The PilZ protein domain is a c-di-GMP-sensing domain

The most thoroughly studied c-di-GMP receptor is a protein domain called the PilZ domain, named for the PilZ protein, PA2960, of *P. aeruginosa*. The PilZ domain was first identified as a possible c-di-GMP receptor through bioinformatics analysis, as it has a similar phyletic distribution to that of c-di-GMP-metabolizing enzymes (2). c-di-GMP binding to the PilZ domain was subsequently confirmed through biochemical analyses (21, 75, 108). Hundreds of PilZ domain proteins have since been identified, and many of these are involved in processes known to be regulated by c-di-GMP (2, 21, 59, 75, 95, 108).

Structural analysis of PilZ domain proteins

Several crystal and NMR structures have been solved for proteins containing PilZ domains, and the roles of conserved residues in binding c-di-GMP have been elucidated (6, 58, 97) (Figure 1.3). The PilZ domain forms a six-stranded anti-parallel β -barrel structure of approximately 100 amino acids in length with conserved residues clustered within the c-di-GMP binding pocket of the domain (97). The most important amino acid motifs for binding c-di-GMP appear to be the highly conserved RxxxR motif at the N-terminus of the PilZ domain, and the (D/N)xSxxG motif, located in the β 2/ β 3 hairpin loop. The two arginines of the RxxxR motif are essential for binding c-di-GMP, as mutation of either arginine results in a PilZ domain that is no longer able to bind this second messenger (21, 58). These arginines form a dual guanidino motif that uses hydrogen bonds and π -stacking interactions to coordinate c-di-GMP in the binding pocket (6, 58) (Figure 1.3). This mechanism of c-di-GMP binding is similar to that of GGDEF domain I-sites, which also rely on dual guanidino motifs to bind c-di-GMP (6, 20). The N-

terminal region containing the RxxxR motif has been referred to as the “c-di-GMP switch”, since in the absence of c-di-GMP it exists disordered in solution, but undergoes a large, entropically unfavorable conformational change upon binding to c-di-GMP (6).

Several residues in the c-di-GMP binding pocket affect the binding affinity of PilZ domains for c-di-GMP. The residue immediately N-terminal of the RxxxR motif, dubbed “Position-X”, has been shown to be an important determinant in the affinity of PilZ domain proteins for c-di-GMP (58) (Figure 1.3). Specifically, the presence of an arginine in this position tends to increase binding affinity due to the addition of extra, potentially stabilizing, contacts with c-di-GMP, while the presence of hydrophobic residues in this position decreases binding affinity, presumably because these residues cannot create bonds with the substrate (58). Additionally, mutation of residues in the (D/N)xSxxG motif have also been shown to alter the affinity of PilZ domains for c-di-GMP (21, 58, 108).

In addition to affecting the affinity of PilZ domains for c-di-GMP, the residue at Position-X also determines the number of c-di-GMP molecules that bind to the PilZ domain. PP4397, from *Pseudomonas putida*, and PA4608, from *P. aeruginosa*, both contain arginines in this position, and both bind two molecules of c-di-GMP as an intercalated dimer (58, 97) (Figure 1.3). Mutation of the Position-X arginine in PP4397 to a bulky hydrophobic residue appears to sterically hinder binding of one of the c-di-GMP molecules in the binding pocket (58). VCA0042 from *V. cholerae* contains a leucine in this location and binds one molecule of c-di-GMP, though the binding pocket can be altered to accommodate a dimer of c-di-GMP if this leucine is mutated to an arginine (6, 58).

The C-terminus of PilZ domains frequently contains alpha helices and tends to be disordered during structural assessment, indicating that this region experiences flexibility (44, 58, 97, 111). The flexible C-terminus in PA4608 has been shown to act as a hinged lid that protects the hydrophobic binding pocket from aqueous solution in the absence of c-di-GMP, and is displaced upon binding to c-di-GMP (44, 111). It is unknown whether C-termini in other PilZ domain proteins perform similar functions.

Transduction of the c-di-GMP signal by PilZ domains

During c-di-GMP signal transduction, the signal is transmitted to a biological output through changes in effector protein structure that occur upon c-di-GMP binding. Since PilZ domain proteins demonstrate low sequence similarities aside from conserved residues of the binding pocket, c-di-GMP signal transduction likely involves different structural mechanisms in different effector proteins. In some multi-domain proteins, binding of c-di-GMP results in changes in the relative orientation of these domains. VCA0042 is a two-domain protein consisting of an N-terminal YcgR-N* domain and a C-terminal PilZ domain. Binding of c-di-GMP to the PilZ domain in this protein results in a large conformational change in the switch region, which dramatically alters the orientation of these domains with respect to each other, likely affecting how this protein interacts with its target (6). In other PilZ domain proteins, the binding of c-di-GMP causes a change in oligomerization state. Such is the case with PP4397, a homologue of VCA0042 that exists as a dimer in the absence of c-di-GMP. Binding to c-di-GMP induces a dimer-to-monomer conversion due to the disruption of important contacts

between the individual units of the dimer (58). Neither VCA0042 nor PP4397 demonstrate significant structural change in the domains themselves upon c-di-GMP binding; rather it is through the conformational shifts between domains or protein subunits that c-di-GMP likely transduces its signal. However, other PilZ domain proteins likely transduce the c-di-GMP signal by conformational rearrangements in the PilZ domain itself upon c-di-GMP binding. For example, PA4608 binding to c-di-GMP induces clustering of negative charges on one face of the protein (44). This may result in electrostatic interactions between PA4608 and its downstream target.

Targets affected by c-di-GMP signaling

The targets of several PilZ domain proteins have been studied in some detail. Several PilZ domain proteins have been found to directly affect motility in the presence of c-di-GMP, such as DgrA and DgrB from *C. crescentus*, and YcgR from *S. Typhimurium* and *E. coli* (21, 59, 108) (Figure 1.5E). Recent studies have determined that YcgR directly affects cellular motility by binding to components of the flagellar apparatus. Other PilZ domain proteins regulate the production of exopolysaccharide. Alg44 is a PilZ domain protein in *P. aeruginosa* that is required for the production of alginate in this organism (75). The protein that regulates cellulose synthesis in *G. xylinus* by binding c-di-GMP is also a PilZ domain protein (2, 108). Other PilZ domain proteins, such as PA2989, seem to be involved in both motility and biofilm formation (75). Much remains to be learned about the molecular mechanisms by which PilZ domain proteins exert their effects on downstream processes.

Degenerate GGDEF or EAL domains can act as c-di-GMP receptors

Another class of c-di-GMP receptors includes GGDEF and EAL domain proteins in which the GGDEF or EAL domain has lost catalytic activity but retains its ability to bind c-di-GMP, presumably *via* the I-site of the GGDEF domain or the catalytic pocket of the EAL domain. PopA, an important regulatory factor of the cell cycle in *C. crescentus*, is an example of a GGDEF domain protein that acts as a c-di-GMP receptor. PopA harbors a degenerate GGDEF domain with an intact I-site that binds c-di-GMP with an affinity of 2.4 μM (28). In swarmer cells of *C. crescentus*, the level of c-di-GMP is kept low, and chromosomal replication is prevented by the replication inhibitor CtrA. When the swarmer differentiates into a stalked cell, the concentration of c-di-GMP rises high enough to bind to PopA, which then binds CtrA and facilitates its degradation by the cellular protease ClpXP (28, 90, 96). Another example of c-di-GMP binding to a degenerate GGDEF domain by means of an RxxD I-site is the *P. aeruginosa* protein PelD, which binds c-di-GMP with an affinity of 1.9 μM . PelD bound to c-di-GMP stimulates the production of Pel polysaccharide, which is important for biofilm formation in this organism (68, 142). The *P. aeruginosa* FimX protein, on the other hand, binds c-di-GMP in its degenerate EAL domain (80). Binding of FimX to c-di-GMP is important in the generation of Type IV Pili in *P. aeruginosa* (50, 80).

Transcription factors that bind c-di-GMP

In addition to proteins with PilZ, GGDEF, and EAL domains, a number of transcription factors have also been shown to bind c-di-GMP through diverse or unknown mechanisms. Clp, a transcriptional regulator in the plant pathogen *X. campestris*, consists of a C-terminal helix-turn-helix DNA binding domain and an N-terminal cNMP binding domain that binds c-di-GMP with an affinity of 161 nM (126). Interestingly, Clp is a paralog of the classical cAMP-binding protein CRP that seems to have lost the ability to bind cAMP and instead binds c-di-GMP. c-di-GMP binding to Clp affects its activity on target promoters involved in the expression of virulence factors (19, 126). Reducing the affinity of this protein for c-di-GMP abrogates the virulence of this organism (126). Two transcriptional regulators in *V. cholerae*, VpsR and VpsT, have both been found to directly bind c-di-GMP with affinities of 1.6 and 3.2 μ M, respectively (61, 120). Additionally, FleQ, a transcription factor in *P. aeruginosa*, also binds c-di-GMP, with an affinity of 15-25 μ M (5, 46). These transcription factors inversely regulate genes involved in motility and expolysaccharide production, and their activities are altered upon binding to c-di-GMP.

RNA molecules can act as c-di-GMP receptors

In addition to binding protein partners, c-di-GMP has also been shown to bind RNA molecules, thereby regulating the transcription or translation of target proteins. Riboswitches in both *V. cholerae* and *Clostridium difficile* have been shown to bind c-di-GMP with a very high affinity (K_d of 0.2 – 1 nM) (67, 123). In *V. cholerae*, a c-di-GMP-binding riboswitch controls the expression of flagellar and pilus biosynthetic genes, as well as virulence components (123).

The *C. difficile* riboswitch is actually a ribozyme: binding of c-di-GMP results in autocleavage of the RNA, thereby revealing a perfect ribosome binding site that can then direct transcription of downstream genes (67). Thus, c-di-GMP binds to many diverse target macromolecules to exert its effects on the cell.

Methods to analyze intracellular c-di-GMP concentrations

The ability to correlate specific cellular phenotypes directly to intracellular c-di-GMP concentrations is essential to unravel the mechanisms of c-di-GMP signaling. Currently, there exist two general approaches for measuring intracellular c-di-GMP: extraction of nucleotides from cell lysate followed by quantification using chromatography-based methods, and measurement in live cells using a method based on Forster resonance energy transfer (FRET). These techniques have allowed for comparisons of intracellular c-di-GMP concentrations between different bacterial species, or between various growth or differentiation phases of the same species (23, 114, 119). Methods to measure intracellular c-di-GMP levels are also applied to analyze the activities of various DGCs and PDEs, or other components that affect c-di-GMP levels, through their inactivation or overexpression *in vivo* (8, 12, 23, 46, 48, 55).

Quantification of intracellular c-di-GMP by chromatography-based methods

The most commonly used methods for measuring intracellular c-di-GMP concentrations involve extraction of nucleotides from the cell cytoplasm, separation and purification of these nucleotides using chromatography, and quantification of the c-di-GMP fraction with a detector. Frequently, high-performance liquid chromatography (HPLC) is chosen as the chromatographic method due to the ability to couple this technique to identification and quantification of compounds using a mass spectrometer. To prepare samples from cell cultures for HPLC, nucleotides are extracted from cells, typically using either heat or acid lysis (3, 139). The extract must then be lyophilized and resuspended in water for injection into the HPLC instrument. During HPLC, molecules in the liquid sample are pumped through a column that contains a stationary phase. Compounds in the liquid interact with stationary phase particles based on their chemical and physical properties, and this determines their retention time in the column. As compounds exit the column, they are analyzed, and may be quantified, by a UV detector with an absorption wavelength of the compound to be identified. For c-di-GMP, this absorption wavelength is at 254 nm, at which c-di-GMP demonstrates a characteristic peak. A more sensitive method of quantifying c-di-GMP than assessment of the 254 nm absorbance peak is to couple HPLC to mass spectrometry (46, 114, 119). c-di-GMP quantified using this method is usually expressed as pmol mg⁻¹ protein or pmol mg⁻¹ cells, which can be converted to molarity assuming that an average cell weighs 0.66 pg, that it is composed of 16.5% protein by weight, and that one molecule cell⁻¹ is equivalent to 1 nM (79, 114). Modifications and improvements on these techniques have led to the detection of c-di-GMP at levels as low as 0.1 pmol mg⁻¹ protein, corresponding to approximately 6.6 nM (114). Another chromatographic method for analyzing c-di-GMP is thin layer chromatography (TLC) (10). To prepare nucleotides for analysis by TLC, cells are incubated in the presence of radiolabeled phosphate, which is incorporated into cellular

molecules. Cells are then lysed, nucleotides are extracted with acid, neutralized, and applied to the TLC plate (8, 10, 104, 125). As in HPLC, compounds migrate along the TLC plate at different rates based on their chemical and physical properties, allowing for their separation. The amount of radioactivity corresponding to a spot at the correct retardation factor (Rf) for c-di-GMP is then quantified using a scintillation counter. c-di-GMP is usually represented in relative amounts between samples using this method.

Estimation of intracellular c-di-GMP concentrations in live cells using FRET technology

Recently, a method of measuring c-di-GMP levels in individual live cells based on Förster Resonance Energy Transfer (FRET) has emerged (23) (Figure 1.4). FRET is a very sensitive method that can be used to determine changes in protein structure, such as those that result from the binding of proteins to small molecules. In FRET, the emission wavelength of the donor fluorophore overlaps with the excitation wavelength of the acceptor fluorophore. When these two fluorophores are in proximity, excitation at the donor wavelength thus results in energy transfer and emission at the wavelength of the acceptor fluorophore. To generate a FRET-based c-di-GMP biosensor, the c-di-GMP receptor YcgR was fused between two fluorophores that constitute a FRET pair (23). Binding of this receptor to c-di-GMP results in a conformational change in the YcgR protein, and thus a change in the measured FRET of this biosensor. The YcgR FRET biosensor demonstrates high specificity for c-di-GMP, and does not respond to GTP, cGMP or cAMP (23). This system was used to measure the concentration of c-di-GMP in live cells in real time, based on the binding affinity of YcgR for c-di-GMP (Figure 1.4).

Measurements of physiologically relevant c-di-GMP concentrations

Using the techniques described above, the intracellular concentration of c-di-GMP has been measured at a variety of concentrations in different bacteria. Studies using LC-MS which analyze the total average c-di-GMP levels for cells within a population have been complemented by measurements of c-di-GMP concentrations in individual cells. Using HPLC coupled with ESI-MS, the average c-di-GMP level of *C. crescentus* in log-phase cells has been measured at 1.1 μM (22). Analysis of c-di-GMP levels in individual live cells, however, indicates that the *C. crescentus* population is heterogeneous in its c-di-GMP concentrations, with some cells demonstrating a free c-di-GMP level of greater than 500 nM, and others with less than 100 nM (23). These levels correlated with cellular behavior: stalked, sessile cells demonstrated high levels of c-di-GMP, and motile cells containing flagella had lower levels of c-di-GMP. This population heterogeneity, and its correlation with cellular phenotype, has also been shown for *P. aeruginosa* (23). After cell division of this organism, cells that maintained the flagellum displayed low c-di-GMP levels, whereas unflagellated cells had high c-di-GMP levels. The average total c-di-GMP concentration in *P. aeruginosa* has been shown to be approximately 700 nM by LC-MS at log phase in minimal media (46). In rich media, log-phase *P. aeruginosa* has been shown to have an average c-di-GMP concentration of about half this, around 320 nM (114). This value is lower than that of *V. cholerae* under the same conditions, at 850 nM (114). In *S. Typhimurium* and *E. coli*, the intracellular level of c-di-GMP in rich media in log phase is considerably lower than that of *P. aeruginosa* and *V. cholerae*, estimated at less than 100 nM or below the level of detection (12, 48, 63, 79, 114). The levels of c-di-GMP have been shown to

fluctuate, however, throughout the growth phase. One study on c-di-GMP concentrations at various stages in the growth phase of *E. coli* demonstrated that the level of c-di-GMP rises during growth, peaking at early stationary phase at approximately 830 nM, and then declining (119). In addition to in liquid culture, c-di-GMP has also been measured in cells growing on the surface of agar plates. After 10 hours of growth on LB-agar plates at 28°C, the c-di-GMP concentration of *S. Typhimurium* strain UMR1 has been measured at approximately 233 nM (55, 114). Additionally, analyses in which c-di-GMP-metabolizing enzymes are inactivated or overexpressed can give insights regarding the functions and activities of these enzymes. In *P. aeruginosa*, a mutation in *wspF*, a negative regulator of a DGC, resulted in four-fold higher c-di-GMP levels compared to wild-type cells (46). Surprisingly, inactivation of some DGCs and PDEs that are known to affect cellular phenotypes in a c-di-GMP-dependent manner do not appear to affect detectable total cellular c-di-GMP levels as analyzed by LC-MS (109, 112). Overexpression of some DGCs can lead to a measurable increase in c-di-GMP levels, though the extent of this increase varies depending upon the DGC. Overexpression of the DGC CdgH in *V. cholerae* led to a very large increase in c-di-GMP levels as assessed qualitatively by TLC (8). In *S. Typhimurium*, overexpression of the DGC AdrA raised the total cellular c-di-GMP concentration to 0.64 and to 0.32 nmol mg⁻¹ cells in two separate studies (255.8 μM and 127.9 μM, respectively) (63, 113), while overexpression of the DGCs STM3388 and STM2123 only increased c-di-GMP levels from 0.34 pmol mg⁻¹ cells (137 nM) to 0.93 and 1.5 pmol mg⁻¹ cells (373 and 602 nM, respectively) (55). This demonstrates the huge dynamic range between different c-di-GMP-metabolizing enzymes in their ability to affect the intracellular concentration of c-di-GMP.

The c-di-GMP signaling network in *Salmonella* Typhimurium: a model system

Salmonella enterica serovar Typhimurium is a pathogenic Gram-negative bacterium considered to be a model organism for the study of fundamental cellular processes, including those involved in pathogenesis, due to the large availability of tools for genetic manipulation for this organism (88). In healthy humans, infection with *S. Typhimurium* causes a self-limiting gastroenteritis, though infection can be life-threatening in immunocompromised individuals. The virulence of *S. Typhimurium* can be studied in tissue culture, or in mouse models of infection, in which this organism causes a systemic disease similar to that caused by *S. Typhi* or *S. Paratyphi* in humans. Since *S. Typhimurium* is transmitted through the fecal-oral route between hosts, it must be capable of surviving both inside and outside of the host, environments that present very unique challenges. This indicates that *S. Typhimurium* harbors strategies for adaptation to a variety of different environmental niches.

The c-di-GMP signaling network in *S. Typhimurium* has been the subject of much study in the last decade. *S. Typhimurium* harbors five GGDEF and seven EAL domain proteins, and seven additional proteins that contain both domains. Eight of the GGDEF domain proteins have an intact GGDEF or GGEEF motif (37); the other four contain degenerate GGDEF motifs and thus are not expected to act as functional DGCs. *S. Typhimurium* has three known cellular behaviors that are regulated by c-di-GMP: flagellar-based motility, the production of curli fimbriae, and cellulose production (Figure 1.5). Two of these processes are linked to a particular PilZ domain protein in *S. Typhimurium*: YcgR, which controls motility; and BcsA, the bacterial cellulose synthase. An increase in intracellular c-di-GMP levels results in a decrease in swimming motility (through YcgR), and the production of curli fimbriae and cellulose (through

BcsA), which allows *S. Typhimurium* to attach to surfaces and form biofilms (Figure 1.5). Thus, as in other organisms, c-di-GMP controls the switch between cellular motility and sessility in *S. Typhimurium*.

The PDE YhjH controls motility inhibition through the PilZ domain protein YcgR

YcgR, one of the two PilZ domain proteins in *S. Typhimurium*, has been shown to be an important regulator of flagellar-based motility. YcgR was originally discovered in *E. coli* as a negative regulator of motility in an *hns* mutant (59). The motility defect in an *hns* mutant could be relieved by one of two ways: deletion in the gene *ycgR*, or overexpression of the EAL domain protein YhjH. It was subsequently determined in *S. Typhimurium* that *yhjH* inactivation results in a motility defect that can be partially relieved by a second mutation in YcgR, which was found to bind c-di-GMP, indicating that YcgR acts downstream of YhjH activity (108). Overexpression of YhjH results in a decrease in the total cellular level of c-di-GMP and an increase in swimming, and this is dependent upon a functional EAL motif in YhjH (113). The *E. coli* YhjH protein has been purified and shown to demonstrate c-di-GMP-hydrolyzing activity (92). Thus YhjH is a phosphodiesterase, and its inactivation likely leads to a rise in c-di-GMP levels, which may then bind to the YcgR protein to inhibit motility. The transcription of both the *yhjH* and *ycgR* genes is driven by a flagellar class III promoter, and is thus under positive regulation by FliA, with maximal expression during exponential phase (33, 40, 59, 135). The fact that *yhjH* is co-expressed with *ycgR*, and that *yhjH* deletion results in motility inhibition through YcgR, indicates that YhjH acts as the c-di-GMP-degrading PDE for the c-di-GMP

module involving YcgR (see Figure 1.2). However, deletion of *yhjH* does not result in a significant increase in c-di-GMP levels in *S. Typhimurium*, as determined by LC-MS (112). More work is needed to elucidate the exact mechanism by which *yhjH* inactivation inhibits motility in *S. Typhimurium*.

What are the specific DGCs that produce the c-di-GMP that inhibits motility by YcgR? In an *E. coli yhjH* mutant, several GGDEF domain proteins have been linked to decreased swimming: YegE, YeaJ, YfiN, YedQ, YddV, YneF, and YeaI (12, 92, 109). These correspond to the *S. Typhimurium* homologues STM2123 (YegE), STM1283 (YeaJ), STM2672 (YfiN), and STM1987 (YedQ), which share 61%-75% identity to the *E. coli* proteins (YddV, YneF, and YeaI have no homologues in *S. Typhimurium*). No systematic study has analyzed the effect of GGDEF domain proteins in *S. Typhimurium* on motility; however, given the amount of sequence preservation between the *E. coli* and *S. Typhimurium* homologues, it is not unreasonable to assume that some of these DGCs in *S. Typhimurium* may also regulate swimming motility as they do in *E. coli*.

c-di-GMP-bound YcgR inhibits motility by binding to the flagellum

S. Typhimurium swims by the coordinated movement of its peritrichous flagella. The flagellum is a motor that contains a stator (a ring composed of MotA and MotB subunits) and a rotor (a ring of FliG, FliM, and FliN subunits) (7). The energy to rotate the flagellum is generated by the proton motive force. Protons flow through the stator, causing it to exert torque on the rotor, and the flagellum rotates. When all of the flagella are rotating counter-clockwise

(CCW), they form a bundle and the cell swims smoothly (7). When the flagella rotate clockwise (CW), the bundle dissociates and the cell tumbles, randomly reorienting itself in a new direction. Various environmental signals affect cellular motility, through modulation of the tumbling frequency *via* proteins involved chemotaxis, and by controlling the c-di-GMP concentration. c-di-GMP regulates cellular motility by binding YcgR, which then modulates cellular motility by interacting directly with specific components of the flagellar apparatus.

The molecular mechanisms involved in YcgR-based motility inhibition have been the subjects of several recent studies in *E. coli* (12, 30, 89). YcgR is a two-domain protein with domain architecture similar to its homologs VCA0042 and PP4397 (discussed in a previous section): an N-terminal YcgR-N* domain and a C-terminal PilZ domain, which binds two molecules of c-di-GMP (23). Boehm *et al* observed *in vivo* localization of YcgR to the flagellum in the presence, but not in the absence, of c-di-GMP, using FRET fluorescence microscopy (12). They identified point mutations in the MotA stator protein that abolished YcgR flagellar localization and motility inhibition, suggesting that YcgR may bind MotA. By comparing the rotational behavior of tethered wild-type cells to *yjhH* mutant cells, they determined that YcgR acts as a flagellar brake, presumably by binding to components of the rotor and the stator in the presence of c-di-GMP. Like Boehm *et al*, Paul *et al* also found that YcgR acts as a brake, though they could not visualize direct YcgR binding to MotA (89). Instead they identified FliG and FliM, components of the flagellar rotor, as direct protein interaction targets of YcgR, using pull-down assays. Paul *et al* found that YcgR interacts with FliG and FliM even in the absence of c-di-GMP, leading to the hypothesis that c-di-GMP affects the activity of YcgR but not its localization. This is consistent with findings by Fang *et al*, which demonstrate that YcgR interacts with FliG, FliM, and the rotor protein FliN, even when certain critical residues for

binding c-di-GMP are mutated (30). Both Fang *et al* and Paul *et al* determined that YcgR induces a CCW bias in flagellar rotation (30, 89), thereby reducing the frequency of tumbling, which may inhibit the ability of *E. coli* to free itself if it becomes stuck while swimming through viscous media.

c-di-GMP induces the rdar morphotype via the master regulator CsgD

In addition to inhibiting motility through YcgR, c-di-GMP also induces production of an extracellular matrix in *S. Typhimurium* by stimulating the expression of CsgD, a transcriptional regulator of the LuxR/FixJ family. The extracellular matrix consists of curli fimbriae, which are thin, coiled structures of 2-5 nm in length that protrude from the cell and are required for cellular aggregation, and cellulose, a β -(1,4)-D-glucan polymer (140, 151). Expression of these two components on the cell surface results in a rigid, hydrophobic network that causes cells to pack together and stick to surfaces, and provides resistance to environmental stresses such as desiccation (117, 151). Colonies that produce this matrix give an appearance on agar plates of being dry and wrinkly, called the rdar (rough, dry and red) morphotype (100). This matrix can be visualized by a red color on agar plates that contain the dye Congo Red, or by fluorescence of colonies on plates that contain calcofluor, which fluoresces under UV light when it binds to cellulose (Figure 1.5). CsgD controls the rdar morphotype by directly activating the expression of *csgAB*, which encodes the structural subunits of curli fimbriae, and *adrA*, which encodes a DGC required for the production of cellulose (86, 148). CsgD also represses transcription of flagellar class II genes by interfering with FlhDC binding to the promoter (85, 148). Although

the *V. cholerae* CsgD homologue, VpsT, has been shown to directly bind c-di-GMP, CsgD in *S. Typhimurium* and *E. coli* do not bind c-di-GMP (61, 148). Transcriptional regulation of *csgD* is complex, under the control of at least nine different transcription factors, each responding to different environmental conditions (39, 85, 103). *csgD* is not transcribed at temperatures above 30°C, so extracellular matrix production only occurs at temperatures of 30°C or lower (101, 103). Additionally, the production of CsgD is dependent on the stationary-phase sigma factor RpoS, and is linked to nutrient-limited conditions (99, 140). Several DGCs and PDEs have been linked to the expression of CsgD in *S. Typhimurium*. The DGCs STM2123 and STM3388, and the PDEs STM1703, STM1827, and STM4264, have been shown to be involved in c-di-GMP-dependent regulation of CsgD expression (55, 112). Other DGCs that are not normally involved in CsgD expression can still stimulate its production when overexpressed, suggesting that c-di-GMP produced from any DGC can stimulate CsgD expression (55). However, the c-di-GMP receptor that controls CsgD expression remains unknown. One potential candidate is MlrA, which is a positive transcriptional regulator of the *rdar* morphotype in both *E. coli* and *S. Typhimurium* and is highly specific for the *csgDEFG* operon (15).

Cellulose is produced by the bacterial cellulose synthase BcsA

Cellulose is an important structural component of extracellular matrices produced by several different organisms. The genes required for cellulose production were first identified using genetic complementation studies in *G. xylinus* (143). This operon consists of four genes, named *bcsA-D*, all of which are required for cellulose production in this organism (143).

Homologues to *bcsA-C*, but not to *bcsD*, are found in all Enterobacterial genomes analyzed to date (37). In addition to *bcsA-C*, *S. Typhimurium* also requires several other genes to produce cellulose. These are located in the two divergently-transcribed operons, *bcsQABZC* and *bcsEFG* (117, 151). Some of these genes have known functions. *bcsA* encodes the bacterial cellulose synthase, which is a transmembrane protein that contains a glycosyl transferase domain, which is involved in the polymerization of individual UDP-glucose units (124, 150). BcsA also contains a C-terminal PilZ domain, which presumably binds to c-di-GMP to allosterically activate cellulose production. BcsQ encodes a MinD homologue and is localized to the cell pole, where it potentially acts to induce cellulose synthesis (65). BcsZ is a predicted periplasmic protein that contains putative domains involved in the breakdown of cellulose. BcsC is a putative oxidase and contains protein-protein interaction domains. BcsE and BcsG have similarities to other bacterial proteases and endoglucanases. The functions of BcsB and BcsF remain unknown. The transcription of these components does not appear to be regulated by c-di-GMP, CsgD, temperature, or other environmental factors, so these genes are thought to be constitutively transcribed (42, 55, 151).

The DGC AdrA directly stimulates cellulose production

Although CsgD directly activates the transcription of curli fimbriae subunits, its involvement in cellulose production is indirect, and occurs through the transcription of *adrA*, which encodes a DGC that is required for the production of cellulose (102, 151). AdrA is the only DGC that is dependent on CsgD for its expression (151). Because CsgD is only expressed

at temperatures of 30°C or lower, cellulose production only occurs at lower temperatures (55, 102). Deletion of AdrA abolishes cellulose production, indicating that other DGCs cannot compensate for its loss (37). This is surprising, since other DGCs are also expressed at cellulose-producing conditions, and some have been shown to be active, since c-di-GMP is necessary for the expression of CsgD (55, 116). This indicates that AdrA has the ability to selectively target cellulose production that other DGCs lack. The overexpression of other DGCs can result in cellulose production (37), but these overexpression effects are likely to mask specificity (138). AdrA is also unique in that it is capable of producing large amounts of intracellular c-di-GMP. Overexpression of AdrA in *S. Typhimurium* yielded 500-fold higher intracellular c-di-GMP levels than the overexpression of two other *S. Typhimurium* DGCs that are required for the production of CsgD (discussed in a previous chapter) (55, 113). Indeed, under native expression, AdrA is responsible for over half of the c-di-GMP produced in the cell (55). Finally, although AdrA is required for cellulose production during the *rdar* morphotype, which occurs in liquid or solid rich media (117, 151), another DGC, STM1987, is involved in cellulose production during pellicle formation at the air-liquid interface in a liquid starvation media called ATM (37). It is possible that activation of STM1987 may occur in ATM but not during the *rdar* morphotype due to different environmental sensing domains in these enzymes, which would explain why STM1987 cannot compensate for the loss of AdrA.

Other c-di-GMP-binding receptors in S. Typhimurium

The fact that CsgD requires an as-yet unknown c-di-GMP receptor for its expression demonstrates the existence of other c-di-GMP-binding receptors in *S. Typhimurium*. Two c-di-GMP-binding receptors in *S. Typhimurium* may be PNPase and BdcA, since close homologues of these proteins in *E. coli* have been demonstrated to bind c-di-GMP. *E. coli* PNPase, which is 97% identical to the *S. Typhimurium* homologue, is an important 3' to 5' exonuclease that copurifies with a DGC and a PDE that contain PAS domains and is thus thought to modify RNA in response to oxygen levels (131, 132). *E. coli* BdcA is 80% identical to the *S. Typhimurium* homologue and binds c-di-GMP with an affinity of 11.7 μ M (69). BdcA acts to increase motility by binding to, and thus potentially sequestering, c-di-GMP (69). Due to the large amount of sequence conservation between the *E. coli* and *S. Typhimurium* homologs of PNPase and BdcA, it seems reasonable to speculate that these proteins may also be involved in mediating c-di-GMP-regulated processes in *S. Typhimurium*.

The role of c-di-GMP in the virulence of S. Typhimurium

Although the ability to regulate c-di-GMP levels is important in *S. Typhimurium* during infection, the exact role of c-di-GMP during infection is not known. Artificial production of high levels of c-di-GMP during infection abolishes virulence in mice (63). Conversely, a *S. Typhimurium* strain that lacks all 12 GGDEF domain proteins is also completely defective for virulence, though virulence can be restored by complementation with the GGDEF domain protein STM4551, even without an active GGDEF motif (116). One EAL domain protein, YdiV, has been shown to be important for virulence of *S. Typhimurium* in mice (48). However,

enzymatic activity of this protein has not been demonstrated *in vitro*, and YdiV has been shown to inhibit motility and up-regulate CsgD expression, which are not canonical features of a PDE (24, 115). It has more recently been shown that YdiV contributes to the virulence of *S. Typhimurium* by reducing the expression of flagellin on the cell surface, which is an immunostimulatory factor (122). Several studies regarding the involvement of cellulose production during infection have demonstrated conflicting results. The production of cellulose has been shown to be unnecessary for virulence of *S. Typhimurium* (117). In fact, overproduction of cellulose has been shown to inhibit invasion of this organism into gastrointestinal cells (63). Other studies have shown that cellulose contributes to the attachment of *S. Typhimurium* HEp-2 cells and chicken epithelial cells (66). However, cellular aggregation, which is a hallmark of the rdar morphotype, does not appear to be a virulence adaptation, as a strain of *S. Typhimurium* that lacks aggregative factors outcompetes wild-type cells in a competitive assay for virulence in mice (140). Several studies indicate that production of curli fimbriae and cellulose may provide some advantage in the transmission between hosts, but not during infection within the host. The production of cellulose and curli fimbriae has been shown to facilitate attachment to plants, and to protect cells against desiccation and chlorine exposure (42, 64, 117, 141). Finally, although the ability to swim is important for *S. Typhimurium* to access endothelial cells of the host, it is unknown whether a YcgR-mediated decrease in swimming is important at any point during infection.

Conclusions

Although much has been learned about c-di-GMP signaling in the past decade, many questions remain. Why is there such a multiplicity of c-di-GMP signaling components encoded in bacterial genomes? What are the c-di-GMP downstream receptors, and how do they exert their effects on cellular behavior? How are individual c-di-GMP modules able to regulate processes in parallel in the same cell? Examination of the c-di-GMP signaling network in model organisms such as *S. Typhimurium* can provide insight into these questions. The studies highlighted above present a model of c-di-GMP signaling in *S. Typhimurium* in which low levels of c-di-GMP favor motile cells that do not produce adhesive factors, and high levels of c-di-GMP favor the production of an adhesive extracellular matrix. In this organism, under some environmental conditions, cellular motility is allowed through the maintenance of low levels of c-di-GMP by YhjH. Certain environmental cues result in a rise in c-di-GMP levels by the DGCs STM2123 and STM3388 that induces expression of CsgD, which down-regulates flagellar gene expression and activates the production of curli fimbriae and AdrA. c-di-GMP produced by AdrA, or by STM1987 in some circumstances, then results in the production of cellulose. Future experiments analyzing components involved in c-di-GMP signaling, and improvements in the methods for measuring c-di-GMP, will lead to a better understanding of how c-di-GMP affects cellular behavior in *S. Typhimurium* as well as in other organisms.

Figures

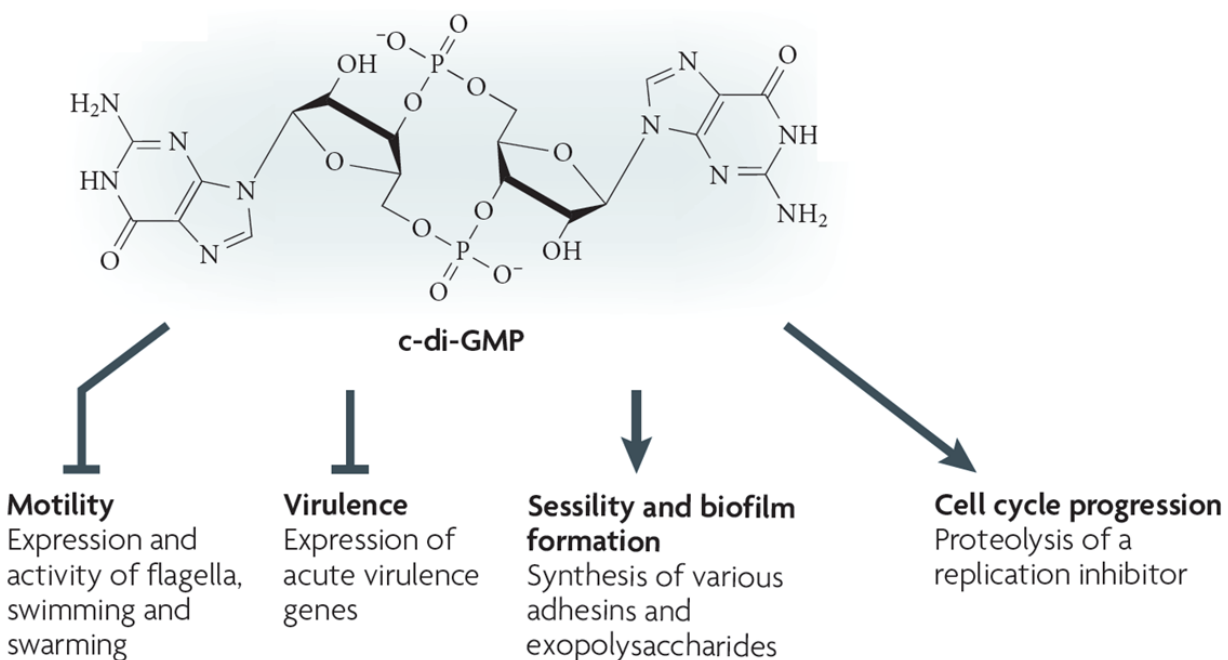


Figure 1.1: c-di-GMP is responsible for the switch between the motile and sessile lifestyle. In many bacteria, c-di-GMP has been shown to inhibit cellular motility, and to stimulate the production of adhesive factors, such as fimbriae and exopolysaccharides. In addition, c-di-GMP has also been shown to be involved in the cell cycle of *C. crescentus*, and in the virulence of many pathogens. (Modified from Hengge, 2009 (45))

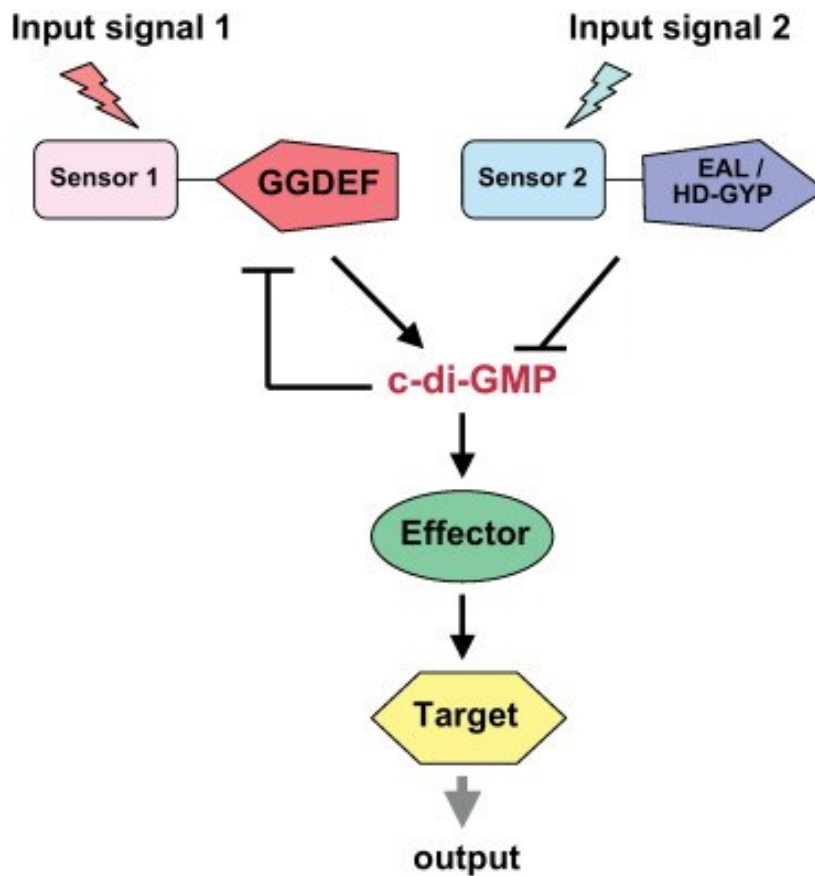


Figure 1.2: The minimal functional module in c-di-GMP signaling. The minimal functional c-di-GMP module consists of a c-di-GMP-generating enzyme that contains a GGDEF domain, a c-di-GMP-degrading enzyme that contains an EAL or HD-GYP domain, an effector molecule that can bind to c-di-GMP, and a target molecule that produces a biologically important output. The c-di-GMP-metabolizing enzymes are physically linked to environmental sensing domains, and thus their activities are controlled by input signals. Many GGDEF domain proteins also display negative feedback inhibition. (Modified from Povolotsky & Hengge, 2011 (94))

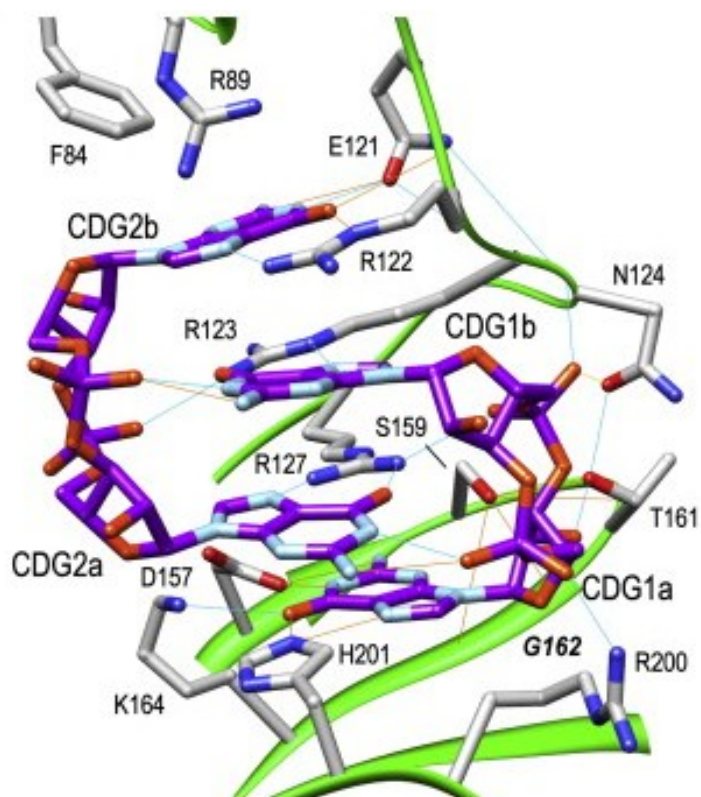


Figure 1.3: The binding pocket of the PilZ domain protein PP4397 bound to c-di-GMP reveals that conserved residues make direct contacts with c-di-GMP. Two molecules of c-di-GMP (CDG1 and CDG2), with individual guanine groups designated as (a) or (b), are shown as a ball-and-stick model (carbon, purple; phosphorous, orange; nitrogen, light blue; oxygen, red). The backbone of PP4397 is shown as a ribbon diagram (green) with atoms of relevant residues of the binding pocket shown as a ball and stick model (carbon, white; nitrogen, blue; oxygen, red). The conserved residues RxxxR (R123 and R127), DxSxxG (D157, S159, G162), and the Position-X residue (R122) are shown as indicated. Hydrogen bonds are indicated by orange or blue lines. (From Ko *et al.*, 2010 (58))

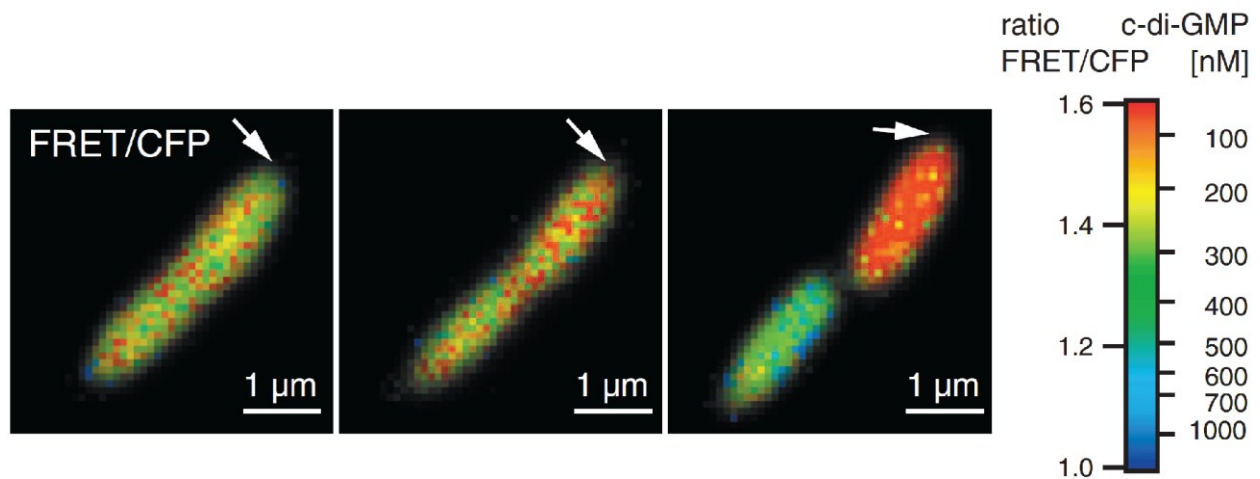


Figure 1.4: A genetically-encoded c-di-GMP biosensor based on the PilZ domain protein YcgR measures c-di-GMP in live cells. Shown are cells of *P. aeruginosa* expressing pYcgR-Spy in which the FRET/CFP ratios have been pseudocolored to reflect the values shown in the figure legend. The FRET/CFP ratio can be specifically correlated to a particular c-di-GMP concentration based on the affinity of YcgR for c-di-GMP. (From Christen *et al.*, 2010 (23))

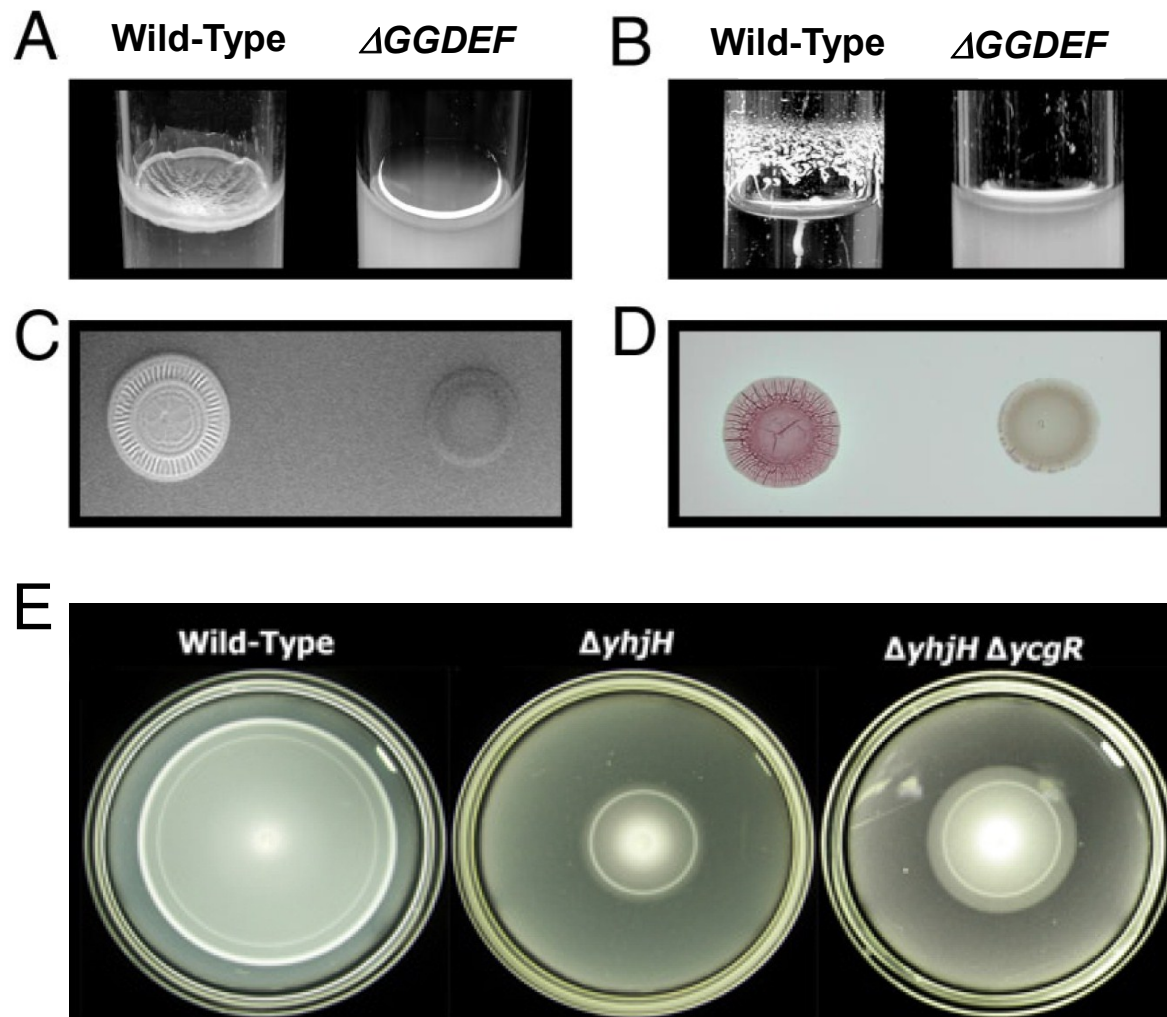


Figure 1.5: c-di-GMP controls motility and rdar morphotype formation in *S. Typhimurium* and *E. coli*. (A-D) Comparison of extracellular matrix production between wild-type *S. Typhimurium* and a strain lacking all twelve genes that encode GGDEF domain proteins. (A, B) Formation of a pellicle in the air-liquid interface of LB (A) or ATM (B) is dependent on c-di-GMP. (C) c-di-GMP stimulates cellulose production, which results in the fluorescence of colonies on agar plates containing calcofluor. (D) Formation of the rdar morphotype on Congo Red agar plates is dependent on c-di-GMP. (E) The ability of *E. coli* to swim through low-agar motility plates is inhibited by a deletion in *yhjH*. This inhibition is partially relieved by a second mutation in *ycgR*. ((A-D) Modified from Solano *et al.*, 2009 (116); (E) Modified from Paul *et al.*, 2010 (89))

CHAPTER 2: MATERIALS AND METHODS

Bacterial Strains

The bacterial strains used in this work are listed in Table 2.1.

Wild-type strains and backgrounds

All *Salmonella* strains used in this work were *S. enterica* serovar Typhimurium ATCC 14028s (53), with the exception of the *ara::DGC* strain used to generate Figures 4.1 and 4.6, which was generated on a *S. Typhimurium* LT2 background (73). *S. Typhimurium* LT2 is over 98% genetically identical to 14028s, and does not contain any differences in genes encoding GGDEF, EAL, and PilZ domain proteins. For cloning purposes, *E. coli* DH5 α or DH10 β cells (Invitrogen) were used. Purified protein was produced in *E. coli* BL21(DE3) (Invitrogen) cells.

Chromosomal mutations

Chromosomal insertions, deletions, and site-directed mutations were generated using the method described by Datsenko and Wanner (25). Antibiotic resistance markers inserted into the genome for the purpose of generating chromosomal mutations were transferred to a genetically unmanipulated strain by P22 transduction, to ensure that the phenotype was due to the intended mutation. Chromosomal deletion mutants were constructed by the substitution of genetic

antibiotic resistance cassettes encoding kanamycin, chloramphenicol, or tetracycline resistance, in such a way that deletion did not affect surrounding genes. To insert *PA1120* or *PA2133* into the arabinose locus, a genetic cassette encoding resistance to tetracycline was first inserted into the chromosome replacing the *araBAD* genes. Then, primers were used to amplify *PA1120* and *PA2133* (62) from *P. aeruginosa* PAO1 genomic DNA. These primers contained homology to the genomic regions immediately flanking the tetracycline resistance cassette such that, upon transformation of the PCR product, *PA1120* or *PA2133* replaced the tetracycline resistance cassette. Strains containing the *PA1120* or *PA2133* genes under the control of the arabinose-inducible promoter were then selected by their growth on agar plates containing chlortetracycline, which selects for tetracycline sensitivity (11). *S. Typhimurium* 14028s expressing FLAG-tagged BcsA protein was generated by chromosomal insertion, using the tetracycline selection described above, of a nucleotide sequence encoding the FLAG tag (DYKDDDDK) just before the STOP codon on the 3' end of the *bcsA* gene. *ycgR R113A* and *bcsA V695R* chromosomal mutants were generated by first inserting a tetracycline antibiotic resistance cassette into the site of the desired mutation. Tetracycline-resistant strains were then transformed with oligonucleotides that encoded the single point mutation into cells flanked by 30 nt on either side of the mutation with DNA that was homologous to the DNA flanking the tetracycline resistance cassette. Mutants containing the mutation in place of the tetracycline resistance cassette were then selected using the tetracycline selection method described above. All gene manipulations were designed using the software program Geneious Pro™, and were verified by PCR amplification of the mutated region and sequencing.

Plasmids

The plasmids used in this work are listed in Table 2.2. All plasmids were designed using the software program Geneious Pro™, and were verified by sequencing.

DGC and YcgR expression plasmids

The plasmids used for expression of proteins inside of live strains of *S. Typhimurium* in this work were generated in a pMMB67EH background encoding ampicillin resistance (34). To make pDGC, *PA1120* from *P. aeruginosa* PAO1 (62) was inserted into pMMB67EH under the control of the *tac* promoter, and the pET15B ribosome binding site (ACTTTAAGAAGGAGATATCAT) was inserted immediately upstream of the *PA1120* start codon. To make pDGC-YcgR, *ycgR* and its corresponding putative promoter region (118 bp upstream of the *ycgR* start codon) were cloned downstream of *PA1120* in pDGC. To prevent read-through of the *ycgR* gene when *PA1120* transcription was induced with IPTG, the transcriptional terminator from phage T4 gene 32 was inserted between the end of *PA1120* and the beginning of the YcgR promoter region (31). The YcgR R113A mutation was generated in this plasmid background using the QuikChange XL™ kit (Agilent) with primers containing the mutation.

FRET-based biosensor plasmids for protein purification

Plasmids encoding PilZ-based FRET constructs for the determination of c-di-GMP binding affinities of PilZ domain proteins were generated in a pET15B plasmid background

containing the N-terminal 6xHis-tagged *yfp-cfp* FRET fusion pair under the control of a *tac* promoter as previously described (23). PilZ domain proteins were cloned into the SpeI and Acc651 sites between the *yfp* and *cfp* genes to generate plasmids that would result in the production of His-tagged, FRET fusion proteins when their expression was induced with IPTG. BcsA from *S. Typhimurium* and Alg44 from *P. aeruginosa* are membrane proteins, so the regions of the genes encoding the PilZ domains of these proteins were cloned into the FRET construct (residues 691-791 for BcsA and 299-389 for Alg44). A truncated version of PA3353 was generated lacking the residues corresponding to the first alpha helix (bases 1-63), since the full-length PA3353 protein did not demonstrate a change in FRET between the bound and unbound states that was large enough to accurately measure binding affinity. The BcsA V695R, YcgR R113A, and YcgR S147A point mutations were made on the corresponding pET15B fusion construct backgrounds using the QuikChange XL™ kit (Agilent) with primers containing the mutation.

FRET-based biosensor plasmids for expression in vivo

pYcgR-Spy, encoding gentamicin resistance and the YcgR FRET-based biosensor, was obtained from Christen *et al* (23). This plasmid contains the gene *mYPet_synthYcgR_mCYPet* under the control of an IPTG-inducible promoter. In this plasmid, the *ycgR* gene, which had been codon-optimized to remove rare codons during expression in *S. Typhimurium*, was cloned between the *mYPet* and *mCYPet* genes in SpeI and ACC651 sites, resulting in mYPet-YcgR-mCYPet fusion protein expression in the presence of IPTG. pYcgRR113A-Spy was generated in

a pYcgR-Spy background by site-directed mutagenesis using the QuikChange® XL II kit (Agilent). pBcsA-Spy was constructed by digesting pET15B-BcsAPilZSpy with the restriction enzymes SpeI and ACC651 (FastDigest®, Fermentas) and ligating the released *bcsA* PilZ region into pYcgR-Spy (Rapid DNA Ligation Kit, Fermentas) that had also been digested with SpeI and ACC651.

Growth conditions

Unless otherwise stated, cells were grown in Luria Broth at 37C with shaking, in the presence of antibiotics, arabinose, IPTG, and/or calcofluor (Fluorescence Brightener 28, Spectrum Chemical MFG) when appropriate. Antibiotic concentrations were: ampicillin, 100 $\mu\text{g ml}^{-1}$; carbenicillin, 100 $\mu\text{g ml}^{-1}$; chloramphenicol, 20 $\mu\text{g ml}^{-1}$; gentamicin, 15 $\mu\text{g ml}^{-1}$; kanamycin, 45 $\mu\text{g ml}^{-1}$; tetracycline, 10 $\mu\text{g ml}^{-1}$.

Protein purification

pET15B plasmids encoding His-tagged PilZ FRET fusion proteins were transformed into *E. coli* BL21(DE3) cells. mYPet - PilZ protein - mCyPet fusion proteins were expressed in BL21(DE3) cells and underwent purification through Ni-NTA resin as previously described (23). For the affinity measurements shown in Figure 4.4 and Figure 5.1, YcgR and BcsA PilZ FRET constructs, and their associated mutants, were further purified by size exclusion chromatography using a Superdex™ 200 10/300 GL column (GE Healthcare). To generate a His-tagged BcsA

PilZ domain lacking fluorophores, this gene was constructed in pET15B without encoding flanking fluorophores. The His-tagged BcsA protein was expressed in BL21(DE3) cells and purified through Ni-NTA resin as described (23). This protein then underwent purification by anion exchange chromatography using a Mono Q™ 5/50 GL column (GE Healthcare) followed by size exclusion chromatography.

Protein identification using mass spectrometry

In order to identify the protein that co-purified with the *S. Typhimurium* His-tagged BcsA PilZ domain when it was expressed in *E. coli*, protein fractions from the size exclusion purification step were separated on a SDS-PAGE gel, stained with Coomassie Brilliant Blue (Thermo Fisher Scientific), and then destained using a solution of 10% acetic acid and 10% methanol. A 30 kDa band was excised from the gel, and this gel slice was dehydrated by incubation at room temperature in alternating 100 mM ammonium bicarbonate and 100% acetonitrile solutions. Proteins were digested in the gel on ice for 45 min with 20 $\mu\text{g ml}^{-1}$ trypsin (Promega) in the presence of 50 mM ammonium bicarbonate. Digested proteins were then extracted from the gel using a solution of 5% acetonitrile with 0.1% trifluoroacetic acid, followed by extraction using 50% acetonitrile with 0.1% trifluoroacetic acid. The solution containing digested proteins was then centrifuged in an Eppendorf Vacufuge® plus to evaporate liquid until only about 10 μL of liquid remained in the tube. Protein fragments were then identified using a LTQ Velos Dual-Pressure Linear Ion Trap Mass Spectrometer (Thermo Scientific). As a control, the band corresponding to the approximate length of the BcsA PilZ

domain protein (about 15 kDa) was also excised from the gel, processed, and submitted for identification. As expected, this protein was identified as the *S. Typhimurium* BcsA PilZ domain.

Fluorescence spectra and kinetic measurements

c-di-GMP was added to purified FRET fusion protein in 96-well black Greiner plates, and the amount of FRET was quantified on an Envision multilabel plate reader (PerkinElmer). Fluorescence spectra were recorded using the quad monochromator (excitation at 425 nm, emission scan from 460 to 560 nm in 1 nm intervals) using 50-500 nM biosensor in PBS pH 7.4 with 10% glycerol, 200 mM NaCl, and 5 mM β -mercaptoethanol. Emission spectra were normalized to the total amount of fluorescence emission over the entire scan. Binding affinity was determined by adding increasing concentrations of c-di-GMP and measuring the resulting FRET/CFP ratio using a filter-based measurement method (CFP excitation filter CWL 430 nm, BW 24 nm; CFP emission filter CWL 485 nm, BW 14 nm; YFP emission filter CWL 535 nm, BW 30 nm, dual dichroic mirror D450/D505 nm) to determine FRET ratios at 24°C to 37°C in 1°C intervals. In the filter-based method, the fraction of FRET biosensor bound to c-di-GMP was calculated for each biosensor by measuring the FRET/CFP ratio at each indicated c-di-GMP concentration, subtracting the unbound FRET/CFP ratio, and dividing this number by the difference between the bound and unbound FRET/CFP ratios. A number of 0 indicates that the FRET biosensor is completely unbound to c-di-GMP, and a number of 1 indicates that the FRET biosensor is completely bound to c-di-GMP. Binding affinities and Hill coefficients were

calculated by fitting a curve to the plot of FRET ratio versus c-di-GMP concentration in either Quantum Soft pro Fit™ or GraphPad Prism™.

Analysis of BcsA protein expression

To compare BcsA protein expression between strains growing at different temperatures, cells of a *S. Typhimurium* strain harboring FLAG-tagged BcsA protein were scraped off of LB plates that had been incubated at either 37°C for 24 hours, or at 24°C (room temperature) for 48-72 hours, into pre-weighed Eppendorf tubes, immediately frozen at -80°C for at least 15 minutes, then resuspended in PBS pH 7.4 at a concentration of 0.2 µg cell wet weight µl⁻¹ with chloramphenicol (20 µg ml⁻¹) to inhibit any protein translation that might occur before and during the sonication process. To verify that the observed FLAG-tagged band represented FLAG-tagged BcsA protein, cells expressing the native untagged BcsA protein grown at 24°C were also included in this analysis. Cells were disrupted by sonication, centrifuged for 10 min at 4°C at full speed in a tabletop Eppendorf centrifuge, and the supernatant containing soluble protein was discarded. The pellet was resuspended in PBS with 1% lauryldimethylamine-oxide to solubilize membrane proteins. The mixture was centrifuged again to remove whole cells. The supernatant, containing membrane proteins, was obtained, and protein content was quantified using a Bradford assay. 5 mg of total protein was run on an SDS-PAGE gel (6% acrylamide), transferred to nitrocellulose membranes, and blocked using PBST containing 0.5% milk. Blots were incubated with a primary antibody (polyclonal anti-FLAG 1:500, Immunology Consultants

Laboratory), washed, incubated with a secondary antibody (1:5000, donkey anti-rabbit conjugated to HRP, GE Healthcare), and developed using X-ray film.

Analysis of cellulose production

Visualization of cellulose production on LB plates

Cellulose production is determined by its binding to the fluorescent dye calcofluor, which fluoresces when it is bound to cellulose. The calcofluor plates used in this work were LB-agar plates containing $50 \mu\text{g ml}^{-1}$ calcofluor (Fluorescence Brightener 28, Spectrum Chemical MFG). Strains were streaked on calcofluor plates and incubated overnight (37°C) or for 2-3 days ($24\text{-}30^{\circ}\text{C}$). Plates were analyzed by illumination using a UVP Bioimaging System© with an excitation wavelength of 365 nm unless otherwise specified, equipped with a digital camera for capturing images.

Quantitative cellulose measurements

For the quantitative cellulose production measurements shown in Figure 4.6, *S. Typhimurium* *ara::DGC*, *ara::DGC bcsA-V695R*, or the *ara::DGC ΔbcsA* mutant were incubated overnight at 37°C . The next day, cells were diluted to an OD_{600} of 0.02, incubated at 37°C with shaking until the OD_{600} reached 3.3, then diluted again to an OD_{600} of 0.0625. 8 μl of

each strain were spotted using a multichannel pipettor into each well of a Greiner 96-well black plate with 200 μl of calcofluor ($3 \mu\text{g ml}^{-1}$) and the indicated amount of arabinose. After incubation at 37°C for 20 hours (a condition at which *Salmonella* does not normally make cellulose), the intensity of calcofluor fluorescence was then quantified by reading the fluorescence values in an ENVISION multilabel plate reader (PerkinElmer). The data was analyzed using a Student's two-tailed T test.

Measurement of cellulose production in swimming agar plates

For determination of cellulose production in swimming agar plates, *S. Typhimurium* strains $\Delta yhjH$, $\Delta yhjH \Delta bcsA$, pDGC, and pDGC $\Delta bcsA$ were inoculated as described below in the “soft-agar motility plate assays” section onto 0.3% agar swimming plates containing $50 \text{ ng } \mu\text{L}^{-1}$ calcofluor. To induce production of the DGC PA1120, IPTG had been added to the plate at a concentration of $100 \mu\text{M}$. Plates were incubated at 37°C for 12 hours, then scanned using an Epson® Perfection 4990 scanner and imaged using a UVP Bioimaging System© with the excitation wavelength at 254 nm.

Cell lysate assay for production of cellulose

To determine whether cells of *S. Typhimurium* contained all of the components required for the production of cellulose when grown at 37°C , an experiment analyzing cellulose production by cell lysates of strains grown at 37°C was performed. Strains were inoculated into

1 liter of LB and shaken at 37°C overnight. The next morning, chloramphenicol was added (20 $\mu\text{g ml}^{-1}$) to stop any new protein translation, and cells were allowed to incubate for another hour. Cells were then rapidly cooled in a dry ice/ethanol bath, pelleted at 4420*g for 15 min at 4°C, and stored at -80°C for at least 15 minutes. Pellets were resuspended in 25 ml of 70 mM Tris pH 7.7 with 50 mM NaCl, 10 mM MgCl₂, 5 mM CaCl₂, 1 mM EDTA, 5 mM β -mercaptoethanol, protease inhibitors, 20 $\mu\text{g ml}^{-1}$ chloramphenicol to prevent protein translation, and 1 $\mu\text{g ml}^{-1}$ lysozyme to degrade the bacterial cell wall. After 30 minutes of incubation on ice, cells were lysed in an Avestin™ EmulsiFlex-C3, and cell lysate was centrifuged 4 times for 15 min at 4°C at 4500*g to remove whole unlysed cells. At this point, 100 μl of lysate was plated onto LB-agar plates to verify that all live cells had been removed. Lysate was then incubated in a solution containing 5% glycerol, 100 μM GTP, 20 mM MgCl₂, 1 mM UDP-glucose, and 50 $\mu\text{g ml}^{-1}$ calcofluor, with or without 6 $\mu\text{g ml}^{-1}$ purified DgcA of *Caulobacter crescentus*, at 37°C for 15 min. 12 replicates of 100 μl each were performed for each strain. After incubation, samples were centrifuged at max speed in a tabletop Eppendorf centrifuge, washed twice in Tris buffer (composition above), resuspended in 100 μl Tris buffer, and transferred to a Greiner 96-well black plate. Calcofluor fluorescence was measured on an Envision multilabel reader (PerkinElmer) by excitation at 365 nm and emission at 420 nm. The data was analyzed using a Student's two-tailed T test.

Soft-agar motility plate assays

Strains were inoculated as overnight cultures in LB at 37°C with shaking. The following morning, strains were diluted to OD₆₀₀ of 0.1. 1.5 μl were then spotted onto 0.3-0.35% agar LB

plates. Plates were incubated at 37°C for 9-13 hours, then scanned using an Epson® Perfection 4990 scanner and imported as TIFF files. The diameter of swimming of each strain was measured by using the magic wand tool in Adobe™ Photoshop™ CS5.

Measurement of *in vivo* FRET/CFP ratios in individual cells

Growth conditions for in vivo biosensor expression – characterization of biosensors (Chapter 5)

To characterize all biosensors for use as *in vivo* c-di-GMP measurement tools, all strains containing biosensor plasmids were grown at 30°C to prevent homologous recombination between the *mYPet* and *mCYPet* genes. To determine FRET/CFP ratios in *ara::DGC* or *ara::PDE* strains expressing biosensors, strains were inoculated into one ml LB with 15 µg ml⁻¹ gentamicin and 75 µM IPTG, and incubated overnight at 30°C with shaking. The next day, strains were diluted to an OD₆₀₀ of 0.04 in 1 ml modified M63 media (1.1 mM KH₂PO₄, 2 mM K₂HPO₄, 750 µM (NH₄)₂SO₄, 100 mM glycerol, 5 µM Fe²⁺NH₄SO₄, 2 mM MgCl₂, 10 mM NaCl, 15 µg ml⁻¹ gentamicin, 500 µM IPTG, 1.3 mM arabinose). M63 media was used in these experiments since LB media demonstrates autofluorescence at the wavelengths used for imaging. Strains were then incubated for 5 hours and 25 minutes at 30°C with shaking. At this point, cells were prepared for fluorescence microscopy.

Growth conditions for in vivo biosensor expression – determination of c-di-GMP concentrations in wild-type vs. ΔyhjH mutant strains (Chapter 4)

To determine FRET/CFP ratios in *S. Typhimurium* 14028s and an isogenic *yhjH* mutant, cells were inoculated into one ml LB with 15 $\mu\text{g ml}^{-1}$ gentamicin and 75 μM IPTG, and incubated at 30°C overnight with shaking. The next day, cells were diluted into 25 ml fresh LB with 15 $\mu\text{g ml}^{-1}$ gentamicin and 500 μM IPTG at an OD_{600} of 0.02. Cells were incubated at 37°C for approximately 2 hours until the OD_{600} reached 0.2. At this point, cells were prepared for fluorescence microscopy.

Sample preparation for fluorescence microscopy

To prepare samples for fluorescence microscopy, cells were centrifuged, washed in M63 media (for strains that had previously been growing in LB), and resuspended in M63 media to an OD of 2.0. 1.5 μl of resuspended cells were then spotted onto 0.75 mm thick agar pads (modified M63 media with 1% agarose) on prewarmed, prewashed 1 mm microscope slides (Thermo Fisher Scientific) and allowed to dry. A prewarmed number 1.5 glass coverslip (Corning Life Sciences) was applied to the agar pads, and the coverslip was sealed to the slide using a glue gun to prevent liquid evaporation.

Image acquisition

Fluorescence microscopy images were acquired using a Nikon Eclipse TIE inverted, wide-field microscope using the same hardware and software as previously published (23). For each experiment, the microscope chamber was prewarmed to the appropriate temperature.

Exposure times for the determination of intensities in the FRET, CFP, and YFP channels were 1000, 1300, and 200 ms, respectively, with a conversion gain of 2x and 2x2 binning.

Image processing

For each image, all channels were exported in a TIFF file format by Nikon Elements analytical software. For each TIFF file, the background intensity was subtracted, and the subpixel shifts were corrected by registering to the CFP channel image using ImageJ version 1.44. Processed images were imported into Nikon NIS Elements software, and regions of interest representing individual cells were selected. The average intensity values for each region of interest were then exported to Microsoft® Excel software. Regions of aggregated FRET protein, represented by localized, unphysiologically high intensity values in either the CFP or YFP channels near one pole of the cell were deselected when observed and were not counted in the analysis. Cells demonstrating an average FRET intensity value of less than three times higher than background were not included in the analysis, unless a clear distinction could be determined between control strains at this intensity value. Net FRET (nFRET) was calculated by subtracting spectral bleedthrough and direct YFP excitation from the FRET intensity value (23, 145). To control for brightness, nFRET was normalized to the intensity of the CFP channel (133). The limit of detection of this technique is 1-2 molecules per pixel, which is hundreds of molecules per individual bacterial cell.

Determination of FRET/CFP ratios of purified biosensors loaded onto Ni-NTA silica beads

Ni-NTA Superflow silica resin was obtained from Qiagen. Purified biosensor was mixed at the concentration of 12.5 nM (for YcgR and YcgR R113A biosensors) or 50 nM (for BcsA PilZ biosensor) with a 1:75 dilution of the Ni-NTA resin and the indicated concentration of c-di-GMP in PBS pH 7.5 with 200 mM NaCl and 5 mM β -mercaptoethanol at 30°C. 100 μ l was transferred to a chamber of an eight-chambered slide (Lab-Tek™, Thermo Fisher Scientific). Biosensor-loaded beads were then imaged using the above protocol, with differences in exposure times for the FRET, CFP, and YFP channels: these were 600, 600, and 100 ms, respectively, with 1x1 binning.

Mouse virulence assays

Healthy adult BALB/cJ mice (Charles River Laboratories) were administered 10 or 100 cells intraperitoneally with *S. Typhimurium* 14028s wild-type, $\Delta bcsA$, $\Delta ycgR$, or $\Delta bcsA \Delta ycgR$ mutants diluted in 100 μ l of PBS. The number of cells in inocula was verified by dilutional plating and found to vary by no more than 25%. The health of infected mice was then monitored over the course of 4-5 days. All procedures were in compliance with the regulations of the Institutional Animal Care and Use Committee of the University of Washington.

Tables

Table 2.1. Description of the strains used in this study.

Strain	Description	Ancestor, Comments, References
<i>E. coli</i>		
<i>E. coli</i> DH5a	Cloning strain	Invitrogen
<i>E. coli</i> DH10b	Cloning strain	Invitrogen
<i>E. coli</i> BL21(DE3)	Strain for protein purification	Invitrogen
<i>S. Typhimurium</i>		
<i>S. Typhimurium</i> 14028s	Wild-type strain, virulent, ATCC14028	Jarvik <i>et al</i> , 2012
<i>S. Typhimurium</i> LT2	Wild-type strain, avirulent, ATCC700720	McClelland <i>et al</i> , 2001
<i>ara::DGC</i>	($\Delta araBAD$)::PA1120	14028s or LT2
<i>ara::PDE</i>	($\Delta araBAD$)::PA2133	14028s
$\Delta yhjH$	$\Delta yhjH$::kan	14028s
$\Delta yhjH \Delta ycgR$	$\Delta yhjH$::kan $\Delta ycgR$::cam	14028s
$\Delta yhjH ycgR$ -R113A	$\Delta yhjH$::kan $ycgR$::R113A	14028s
$\Delta yhjH \Delta bcsA$	$\Delta yhjH$::kan $\Delta bcsA$::tet	14028s
$\Delta adrA$	$\Delta adrA$::kan	14028s
$\Delta ycgR$	$\Delta ycgR$::cam	14028s
$\Delta bcsA$	$\Delta bcsA$::tet	14028s
$\Delta ycgR \Delta bcsA$	$\Delta ycgR$::kan $\Delta bcsA$::tet	14028s
<i>bcsA</i> -FLAG	<i>bcsA</i> ::FLAG	14028s
<i>ara::DGC bcsA</i> -V695R	($\Delta araBAD$)::PA1120 <i>bcsA</i> ::V695R	LT2
<i>ara::DGC \Delta bcsA</i>	($\Delta araBAD$)::PA1120 $\Delta bcsA$::tet	LT2

Table 2.2. Description of the plasmids used in this study.

Plasmid	Description	Source or Reference
pET15B	Protein expression vector. Ampicillin resistance.	
pET15B-YcgRSpy	pET15B::mYPet_synthYcgR_mCYPet	Christen <i>et al</i> , 2010
pET15B-YcgRR113ASpy	pET15B::mYPet_synthYcgRR113A_mCYPet	This work
pET15B-YcgRS147ASpy	pET15B::mYPet_synthYcgRS147A_mCYPet	This work
pET15B-BcsAPilZSpy	pET15B::mYPet_BcsAPilZ_mCYPet	This work
pET15B-PA2960Spy	pET15B::mYPet_PA2960_mCYPet	This work
pET15B-PA3353Spy	pET15B::mYPet_PA3353_mCYPet	This work
pET15B-Alg44PilZSpy	pET15B::mYPet_Al44PilZ_mCYPet	This work
pET15B-PA4324Spy	pET15B::mYPet_PA4324_mCYPet	This work
pMMB67EH	Broad-host expression vector. Gentamicin resistance.	Furste <i>et al</i> , 1986
pYcgR-Spy	pMMB67EH::mYPet_synthYcgR_mCYPet	Christen <i>et al</i> , 2010
pYcgRR113A-Spy	pMMB67EH::mYPet_synthYcgRR113A_mCYPet	This work
pBcsA-Spy	pMMB67EH::mYPet_bcsAPilZ_mCYPet	This work
pDGC	pMMB67EH::PA1120	This work
pDGC-YcgR	pMMB67EH::PA1120_T4 32 trans term_pycgR_ycgR	This work
pDGC-YcgR R113A	pMMB67EH::PA1120_T4 32 trans term_pycgR_ycgR R113A	This work

CHAPTER 3: THE BINDING AFFINITIES OF PILZ DOMAIN PROTEINS SPAN A LARGE RANGE OF C-DI-GMP CONCENTRATIONS

Summary

In many different organisms, c-di-GMP signaling involves complex networks composed of DGCs, PDEs, and c-di-GMP downstream receptors. One major question remaining in the field of c-di-GMP signaling is how specificity is achieved between c-di-GMP-metabolizing enzymes and the downstream processes that they control, when all of these enzymes signal through the same second messenger. Here, we use a FRET-based method to measure the affinities of c-di-GMP-specific receptors, PilZ domain proteins, and demonstrate large ranges of c-di-GMP-binding affinities for these proteins in two different organisms: *S. Typhimurium* and *P. aeruginosa*. We show that the PilZ domain proteins of *S. Typhimurium*, YcgR and BcsA, demonstrated a 43-fold difference in their affinities for c-di-GMP. The eight PilZ domain proteins of *P. aeruginosa* demonstrated a 145-fold difference in binding affinities, spanning from the nanomolar to the micromolar range. Differences in binding affinities of c-di-GMP receptors in these organisms define ranges of intracellular c-di-GMP concentrations in which some receptors, but not others, would be bound to c-di-GMP within the cell. These data, combined with measurements of binding affinities of c-di-GMP receptors from other organisms, suggest that regulation of c-di-GMP signaling by binding affinity may be a conserved mechanism that allows organisms with many c-di-GMP-binding macromolecules to integrate multiple environmental signals into one specific output.

Introduction

c-di-GMP is an intracellular second messenger that regulates motility and exopolysaccharide production in bacteria. Although many bacterial species encode dozens of GGDEF and EAL domain proteins that all metabolize the same second messenger, many of these enzymes have been specifically implicated in certain downstream processes. These observations have led to the conclusion that c-di-GMP signaling may be functionally compartmentalized (45, 92, 138). There are several potential mechanisms for how this compartmentalization could occur. One of these mechanisms involves temporal regulation of c-di-GMP components. In this mechanism, c-di-GMP metabolizing enzymes would be expressed under the same conditions as their downstream receptors and targets. Indeed, some c-di-GMP components are known to be under the transcriptional control of various signals (92, 138); however, others appear to be constitutively expressed, so this mechanism does not adequately account for all observed signaling specificity (116). Another proposed model for signaling specificity involves the spatial sequestration of individual c-di-GMP components, such that generation and degradation of c-di-GMP would act locally on a particular target. Although there is some evidence to support local activity of c-di-GMP metabolizing enzymes (72, 76), the rapid diffusion of c-di-GMP in the bacterial cytoplasm would make it difficult to establish such local pools inside of the bacterial cell (77) (Chapter 6). An alternative, though not mutually exclusive, mechanism by which c-di-GMP signaling specificity could be achieved is through the binding affinities of downstream

receptors (45, 58, 77), wherein downstream receptor affinity for c-di-GMP would determine which receptors are activated at particular c-di-GMP levels.

The hypothesis that regulation of downstream processes occurs at least in part through c-di-GMP receptor binding affinities is supported by the measured affinities of several PilZ domain proteins for c-di-GMP, which have been found to vary considerably. For example, the c-di-GMP binding affinity of DgrA, a PilZ domain protein from *Caulobacter crescentus*, was found to be high, with a K_d of less than 50 nM (21). Conversely, Alg44, a PilZ domain protein in *Pseudomonas aeruginosa* that is required for alginate production, was found to have a low binding affinity, with a K_d of approximately 8.4 μ M (75). It seems unlikely that these differences in binding affinities simply reflect differences in the natural concentrations of c-di-GMP between these organisms, since other, non-PilZ c-di-GMP-binding proteins identified in these organisms also demonstrate very different affinities for c-di-GMP: PopA from *C. crescentus* (2.4 μ M) (28), and FimX, PelD, and FleQ from *P. aeruginosa* (125 nM, 1 μ M, and 15-25 μ M, respectively) (46, 68, 80). This disparity in the affinities of c-di-GMP receptors suggests that the concentrations of c-di-GMP required for receptor activation span a large range even within the same organism.

In this work, we used the same measurement method to measure and compare the binding affinities of all PilZ domain proteins in two organisms: *Salmonella* Typhimurium, which harbors two PilZ domain proteins, and *P. aeruginosa*, which contains eight. We found that the affinities of these proteins varied considerably: the PilZ domain proteins of *S. Typhimurium* differed by 43-fold in their affinities for c-di-GMP, and PilZ domain proteins of *P. aeruginosa* differed by 145-fold. These data provide support to the hypothesis that signaling specificity can occur by the

affinities of downstream receptors, since they indicate that there exist discrete levels of c-di-GMP that would activate some of these c-di-GMP receptors, but not others.

A FRET-based method to measure PilZ domain protein binding affinities for c-di-GMP

In order to measure binding affinities of PilZ domain proteins, we constructed FRET-based biosensors by fusing these proteins to fluorophores that constitute a FRET pair (Figure 3.1). Intramolecular FRET is a very sensitive method for detecting changes in protein conformation (52, 106). FRET technology depends on the use of a donor and acceptor fluorophore, in which the donor emission wavelength overlaps with the acceptor excitation wavelength. In this study, we made use of the two fluorophores mYPet and mCyPet, which are YFP and CFP derivatives, respectively, that have been optimized for use as a FRET pair (81). In the absence of c-di-GMP, upon excitation with the mCyPet fluorophore wavelength, FRET biosensors based on PilZ domain proteins will demonstrate a characteristic FRET profile that is dependent on the relative distance and/or orientation of the two fluorophores with respect to each other (Figure 3.2). Upon binding to c-di-GMP, the PilZ domain protein experiences a conformational change, which results in a change in the FRET output emission spectrum (Figure 3.2). This method has been previously utilized to measure the affinity of YcgR for c-di-GMP in a mYPet-YcgR-mCyPet fusion protein (23), and to measure affinities of other, non-PilZ domain proteins for other second messengers (51, 78, 83, 87, 107).

The binding affinities of *S. Typhimurium* PilZ domain proteins differ by 43-fold

S. Typhimurium harbors two PilZ domain proteins: YcgR and BcsA. We used the FRET-based method to generate a c-di-GMP biosensor using the BcsA PilZ domain in order to compare its c-di-GMP binding properties to those of YcgR. The BcsA protein is predicted to include nine transmembrane helices, a glycosyltransferase domain, and a cytoplasmic PilZ domain located immediately on the carboxyl-terminal side of a transmembrane helix (InterPro - <http://www.ebi.ac.uk/interpro/>). Making a FRET fusion using the entire BcsA protein would not have been possible due to the transmembrane domains of BcsA, so we used the cytoplasmic PilZ domain as the c-di-GMP-detecting sensor. Both YcgR- and BcsA PilZ domain -based c-di-GMP biosensors were purified from *E. coli* BL21(DE3) cells, and their FRET emission spectrum profiles were analyzed in the presence or absence of 40 μ M c-di-GMP using a fluorescence plate reader. For both the YcgR and BcsA PilZ FRET constructs, the presence of c-di-GMP results in a corresponding decrease in FRET of PilZ-FRET fusion proteins (Figure 3.2), suggesting that binding results in an increase in the distance between the amino- and carboxyl-termini in the protein tertiary structure, or a change in their dipole-dipole orientation. The c-di-GMP bound state of the FRET fusion protein can be distinguished from the unbound state by comparing the ratio of YFP (535 nm) to CFP emission (480 nm) (Figure 3.2).

We used this construct to explore the c-di-GMP binding kinetics of the BcsA PilZ domain. The c-di-GMP binding affinities for both PilZ domain protein-based c-di-GMP biosensors were measured by determining their FRET profile in the presence of increasing concentrations of c-di-GMP. This yielded a concentration-responsive curve of the FRET-based proteins for c-di-GMP (Figure 3.3 and data not shown for the YcgR FRET protein). The Hill coefficient was approximately two for the BcsA PilZ domain, similar to Hill coefficients

measured for other PilZ domains (58, 97), suggesting binding to two molecules of c-di-GMP and indicating positive cooperativity in c-di-GMP binding (Table 3.2). Unexpectedly, we observed a Hill coefficient closer to 1.5 for the YcgR FRET-based biosensor at 25°C, compared to the Hill coefficient previously published of 2 for this protein (23); however, as temperature increased, the Hill coefficient approximated 2 for this protein (Table 3.2). We were able to measure the equilibrium binding constant K_d by fitting a line to the concentration-responsive curve. The affinities for c-di-GMP binding were 191 ± 18 nM for YcgR (similar to the value of 195 nM previously published for this FRET-based biosensor (23)) and 8240 ± 238 nM for BcsA at 25°C (Table 3.1). This represents an approximately 43-fold difference in affinity for c-di-GMP between these two proteins. Additionally, the c-di-GMP binding affinity of each PilZ domain protein measured was highly dependent on temperature, since the affinity dropped by approximately 15% for every increase in °C (Figure 3.3, 3.5 and data not shown). This indicates that the binding is entropically unfavorable, as was also determined for the binding of the *Vibrio cholerae* PilZ domain protein VCA0042 to c-di-GMP (6). The disparity in binding affinities between YcgR and BcsA was maintained at every temperature measured (Table 3.2). Comparing the binding curves of these two proteins suggests that there exists a range of intracellular c-di-GMP concentrations that would stimulate binding to YcgR but would not be high enough to stimulate binding to BcsA (Figure 3.4), and implies that their specific binding affinities for c-di-GMP may thus be important for their biological functions (Chapter 4).

The binding affinities of PilZ domain proteins of *P. aeruginosa* differ by 145-fold

Next we compared the binding affinities of the eight PilZ domain proteins of *P. aeruginosa* using the same sensitive FRET-based method (2). This method has previously been used to measure the affinities of four *P. aeruginosa* PilZ domain proteins by our research group (Table 3.1) (23). We generated FRET-based c-di-GMP biosensors for the remaining PilZ domain proteins and measured their affinities for c-di-GMP. Alg44 is a membrane protein, and so the PilZ domain alone of this protein was used in the FRET-based biosensor. We found that PA2960, the protein from which PilZ proteins derived their name, did not appear to bind c-di-GMP, as no FRET shift was observed. This is not surprising since PA2960 has been shown to not bind c-di-GMP in another study (75), likely because it lacks the RxxxR motif required for binding c-di-GMP (2, 21, 108). Interestingly, the binding curve for PA3353 suggested two binding sites that differed by about eight-fold, one at an approximate c-di-GMP concentration of 88 nM and one at 732 nM (Figure 3.5, Table 3.1). Further work is needed to determine the structural basis of c-di-GMP binding at two sites in this protein.

As in *S. Typhimurium*, the c-di-GMP-binding affinities of *P. aeruginosa* PilZ domain proteins spanned a sizable range of c-di-GMP concentrations. The highest and lowest affinities of *P. aeruginosa* PilZ domain proteins for c-di-GMP measured in this work differed by 145-fold (Table 3.1). The Hill coefficient approximated two for every *P. aeruginosa* PilZ domain protein measured, and all measured binding affinities decreased as temperatures increased (Figure 3.5 and data not shown). Other published binding affinities of three other non-PilZ c-di-GMP-receptors in *P. aeruginosa* fit into this concentration range (Table 3.1), although it should be noted that the binding affinities of these proteins were not measured at 25°C. Together these binding affinities represent at least a 250-fold difference in concentration of c-di-GMP required to activate c-di-GMP receptors in *P. aeruginosa*.

Discussion

In this study, the binding affinities of PilZ domain proteins from *S. Typhimurium* and *P. aeruginosa* were measured using the same FRET-based method and were found to vary considerably. For *S. Typhimurium*, affinities differed by 43-fold, and for *P. aeruginosa*, they differed by 145-fold. This implies that physiological c-di-GMP levels can vary in these bacteria from the low nanomolar range up to the micromolar range. This disparity in affinities of c-di-GMP receptors has also been shown to exist in other bacteria. c-di-GMP-binding molecules from *Caulobacter crescentus* and *Vibrio cholerae* also exhibit large differences in binding affinities, implying that binding affinities may play an important role in c-di-GMP signaling in many different bacterial species (Table 3.1). This suggests that intracellular c-di-GMP concentrations can span a large range in these organisms, and that under certain conditions the cellular c-di-GMP level would be high enough to stimulate binding to one subset of c-di-GMP-binding proteins while not activating others.

It is interesting to note that the c-di-GMP-binding molecules shown or suspected to be involved in motility tend to have high binding affinities in the nanomolar range (DgrA, YcgR and its homologues VCA0042 and PA3353), and those with lower affinities in the micromolar range tend to be linked to EPS production (like FleQ, Alg44, BcsA, and VpsT) (Table 3.1). Possibly this is because it is always beneficial to inhibit swimming when EPS is produced, while there may be other situations in which it is advantageous to decrease swimming, or perform other c-di-GMP-controlled activities, without investing energy in an extracellular matrix. In addition, many DGCs are negatively feedback-inhibited via binding of c-di-GMP to an allosteric I-site, allowing them to maintain homeostasis of c-di-GMP concentrations (20). It is attractive to

speculate that DGC feedback inhibition may work synergistically with downstream receptor binding affinities, such that some DGCs would produce enough c-di-GMP to “communicate” with receptors with low c-di-GMP-binding affinity, while other DGCs with high affinity for c-di-GMP at the I-site would be limited to activating only receptors with a high affinity for c-di-GMP. Finally, the *P. aeruginosa* PilZ domain protein PA3353 demonstrated the presence of two binding sites in this study. PA3353 might thus act as a bandpass filter, active (or inactive) only within a narrow range of c-di-GMP levels.

To verify that the c-di-GMP-binding affinity of the FRET-based BcsA PilZ domain biosensor was not significantly altered by the presence of the fused fluorophores, a BcsA PilZ domain protein lacking these fluorophores was produced for the purpose of examination of binding affinity by isothermal titration calorimetry, an established method for measuring binding affinities of proteins for small molecules. However, this protein could not be separated from another protein of about 30 kDa during purification process, and thus ITC could not be performed on the BcsA PilZ domain as pure protein could not be obtained using this method. The FRET BcsA PilZ fusion construct did not demonstrate co-purification with this 30 kDa protein. The constituent proteins of this 30 kDa band were identified using a mass spectrometer. Approximately 20 proteins were identified to be associated with this band. One of these proteins, β -hexosaminidase from *E. coli*, was present in the sample at high coverage. This protein has a *S. Typhimurium* homologue that is very similar in sequence. Since this enzyme is involved in maintenance of the peptidoglycan layer, it is not clear what physiological relevance, if any, is represented by the co-purification of this protein with the BcsA PilZ domain in *E. coli*.

The binding affinities of PilZ domain proteins measured in this work using the FRET-based method is comparable to affinities for these proteins measured using other methods. The

S. Typhimurium protein YcgR demonstrated a binding affinity of 191 ± 18 nM in this assay. This is very similar to the affinity of this protein previously measured by crosslinking to radiolabeled c-di-GMP, of 182 ± 29 nM (21) (Table 3.1). PA3353 has also been measured by another group using surface plasmon resonance to be 262 ± 66 nM (Table 3.1), although this binding affinity was measured at 20°C (29). We have found that the binding affinity varies with temperature, and that for every °C increase in temperature, the binding affinity decreases by approximately 15% (Table 3.2). Therefore this measurement of 262 ± 66 nM at 20°C would be estimated to be approximately 530 ± 100 nM at 25°C, comparable to the affinity measured by us of 732 ± 122 nM for PA3353 at 25°C. The published affinity for Alg44 (PA3542) is 8.4 μM, which is slightly higher than the affinity for Alg44 measured by us of 12.7 ± 1.7 μM (75) (Table 3.1). This could be because the published affinity was measured using isothermal titration calorimetry, which is a method that is fairly inaccurate in measuring the affinities of proteins for small molecules when these affinities are low, and cannot resolve binding affinities of less than approximately 10 μM (98). Thus, the small difference in the binding affinity of Alg44 as measured by us and the published binding affinity could be due to differences in measurement methods.

How could differences in binding affinities be achieved? Mutational studies on Position-X of the PilZ domain clearly demonstrate that even differences in single amino acids can result in drastic disparities in binding affinities of PilZ domain proteins for c-di-GMP (58). These amino acid differences may result in dissimilarities in the specific interactions of amino acid residues with c-di-GMP in the binding pocket. Indeed, Alg44, which demonstrates a low affinity for binding c-di-GMP in this study and in others, maintains an alanine in this position, instead of the arginine that is typically associated with PilZ domain proteins that bind with a higher

affinity; other PilZ domain proteins in *P. aeruginosa* demonstrate an arginine, a lysine, or a glutamine in this position.

The differences in binding affinities of c-di-GMP receptors in *S. Typhimurium* and *P. aeruginosa* indicates a potential mechanism for determining specificity in c-di-GMP signaling. In order to analyze how binding affinities of PilZ domain proteins affect their biological output functions, we chose to pursue this study further in *S. Typhimurium*, which has two PilZ domain proteins, both with published phenotypes (Chapter 4).

Tables and Figures

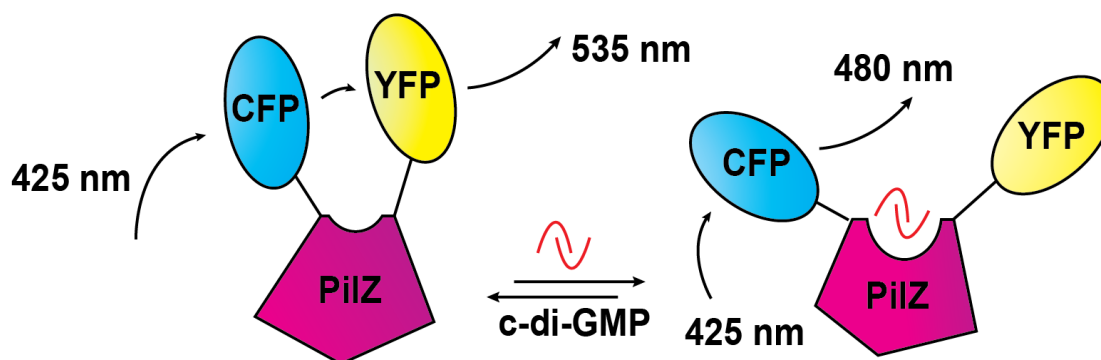


Figure 3.1: The FRET-based biosensor method. PilZ domain FRET proteins were generated by the fusion of the fluorophores mYPet (YFP) and mCyPet (CFP) to either termini of a PilZ domain protein. This protein demonstrates a characteristic FRET signal when excited at the excitation wavelength of mCyPet (425 nm). The amount of FRET is dependent on the particular PilZ domain protein used to generate the construct. Binding of c-di-GMP to the PilZ domain changes the conformation of the PilZ domain protein, which results in a shift in the emission ratio of mYPet (535 nm) to mCyPet (480 nm). In this figure, binding of c-di-GMP results in a decrease in FRET, though c-di-GMP binding can also result in a FRET increase depending on the PilZ domain protein used.

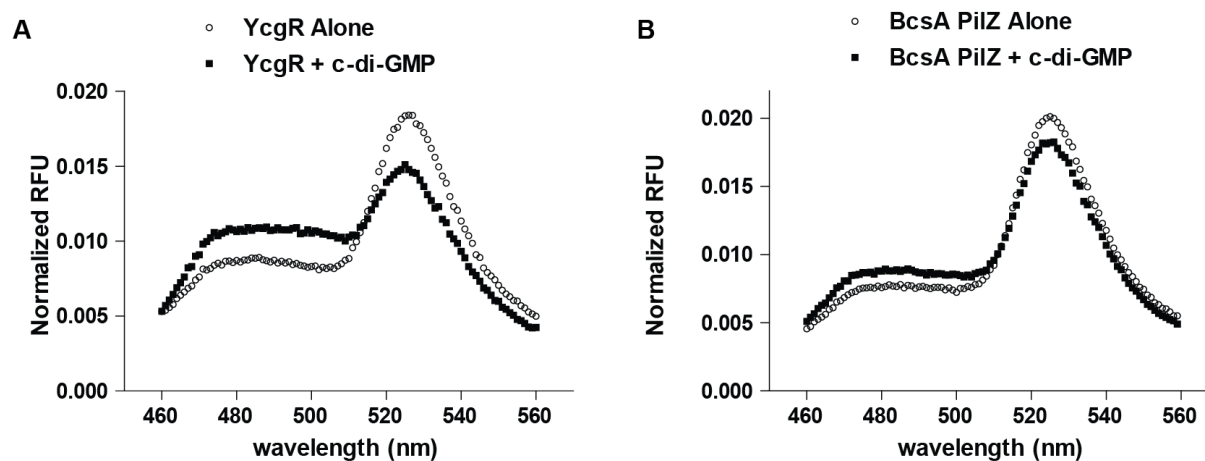


Figure 3.2: YcgR- and BcsA PilZ-based biosensors demonstrate a decrease in FRET in the presence of c-di-GMP. Emission spectra were determined using a fluorescence plate reader upon excitation of CFP at 425 nm. Shown are the emission spectra in the presence (closed circles) and absence (open circles) of 40 μ M c-di-GMP. For both biosensors, the addition of c-di-GMP results in a decrease in the amount of FRET. (a) YcgR biosensor, (b) BcsA PilZ biosensor.

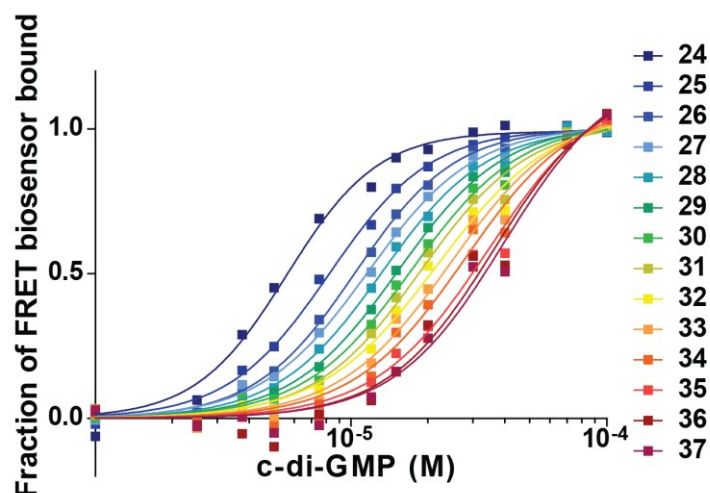


Figure 3.3: The effect of temperature on the binding affinity of the BcsA PilZ domain for c-di-GMP. Shown are binding curves of the BcsA PilZ domain FRET construct for c-di-GMP at temperatures ranging from 24°C to 37°C at 1°C intervals as indicated by the legend. Binding affinity decreases as temperature increases. At each temperature, the fraction of FRET biosensor bound to c-di-GMP was calculated by determining the FRET/CFP ratio at each indicated c-di-GMP concentration, subtracting the unbound FRET/CFP ratio, and dividing this number by the difference between the bound and unbound FRET ratios. A number of 0 indicates that the FRET biosensor is completely unbound to c-di-GMP, and a number of 1 indicates that the FRET biosensor is completely bound to c-di-GMP.

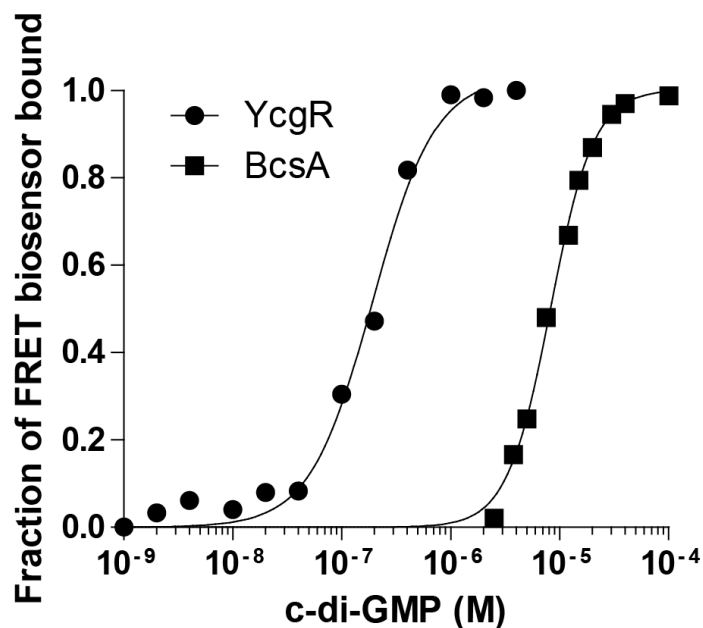


Figure 3.4: The binding affinities of YcgR and the BcsA PilZ domain differ by 43-fold. c-di-GMP binding curves for YcgR (circles) and BcsA (squares) biosensors as measured by FRET. For each biosensor, the fraction of FRET biosensor bound to c-di-GMP was calculated by determining the FRET/CFP ratio at each indicated c-di-GMP concentration, subtracting the unbound FRET/CFP ratio, and dividing this number by the difference between the bound and unbound FRET ratios. A number of 0 indicates that the FRET biosensor is completely unbound to c-di-GMP, and a number of 1 indicates that the FRET biosensor is completely bound to c-di-GMP.

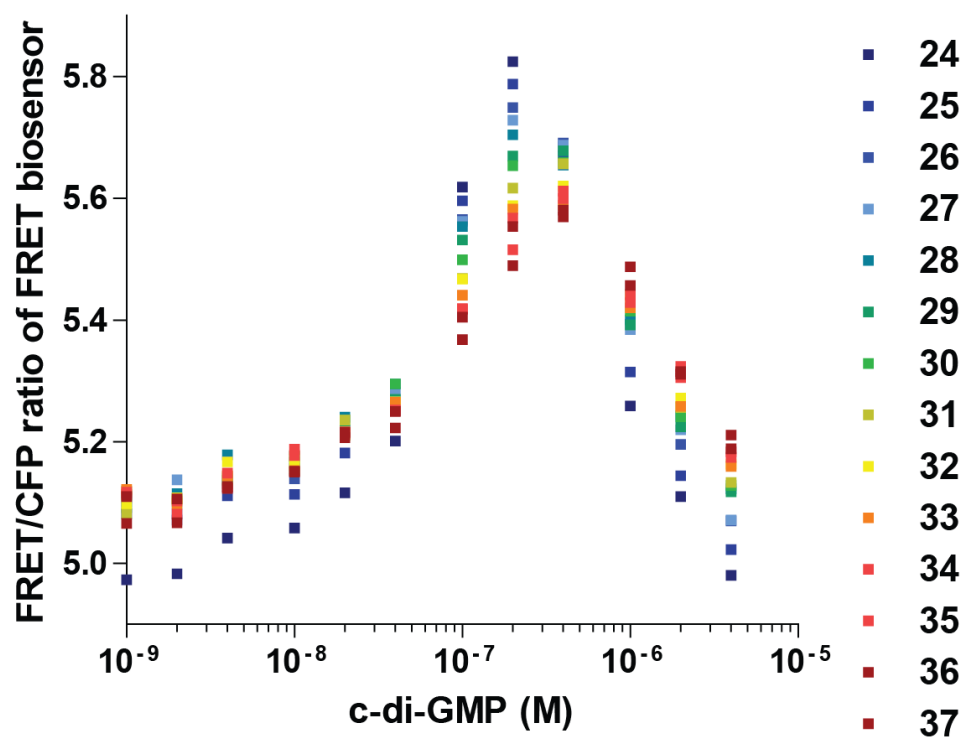


Figure 3.5: Binding curves of PA3353 for c-di-GMP suggest two binding sites. Shown are binding curves of the PA3353 FRET construct for c-di-GMP at temperatures ranging from 24°C to 37°C at 1°C intervals as indicated by the legend.

Table 3.1: Affinities of c-di-GMP-binding molecules in selected bacteria

Protein	Binding Affinity (nM)		Binding Motif	Temp (°C)	Measurement Method	Reference
	This Work	Published				
<i>Salmonella Typhimurium</i>						
YcgR (STM1798)	191 ± 18	182 ± 29	PilZ	25	FRET, ³³ P-Labeled c-di-GMP	This work, Christen 2007
BcsA (STM3619)	8240 ± 238		PilZ	25	FRET	This work
<i>Pseudomonas aeruginosa</i>						
PA3353 site 1 ^a	88 ± 17		PilZ	25	FRET	This work
PA3353 site 2 ^a	732 ± 122	262 ± 66 ^b	PilZ	25, 20	FRET, surface plasmon res	This work, Duvel 2012
FimX (PA4959)		125	EAL	20	ITC	Navarro 2009
PA2989		288	PilZ	25	FRET	Christen 2010
PA0012		402 ± 39	PilZ	25	FRET	Christen 2010
PA4324	735 ± 474 ^c		PilZ	25	FRET	This work
PelD (PA3061)		1900	RXXD I-Site	20	ITC	Whitney 2012
PA2799		1998 ± 448	PilZ	25	FRET	Christen 2010
PA4608		6126 ± 525	PilZ	25	FRET	Christen 2010
Alg44 (PA3542)	12739 ± 1680	8400	PilZ	25	FRET, ITC	This work, Merighi 2007
FleQ (PA1097)		15000-25000	Unknown	37	³² P-Labeled c-di-GMP	Hickman 2008
PA2960	DNB ^d	DNB ^d	Not Applicable	25	FRET, ITC	This work, Merighi 2007
<i>Vibrio cholerae</i>						
Vc2 Riboswitch		1	GEMM	23	In-Line P ³² RNA Probing	Sudarsan 2008
PlzD		100 ± 18	PilZ	25	ITC	Benach 2007
PlzC		314	PilZ	on ice	³² P-Labeled c-di-GMP	Pratt 2007
VpsR		1600	Unknown	RT	³² P-Labeled c-di-GMP	Srivastava 2011
VpsT		3180	W[F/L/M][T/S]R	20	ITC	Krasteva 2010
<i>Caulobacter crescentus</i>						
DgrA		<50 ± 14	PilZ	on ice	³³ P-Labeled c-di-GMP	Christen 2007
DgrB		132 ± 36	PilZ	on ice	³³ P-Labeled c-di-GMP	Christen 2007
DgcA		960	RXXD I-Site	30	Enzymatic Inhibition Assay	Christen 2006
PopA		2400	RXXD I-Site	on ice	³³ P-Labeled c-di-GMP	Duerig 2009
PleD		5800	RXXD I-Site	30	Enzymatic Inhibition Assay	Christen 2006

^aPA3353 binding curves indicate two binding sites

^bThe published affinity of this protein was measured at approximately 20°C, corresponding to ~530 nM at 25°C.

^cThe dynamic range of FRET for PA4324 between bound and unbound states was small, resulting in a high error for the K_d of this protein

^dDoes not bind to c-di-GMP

Table 3.2: Binding affinities and Hill coefficients of YcgR and the BcsA PilZ domain at various temperatures

Temp (°C)	Kd (nM)		Hill Coefficient	
	YcgR	BcsA PilZ	YcgR	BcsA PilZ
24	125 ± 11	5606 ± 226	1.6 ± 0.19	2.4 ± 0.22
25	191 ± 18	8240 ± 238	1.5 ± 0.18	2.2 ± 0.11
26	220 ± 24	10350 ± 220	1.5 ± 0.21	2.2 ± 0.08
27	266 ± 16	11640 ± 345	1.8 ± 0.17	2.1 ± 0.11
28	286 ± 13	13200 ± 400	1.9 ± 0.14	2.1 ± 0.11
29	291 ± 16	15330 ± 610	1.9 ± 0.17	2.1 ± 0.14
30	320 ± 19	17400 ± 740	1.8 ± 0.17	2.0 ± 0.14
31	371 ± 13	18930 ± 1030	1.9 ± 0.11	2.1 ± 0.18
32	406 ± 24	22130 ± 1620	2.2 ± 0.23	1.9 ± 0.18
33	437 ± 30	25250 ± 1980	1.7 ± 0.16	1.9 ± 0.19
34	476 ± 27	29360 ± 3120	1.9 ± 0.15	1.9 ± 0.23
35	522 ± 53	36080 ± 4540	2.2 ± 0.37	1.9 ± 0.25
36	571 ± 39	38670 ± 5960	1.6 ± 0.12	2.0 ± 0.34
37	621 ± 32	41830 ± 6400	1.6 ± 0.10	2.0 ± 0.30

CHAPTER 4: THE BINDING AFFINITIES OF *SALMONELLA* TYPHIMURIUM PILZ DOMAIN PROTEINS AFFECT THEIR BIOLOGICAL FUNCTIONS

Summary

c-di-GMP controls cellular processes by binding to receptor macromolecules including proteins that contain the PilZ domain. The two PilZ domain-containing c-di-GMP receptors in *S. Typhimurium*, YcgR and BcsA, regulate cellular motility and cellulose production, respectively. In the previous chapter, we showed that these two proteins demonstrate a 43-fold difference in their affinities for binding c-di-GMP. Here, we present evidence that the binding affinities of *S. Typhimurium* PilZ domain proteins affect their biological functions. Alteration of the affinities of YcgR and BcsA altered their levels of activation in different conditions, suggesting that the disparate affinities of these proteins for c-di-GMP may be optimized for their specific functions. Inactivation of the EAL domain protein YhjH resulted in a significant increase in the fraction of cells that demonstrate c-di-GMP levels that are high enough to bind to the higher-affinity YcgR and inhibit motility, but not high enough to bind to the lower-affinity BcsA and stimulate cellulose production. This work supports the hypothesis that regulation of c-di-GMP-controlled processes can occur through the affinities of downstream receptors for c-di-GMP.

Introduction

In the previous chapter, we discussed a potential mechanism by which the observed signal transduction specificity between c-di-GMP metabolizing enzymes and their downstream receptors could be achieved: through the variable binding affinities of c-di-GMP downstream receptors. This model is based on the observation that the binding affinities of several c-di-GMP-binding macromolecules span a large range of c-di-GMP concentrations even within the same organism (Table 3.1). This observation, combined with the fact that some DGCs are limited in their ability to generate c-di-GMP due to inhibitory I-sites (20), led us to hypothesize that binding affinities may play a role in the selective activation of c-di-GMP receptors. To explore this hypothesis, we targeted the c-di-GMP signaling system in *Salmonella* Typhimurium.

S. Typhimurium has three defined processes known to be regulated by c-di-GMP: flagellar-based motility, CsgD expression (and therefore generation of curli fimbriae), and cellulose production (55, 108, 117, 151) (Chapter 1). Like most Enterobacteria, *S. Typhimurium* has two PilZ domain proteins that act as c-di-GMP receptors: YcgR, which controls flagellar-based motility, and BcsA, the bacterial cellulose synthase. YcgR was originally identified in *E. coli* as an inhibitor of motility in an *hns* mutant, and has since been found to bind specifically to the flagellar complex to inhibit torque generation and thus decrease motility when it binds to c-di-GMP (12, 30, 59, 89, 108). c-di-GMP stimulates cellulose production presumably by binding to the PilZ domain of BcsA (117, 151). Thus, a rise in c-di-GMP concentration results in a decrease in motility (through YcgR) and an increase in cellulose production (through BcsA). Several of the 20 GGDEF/EAL domain proteins of *S. Typhimurium* have been linked to one of these processes. AdrA, a DGC that is dependent on CsgD for its expression, controls cellulose production; its loss cannot be complemented by the native expression of any other DGC (37,

102, 151). However, other DGCs that are expressed under both cellulose-producing and non-cellulose-producing conditions (116) seem to be involved in controlling motility. The phosphodiesterase that appears to be the most important for maintaining c-di-GMP levels low enough to allow flagellar motility is YhjH (59, 89, 108). Like YcgR, YhjH is a member of the flagellar regulon and is expressed from a flagellar class III promoter (33, 59, 136).

In the previous chapter, we showed that the c-di-GMP binding affinities of *S. Typhimurium* PilZ domain proteins differ by about 43-fold. Here we present evidence that the binding affinities of these proteins affect their biological functions. First, we establish that the regulation of BcsA activity occurs on a post-translational level by c-di-GMP binding. Then, to analyze the effects of binding affinity on phenotype, we undergo a strategy of site-directed mutagenesis to generate PilZ domain protein mutants that have altered affinities but otherwise retain the functions of the native proteins, and tested these proteins in established phenotypic assays. We found that the binding affinities of these proteins affected the conditions or the extent to which each PilZ domain protein was activated. Finally, we determine that inactivation of YhjH results in an increase in the amount of cells that demonstrate a level of c-di-GMP high enough to bind to YcgR, but not to the BcsA PilZ domain. This work implies that regulation by binding affinity of downstream receptors is a possible mechanism for the selective activation of c-di-GMP-controlled processes in *S. Typhimurium*.

Cellulose synthesis by BcsA is predominantly regulated at a post-translational level by c-di-GMP

The production of cellulose in rich media by BcsA is dependent upon the DGC AdrA, which is the only DGC in *S. Typhimurium* that displays temperature-dependent expression: AdrA is expressed at temperatures of 30°C or lower but not at 37°C (36, 45, 116, 151). Accordingly, cellulose production can be observed in *S. Typhimurium* grown on LB agar plates at 30°C or lower, but not at 37°C (Figure 4.1). We found that a strain of *S. Typhimurium* that lacks *adrA* is incapable of producing cellulose at 24°C, as demonstrated by a comparison of the $\Delta adrA$ mutant strain to a $\Delta bcsA$ mutant, similar to results obtained by other groups (37, 102, 151) (Figure 4.1B). Deletion of *yhjH*, which encodes an EAL domain protein that acts to prevent motility inhibition by YcgR, did not result in any increased cellulose production at 24°C, 30°C, or 37°C (Figure 4.1A and data not shown). Heterologous expression of the DGC PA1120 from *P. aeruginosa* was able to induce the production of cellulose even at 37°C (Figure 4.1A), confirming previous results that cellulose synthesis can be stimulated by increasing the intracellular c-di-GMP concentration through the expression of an exogenous DGC (116). The production of cellulose in this DGC-expressing strain was entirely dependent upon BcsA, since a $\Delta bcsA$ deletion mutant failed to demonstrate any calcofluor binding, which is indicative of cellulose production (Figure 4.1A).

Since AdrA is required for the production of cellulose, and because AdrA has been shown to be responsible for over half of the c-di-GMP produced under cellulose-producing conditions, we hypothesized that the reason why cellulose is not produced at 37°C is because the level of c-di-GMP is not high enough to bind to BcsA due to its lower affinity for this second messenger. In order to examine the effects of BcsA binding affinity on its phenotype, we had to first determine the mechanism of action of c-di-GMP on cellulose production. c-di-GMP could stimulate cellulose production directly, through post-translational interaction with the BcsA PilZ

domain, or it could stimulate the expression of BcsA or other factors that are important for cellulose production at lower temperatures. To determine whether the expression of the BcsA protein was dependent on temperature, a FLAG tag was encoded on the 3' end of the chromosomal *bcsA* gene in *S. Typhimurium*. This strain did not demonstrate any deficiency in cellulose production as determined by fluorescence on LB-calcofluor agar plates at 24°C (Figure 4.2A). An anti-FLAG Western blot was then performed on cell lysates isolated from cells grown at either 24°C or 37°C. Differences in cellulose production between 37°C and 24°C were not due to the differential expression of BcsA protein, since protein extracts from strains harboring a FLAG-tagged BcsA demonstrated similar amounts of this protein independent of temperature (Figure 4.2B). This is consistent with previous work showing that genes of the *bcs* locus are constitutively expressed (55, 151).

Although this experiment demonstrates that the BcsA protein is present in cells grown at 37°C, it is not informative regarding the presence of other components which may be necessary to stimulate cellulose production at this temperature. To determine whether all of the components necessary to produce cellulose were present in cells grown at 37°C, cell lysates were prepared from *S. Typhimurium* grown at this temperature, and were then incubated with a DGC *in vitro* at 37°C in the presence of calcofluor. Calcofluor fluorescence was then assessed by the analysis of these samples in a fluorescence plate reader. These cell lysates were capable of generating cellulose in the presence of the DGC, implying that the cellulose synthase complex is functional in cells grown at 37°C (Figure 4.2C). This cellulose production was dependent on a functional BcsA, as lysate prepared from a strain lacking BcsA showed no cellulose production upon DGC addition. These experiments support the hypothesis that cellulose is not produced at 37°C because the level of c-di-GMP is below its affinity for binding BcsA.

Mutation of the amino acid immediately N-terminal to the RxxxR motif alters the affinities of *S. Typhimurium* PilZ proteins for c-di-GMP

In order to test the effects of binding affinities of PilZ domain proteins on their phenotypes in *S. Typhimurium*, we used a strategy of rational, site-directed mutagenesis to alter c-di-GMP-binding affinity. Crystal and NMR studies of PilZ domain proteins in complex with c-di-GMP have elucidated the roles of residues of the binding pocket, especially those of the so-called switch region including the RxxxR motif, in binding to c-di-GMP (6, 58, 111) (Chapter 1). Specifically, the presence of an arginine at the position immediately N-terminal of the RxxxR motif (dubbed “Position-X”) has been shown in the *P. putida* YcgR homologue, PP4397, to be an important determinant of the affinity for c-di-GMP-binding (58) (Figure 1.3).

The *S. Typhimurium* YcgR protein is very similar to the PP4397 protein, demonstrating 21% identity to the length of the protein. Homology modeling indicates that these two proteins adopt very similar structures (Figure 4.3A). *S. Typhimurium* YcgR also has an arginine at Position-X (arginine-113) (Figure 4.3B, 4.4A), so we reasoned that mutation of this arginine to an alanine might decrease binding affinity for c-di-GMP as it does for PP4397. Indeed, mutation of arginine-113 to alanine resulted in a YcgR variant that bound c-di-GMP with an affinity of 3.2 μM , which was approximately 17-fold lower than the affinity measured for the wild-type YcgR protein (Figure 4.4B).

The BcsA PilZ domain has a low binding affinity for c-di-GMP compared to YcgR (8.2 μM compared to 191 nM), so our goal for BcsA was to increase its affinity. BcsA has a valine at Position-X (Figure 4.4A). The *V. cholerae* YcgR homologue, VCA0042, also has a large

hydrophobic residue, a leucine, in this position. Mutation of this leucine to arginine increased the binding affinity of VCA0042 for c-di-GMP by approximately three-fold (58). Although BcsA is not similar in sequence to VCA0042 outside of conserved residues of the binding pocket, we reasoned that mutation of the valine in Position-X of BcsA to an arginine might increase binding affinity in a similar manner as mutation of leucine to arginine in Position-X of VCA0042. Mutating this valine to an arginine increased the affinity of BcsA for c-di-GMP to 4.2 μM at 25°C, which is roughly two-fold greater than that of the WT protein (Figure 4.4C). These mutations did not change the wild-type binding stoichiometries of c-di-GMP to PilZ domain, indicating that the change in affinity was the major determinant of change in downstream function. Therefore we were able by site directed mutagenesis to generate PilZ domain proteins with altered binding affinities for c-di-GMP.

A *S. Typhimurium* strain harboring a BcsA protein with a lower c-di-GMP binding affinity demonstrates an increase in cellulose production at low levels of c-di-GMP

Once we had generated binding affinity mutants of PilZ domain proteins, we needed functional assays to determine the effects of these mutations on phenotype. To compare cellulose production between strains of *S. Typhimurium*, we constructed a strain in which the level of c-di-GMP can be controlled by the addition of arabinose. This is due to the presence of an arabinose-inducible DGC (PA1120 from *P. aeruginosa*) located on the chromosome under the control of the native arabinose-inducible *pBAD* promoter. In this strain, addition of arabinose to the growth media results in induction of the DGC and cellulose production (Figure 4.5). Thus, in

this strain, the presence of arabinose induces the production of the DGC, which in turn makes c-di-GMP and stimulates cellulose production.

To examine whether the twofold increase in binding affinity in the BcsA V695R mutant affects cellulose production, we generated a strain that harbored the *bcsA-V695R* mutation on the chromosome in the background of this arabinose-inducible DGC. We analyzed differences in cellulose production, as determined by cellulose binding to the fluorescent dye calcofluor, between the *ara::DGC*, *ara::DGC ΔbcsA* and *ara::DGC bcsA-V695R* strains at different expression levels of the DGC by varying the arabinose concentrations. At low arabinose levels, the *bcsA V695R* mutant generated a small, but reproducible, increase in calcofluor fluorescence compared to the BcsA wild-type strain (Figure 4.6), implying that this strain produces more cellulose at low levels of arabinose than the wild-type strain. Thus, the binding affinity of BcsA for c-di-GMP does affect its biological function. Upon addition of higher amounts of arabinose, the amount of cellulose synthesis between these strains was not significantly different, suggesting that higher DGC levels result in a cellular c-di-GMP concentration above the K_d values for both BcsA mutant V695R and BcsA wild-type enzymes, and thus results in cellulose production by both enzymes. The *bcsA-V695R* mutation did not result in increased cellulose production at 37°C as visualized by eye (data not shown), possibly because the difference in c-di-GMP binding affinities of the wild-type and the V695R mutant BcsA proteins is not large enough to stimulate c-di-GMP binding, and thus cellulose production, under this condition.

A *S. Typhimurium* strain harboring YcgR with a lower c-di-GMP binding affinity requires higher levels of c-di-GMP to demonstrate motility inhibition

Next we wanted to determine whether the R113A mutation of YcgR, which results in a 17-fold lower affinity for c-di-GMP, affects motility in *S. Typhimurium*. *S. Typhimurium* YcgR has been shown to decrease the swimming diameter of colonies on motility agar plates when intracellular levels of c-di-GMP are artificially raised (108). We hypothesized that the YcgR R113A mutant protein would require a higher concentration of c-di-GMP than the wild-type YcgR protein in order to inhibit *S. Typhimurium* swimming in this assay. To test this hypothesis, *S. Typhimurium* strains containing a plasmid that expresses the DGC PA1120 from an IPTG-inducible *tac* promoter were constructed and evaluated. The addition of IPTG results in a decrease in swimming motility in this strain, as visualized by a decrease in the halo diameter on motility agar plates. In contrast, a $\Delta ycgR$ deletion mutant does not demonstrate as severe of a decrease in swimming diameter compared to the wild-type strain, indicating a partial relief of c-di-GMP-induced swimming inhibition in this strain (Figure 4.7A). Expressing YcgR from its native promoter on a plasmid complemented the $\Delta ycgR$ mutation (Figure 4.7A).

To determine whether the YcgR R113A mutation affected swimming, we complemented the $\Delta ycgR$ mutant strain with wild-type YcgR or the YcgR R113A mutant protein and analyzed the diameter of the swimming halo at different concentrations of IPTG. Complementation with YcgR partially inhibited swimming even in the absence of IPTG, which could be an overexpression effect of YcgR as has been observed previously (89) (Figure 4.7B). Increasing the IPTG concentration decreased the ability of *S. Typhimurium* harboring pDGC-YcgR to swim, indicating that c-di-GMP-bound YcgR was inhibiting motility (Figure 4.7B). At 20 μ M IPTG, the YcgR wild-type protein completely inhibited swimming. Unlike the wild-type YcgR protein, complementation of the $\Delta ycgR$ mutation with YcgR R113A had no effect on swimming

at 0 μM IPTG. Increasing IPTG also decreased motility in the YcgR R113A complemented strain as in the YcgR wild-type strain, but 50 μM IPTG was required to completely inhibit swimming in this strain (Figure 4.7B). This indicates that the YcgR R113A protein requires a higher concentration of c-di-GMP than the wild-type YcgR protein to inhibit swimming, which is consistent with its lower binding affinity, thereby correlating affinity with behavior.

Mutation in *yhjH* results in an increase in the fraction of *S. Typhimurium* cells that demonstrate c-di-GMP levels that are high enough to bind YcgR

Another way to explore the affinity hypothesis is in the context of a mutation of the PDE YhjH. YcgR is most frequently studied in the context of a *yhjH* mutant background, in which a second mutation in *ycgR* partially relieves the swimming defect that is caused by inactivation of YhjH (12, 30, 89, 108). In *E. coli*, cells that harbor a mutation in *yhjH* demonstrate increased c-di-GMP levels compared to wild-type cells (12). However, it has been demonstrated that mutation in *yhjH* in *S. Typhimurium* does not result in a significant difference in total c-di-GMP levels in this strain compared to a wild-type strain (112). In order to determine whether the *yhjH* mutation results in a rise in c-di-GMP levels that are high enough to stimulate binding to, and motility inhibition by, YcgR, we analyzed the binding of a synthetic YcgR-FRET construct *in vivo*, encoded on the plasmid pYcgR-Spy (23). This construct is described in Chapter 5. Since this construct is based on YcgR, it allows for an accurate determination of the bound state of YcgR when expressed inside of live cells.

Wild-type *S. Typhimurium*, or an isogenic *ΔyhjH* mutant strain, both harboring pYcgR-Spy, were grown in liquid LB media at 37°C to an OD₆₀₀ of 0.20. At this point, cells were collected and imaged using fluorescence microscopy, and their net FRET (nFRET)/CFP intensity ratios were calculated. The nFRET/CFP ratio provides a readout as to whether the YcgR protein is bound to c-di-GMP or unbound (see Chapter 5 for a more detailed discussion). Control strains expressing either the DGC PA1120 (*ara::DGC*) or the PDE PA2133 (*ara::PDE*), and pYcgR-Spy, were used to determine the bound and unbound nFRET/CFP ratios for the YcgR FRET construct in this *in vivo* assay. As expected, these control strains defined homogeneous populations of cells, based on the nFRET/CFP ratios of individual cells (these control strains are described in Chapter 5) (Figure 4.8B upper panel, Figure 5.3). Interestingly, in the wild-type strain expressing pYcgR-Spy, a heterogeneous population of c-di-GMP concentrations was observed, even though all cells experienced the same environment of liquid batch culture with shaking (Figure 4.8A, upper panel). This heterogeneity in c-di-GMP concentrations has also been observed previously for other bacterial species, and it is hypothesized that this phenomenon is due to the production of progeny cells after cell division that harbor different c-di-GMP concentrations, and therefore demonstrate different cellular behaviors, in order to promote a diversification strategy that may enhance survival of the bacterial species (23). In the wild-type strain, 43.7% of cells demonstrated a nFRET/CFP ratio higher than 0.9, indicative that YcgR was unbound to c-di-GMP in these cells (Figure 4.8). In contrast, in the *yhjH* mutant, only 4.8% of cells demonstrated a nFRET/CFP ratio higher than 0.9, a 10-fold lower fraction than in wild-type cells. The remainder of cells demonstrated a nFRET/CFP ratio of 0.9 or less, indicating that at least some of the YcgR FRET constructs were bound to c-di-GMP in these cells. As demonstrated by Boehm *et al*, binding of c-di-GMP to only a fraction of the YcgR molecules

present in the cell can lead to a decrease in swimming motility, with swimming inhibition increasing as the number of YcgR molecules bound to c-di-GMP in the cell increases (12). Thus it is possible that the $\Delta yhjH$ mutant strain is inhibited for motility because a higher fraction of the YcgR proteins in these cells are bound to c-di-GMP. This experiment demonstrates that mutation of $yhjH$ does result in an increase in the fraction of cells with an average level of c-di-GMP that is high enough to bind to the YcgR protein, which is then able to inhibit swimming.

A *S. Typhimurium* strain harboring the lower-affinity *ycgR* R113A mutation does not demonstrate YcgR-dependent motility inhibition in a $\Delta yhjH$ mutant

Once we had established that mutation in $yhjH$ results in an increase in average intracellular c-di-GMP levels, we wanted to assess the effect of the YcgR R113A mutation in the context of a $yhjH$ mutant background. To examine this, a $\Delta yhjH$ deletion mutation was generated on a *ycgR* wild-type, *ycgR-R113A*, or $\Delta ycgR$ deletion mutant background of *S. Typhimurium*. As has been demonstrated previously, the $\Delta yhjH$ mutant strain exhibited decreased swimming compared to the wild-type strain as visualized by the swimming halo in a soft-agar motility plate assay (Figure 4.9). The swimming diameter of the $\Delta yhjH$ mutant was roughly 35% of that observed by the wild-type strain. Swimming was partially restored in the $\Delta yhjH$ mutant by a second mutation in *ycgR* (66% swimming diameter of the wild-type strain). Remarkably, chromosomal replacement of the *ycgR* codon encoding arginine-113 with a codon that encodes alanine resulted in a phenotype practically indistinguishable from that of the deletion mutant (69% swimming diameter of the wild-type strain) in this assay, which implies

that the YcgR R113A mutant protein cannot complement for the loss of YcgR in this experiment (Figure 4.9). This suggests that the $\Delta yhjH$ mutation causes the intracellular concentration of c-di-GMP to rise high enough to bind to YcgR, but not high enough to bind to YcgR R113A.

Mutation in *yhjH* does not result in cellulose production in soft-agar motility plates

Our data indicates that mutation in *yhjH* results in an increase in the fraction of cells that contain c-di-GMP levels that are high enough to bind to the wild-type YcgR protein, but not high enough to bind to the R113A mutant YcgR protein. Since the affinity of the BcsA PilZ domain for c-di-GMP is less than that of the YcgR R113A mutant protein, we reasoned that $\Delta yhjH$ mutation would result in a c-di-GMP level high enough to bind to YcgR, but not high enough to bind to the BcsA PilZ domain. To test this, we first expressed a BcsA PilZ FRET-based construct inside of live cells and monitored their nFRET/CFP ratios in a similar manner to that of the YcgR FRET construct (the development and testing of this BcsA PilZ-based FRET construct is described in Chapter 5) (Figure 4.8). As for the YcgR FRET construct, *ara::DGC* and *ara::PDE* strains harboring the BcsA PilZ FRET construct defined homogeneous populations based on their nFRET/CFP ratios (Figure 4.10B, upper panel; Figure 5.5). Unlike cells expressing the YcgR FRET construct, wild-type cells expressing the BcsA PilZ construct were homogeneous in their nFRET/CFP ratios (Figure 4.10). The $\Delta yhjH$ mutant strain did not demonstrate nFRET/CFP ratios that were significantly different than that of the wild-type strain, and in both strains, these ratios matched that of the *ara::PDE* strain, indicating that the BcsA

PilZ domain was unbound to c-di-GMP in this assay (Figure 4.10). Thus, the $\Delta yhjH$ mutation does not result in a change in c-di-GMP levels large enough to affect the BcsA PilZ construct.

Since no binding of c-di-GMP to the BcsA PilZ domain was observed in the $\Delta yhjH$ mutant strain, this implies that even though $\Delta yhjH$ mutation stimulates motility inhibition, it does not result in the production of cellulose. This was observed during growth on solid agar plates, implying that the increased c-di-GMP concentration that results from $\Delta yhjH$ deletion does not induce BcsA activity (Figure 4.1A); however, bacterial detection of solid surfaces may result in different levels of c-di-GMP on solid agar plates than in the low-agar swimming plate assay (43). Therefore, we analyzed the production of cellulose on motility agar plates under the same conditions at which YhjH-dependent motility inhibition is observed. As a control, the *S. Typhimurium* pDGC and $\Delta bcsA$ pDGC strains were included. Induction of the DGC results in the production of a level of c-di-GMP that completely inhibits motility (Figure 4.11). In the soft-agar motility plate assay, cellulose production was observed in the pDGC strain by its binding to the fluorescent dye calcofluor (Figure 4.11). In contrast, no calcofluor binding was observed, as expected, to the pDGC strain lacking *bcsA*. Although the $\Delta yhjH$ deletion strain demonstrated an inhibition in swimming motility in this assay, no calcofluor binding in this strain was observed (Figure 4.11). The calcofluor fluorescence of this strain was indistinguishable from that of a $\Delta yhjH \Delta bcsA$ double mutant (Figure 4.11). This demonstrates that the $\Delta yhjH$ mutation results in motility inhibition but does not stimulate the production of cellulose.

***S. Typhimurium* PilZ domain proteins are not essential for virulence**

c-di-GMP has been implicated in the virulence of many bacterial pathogens (Chapter 1). In *S. Typhimurium*, both the artificial up-regulation of c-di-GMP production, and the deletion of all GGDEF domain proteins from the genome, result in avirulent phenotypes in a mouse model of infection, indicating that the relationship of c-di-GMP to virulence in this organism is complex (63, 116). To determine whether PilZ domain proteins are involved in the virulence of *S. Typhimurium*, strains harboring mutations in the *ycgR* or *bcsA* genes, or in both genes, were inoculated intraperitoneally into mice, and the survival of infected mice was monitored over several days. None of the *S. Typhimurium* strains in this experiment demonstrated a virulence defect compared to the wild-type strain in this infection model (Table 4.1). This is in agreement with previous findings demonstrating that a mutant *S. Typhimurium* strain lacking *bcsC* is fully virulent upon intraperitoneal injection into chickens (117). However, it remains possible that the PilZ domain proteins YcgR or BcsA may be important for virulence during oral infection.

Discussion

In this work, we analyzed the role of c-di-GMP-binding affinities of *S. Typhimurium* PilZ domain proteins on their biological functions. Using site-directed mutagenesis of Position-X residues, we generated PilZ domain proteins with altered c-di-GMP binding affinities (Figure 4.4). For YcgR, mutation of arginine-113 to alanine in Position-X likely led to the loss of important H-bond and/or π -stacking interactions with c-di-GMP, thereby reducing binding affinity. For BcsA, the effect of mutation of valine-695 to arginine is less clear. It was hypothesized that mutation of leucine to arginine in Position-X of VCA0042 caused only a minor

increase in binding affinity because the mutation to arginine did not generate any new bonds to c-di-GMP (58). If this is also true for the BcsA V695R mutation, this could explain why this mutation caused only a twofold increase in binding affinity. Phenotypic analyses of these PilZ domain protein mutants demonstrated that the binding affinity of these proteins for c-di-GMP is a critical determinant in their biological functions. The BcsA V695R mutation resulted in an increased production of cellulose at lower levels of c-di-GMP (Figure 4.6), while the YcgR R113A mutation resulted in the requirement for a higher concentration of c-di-GMP to inhibit motility (Figure 4.7). Analysis of a chromosomal *ycgR R113A* strain of *S. Typhimurium* demonstrated that this mutation abolished the ability of YcgR to inhibit motility in a $\Delta yhjH$ mutant (Figure 4.9). This demonstrates that the affinities of these proteins for c-di-GMP determine the conditions and the extent to which they are active.

This hypothesis is supported by the fact that mutation of *yhjH* appears to result in c-di-GMP levels that are high enough, in most cells, to affect YcgR, but are not high enough stimulate cellulose production by binding to BcsA. The $\Delta yhjH$ mutation results in a considerable increase in the fraction of the population that contains c-di-GMP levels that are high enough to demonstrate at least partial binding to a YcgR FRET construct (Figure 4.8). Binding of YcgR to c-di-GMP then acts to inhibit motility by its interactions with components of the flagellar apparatus (12, 30, 89). However, a BcsA PilZ FRET construct, which demonstrates a lower affinity for c-di-GMP than YcgR (Chapter 3), remained entirely unbound to c-di-GMP in both wild-type and $\Delta yhjH$ mutant strains (Figure 4.10). This, combined with the observation that the $\Delta yhjH$ mutation does not appear to affect motility inhibition by the lower-affinity YcgR R113A mutant protein (Figure 4.9), provides evidence that the rise in c-di-GMP levels in the $\Delta yhjH$ *S. Typhimurium* mutant is small. This explains why a previous comparison of the total c-di-GMP

concentrations in wild-type and $\Delta yhjH$ mutant strains of *S. Typhimurium* did not find a significant difference in c-di-GMP concentration between these strains (112). Additionally, this hypothesis is consistent with our data demonstrating that the $\Delta yhjH$ mutation fails to stimulate cellulose production at 37°C despite the presence of a functional cellulose synthase complex (Figure 4.1, 4.2, 4.11). It is possible that in wild-type *S. Typhimurium*, YhjH maintains the level of c-di-GMP close to the K_d for binding YcgR. Changes detected in the environment that result in a decrease in YhjH activity could then very quickly result in an increase of c-di-GMP levels that are just above the K_d of YcgR, and are therefore just large enough to be biologically relevant to the YcgR protein. These data support the hypothesis that YhjH acts as the phosphodiesterase that specifically regulates the motility-inhibition module in *S. Typhimurium* by controlling the c-di-GMP levels that are available to YcgR.

Based on this evidence, we propose the following model to illustrate c-di-GMP signaling regulation in *S. Typhimurium* in rich media (Figure 4.12). This model involves the sequential activation of c-di-GMP receptors in *S. Typhimurium* through increasing c-di-GMP levels, which is consistent with the progression of biofilm formation. While the cytoplasmic c-di-GMP concentration is maintained at a low level by YhjH, it does not bind to either YcgR or to BcsA, resulting in a cell that is motile and does not produce cellulose. Upon sensing biofilm-forming conditions, c-di-GMP levels rise, which have the immediate impact of decreasing swimming motility through YcgR. This is an important early step in biofilm formation since cellular motility is inhibitory during initial biofilm development (109). Increased c-di-GMP levels induce the expression of CsgD, which would then directly activate the transcription of curli fimbriae, an important attachment and aggregative factor in *S. Typhimurium* (100). CsgD expression also results in the production of AdrA, which, upon sensing cellulose-producing

conditions, raises the intracellular level of c-di-GMP even higher, resulting in cellulose production through c-di-GMP binding to BcsA, and thus the mature biofilm is formed. The requirement for a higher level of c-di-GMP to induce cellulose production, but not to activate the production of curli fimbriae, is potentially due to the fact that cells that produce cellulose before generating curli fimbriae appear to be deficient in initial attachment to surfaces (42). There are several lines of evidence that suggest that AdrA produces a large amount of c-di-GMP inside of the cell. During cellulose-producing conditions, AdrA has been shown to be responsible for producing most of the c-di-GMP present inside of the cell (55). AdrA is capable of producing more c-di-GMP than other *Salmonella* DGCs tested. Its overexpression has been found to raise the cellular c-di-GMP level by 10,000-fold, compared to two other *Salmonella* DGCs that have been shown to affect motility and CsgD expression, which raise the c-di-GMP level by no more than 6-fold (55). In another study, the overexpression of AdrA resulted in 255 μ M c-di-GMP produced, indicating that it is capable of producing c-di-GMP that is high enough to bind to BcsA (113) (Chapter 1). If the affinity of the BcsA PilZ domain were closer to that of YcgR, low level of c-di-GMP might both inhibit motility and stimulate cellulose production simultaneously, a behavior that would be detrimental to biofilm formation. Additionally, there may be situations in which it would be advantageous to decrease swimming motility through YcgR but not to produce cellulose. This work suggests that the disparate binding affinities of YcgR and BcsA are important in the regulation of the biological functions of these proteins.

Tables and Figures

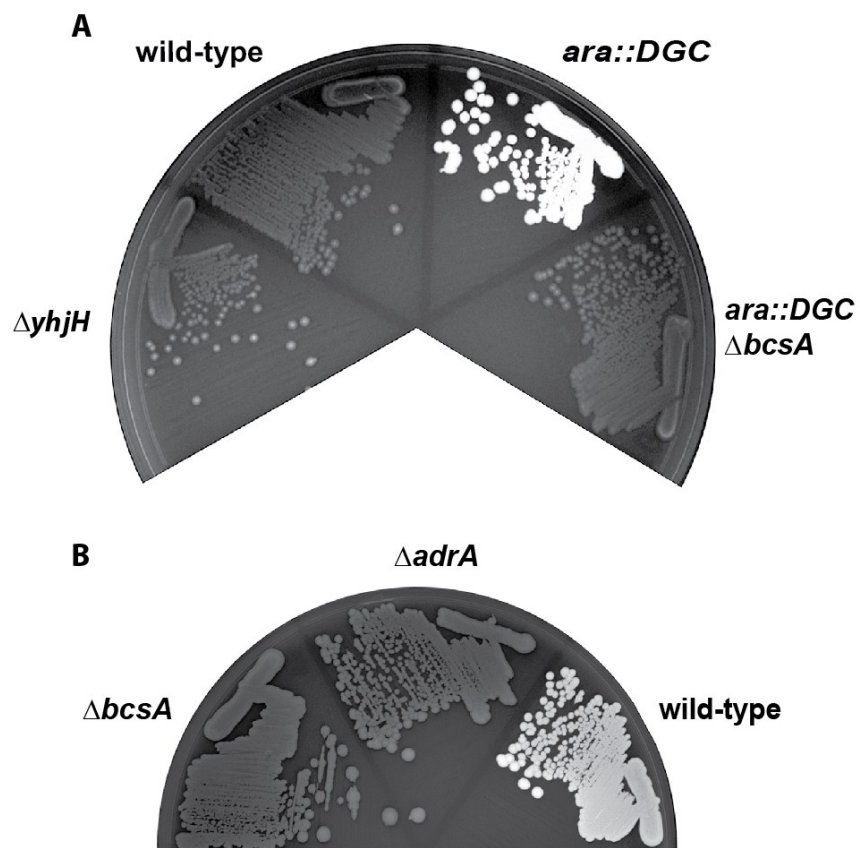


Figure 4.1: *S. Typhimurium* makes cellulose at 24°C, but not at 37°C, in a manner that is dependent on both AdrA and BcsA. LB-calcofluor agar plates inoculated with the indicated strains incubated at either 37°C for 24 hours (a), or 24°C for 72 hours (b). The plate in (a) was supplemented with 0.001% arabinose. Plates were exposed to UV light with an excitation wavelength of 365 nm, which is a wavelength that stimulates fluorescence of calcofluor when it is bound to cellulose. White or light coloring indicates calcofluor binding to cellulose. *ara::DGC* signifies a strain of *S. Typhimurium* that harbors an arabinose-inducible DGC on the chromosome.

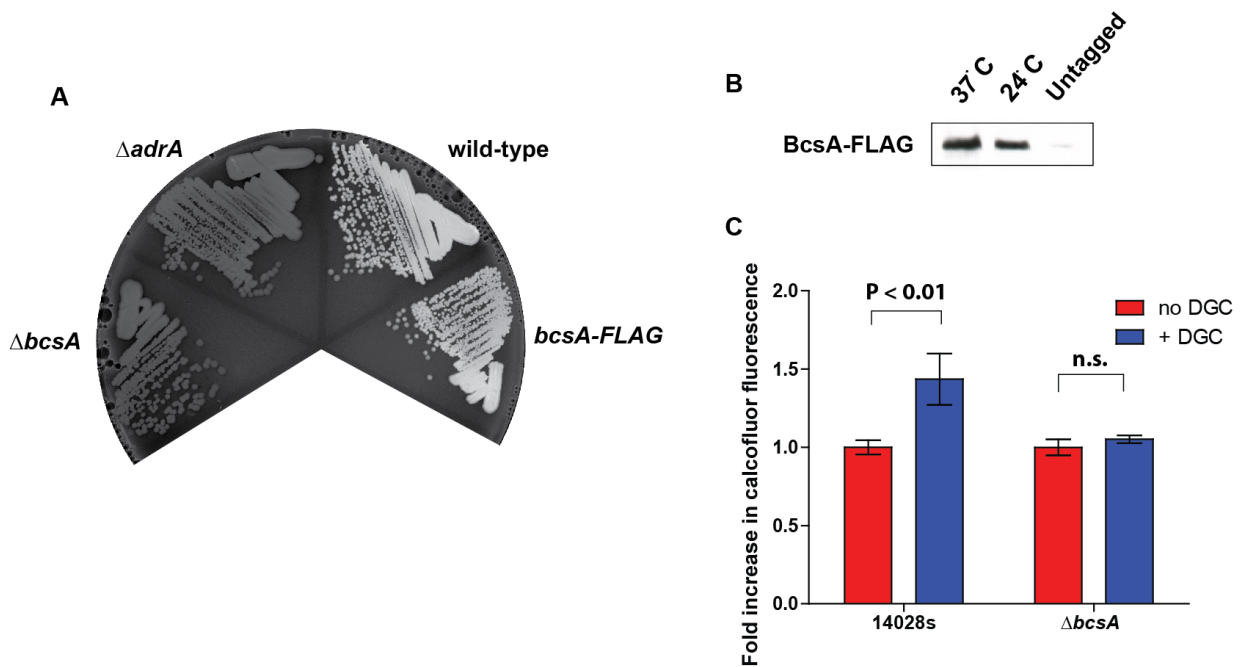


Figure 4.2: Cellulose is predominantly regulated on a post-translational level by intracellular c-di-GMP. (a) A C-terminal FLAG tag on the BcsA protein does not affect its ability to produce cellulose. Shown is a calcofluor agar plate inoculated with the indicated strains and incubated for 72 hours at 24°C, after which the plate was exposed to UV light with a wavelength of 365 nm. (b) Western blot using anti-FLAG antibodies on membrane proteins isolated from *S. Typhimurium* *bcsA-FLAG* or a wild-type strain with untagged BcsA that had been incubated at either 37°C or 24°C. 5 mg total protein was added to each lane. (c) Fold increase in calcofluor fluorescence of lysate generated from *S. Typhimurium*, or a $\Delta bcsA$ deletion strain, at 37°C, incubated *in vitro* with a DGC, compared to the amount of calcofluor fluorescence of lysate without DGC addition. n.s. = not significant.

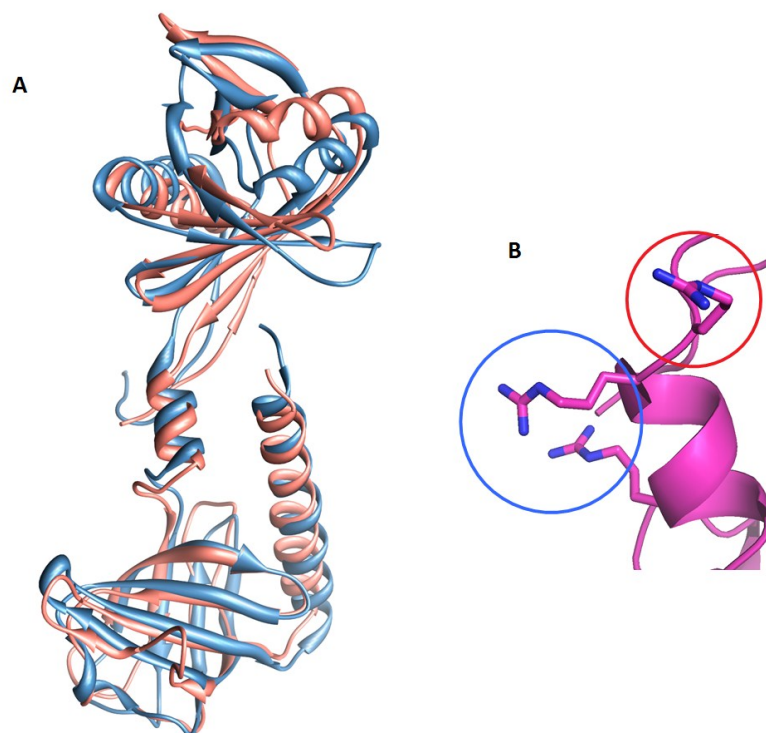


Figure 4.3: The *S. Typhimurium* YcgR protein contains an arginine in “Position-X”. (a) Structural alignment comparing the *S. Typhimurium* YcgR protein (pink) with the *P. putida* PP4397 protein (blue). Image was generated using UCSF Chimera©, production version 1.6.2. (b) Close-up view of the essential arginines (circled in blue) of the RxxxR motif, and the Position-X arginine (circled in red) of the *S. Typhimurium* YcgR protein. Protein backbone and carbon atoms are shown in pink. Nitrogen atoms are shown in blue. Image was generated using PyMOL© version 1.5.0.3.

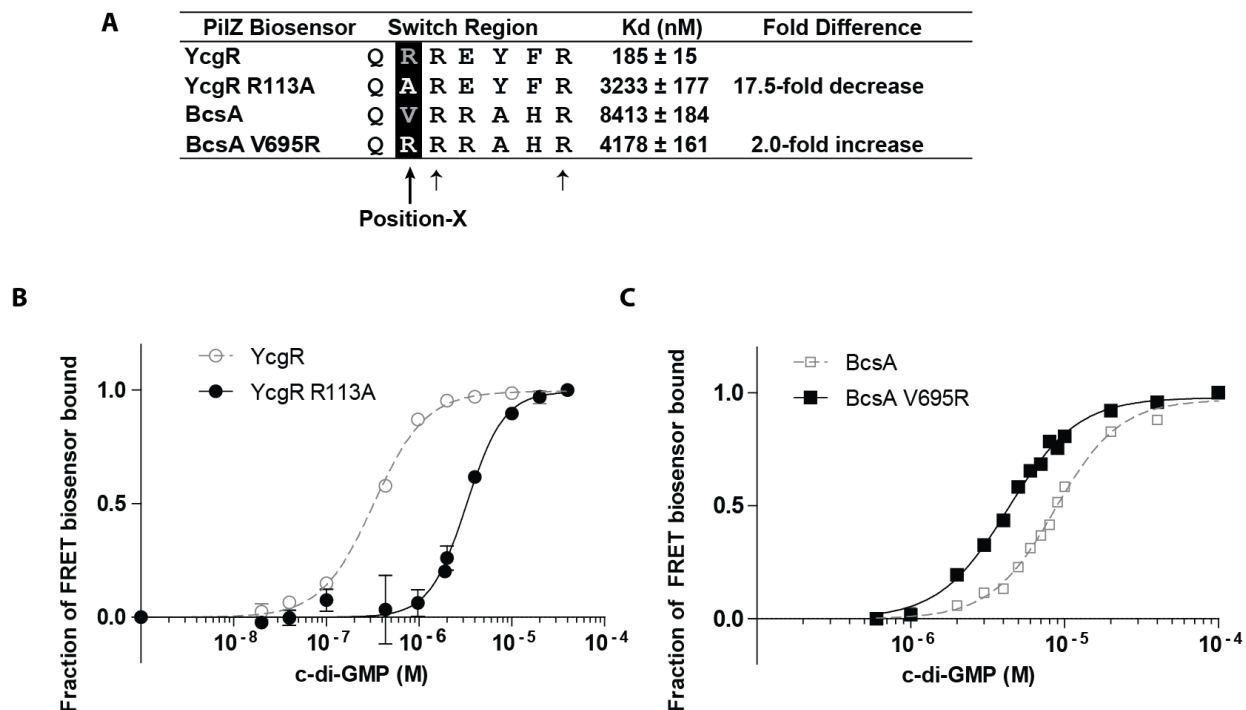


Figure 4.4: Mutation of the “Position-X” residues in *S. Typhimurium* PilZ domain proteins alters their affinities for c-di-GMP. (a) Table showing the c-di-GMP switch region for YcgR and BcsA. Shown in white are mutated residues. Small arrows indicate the positions of the invariant arginines of the RxxxR motif. The affinities shown are for proteins measured at 25°C. (b) c-di-GMP titration curve for YcgR wild-type (open circles) and YcgR R113A (closed circles) FRET biosensors at 25°C. (c) c-di-GMP titration curves for BcsA PilZ wild-type (open squares) and BcsA PilZ V695R (closed squares) FRET biosensors at 25°C.

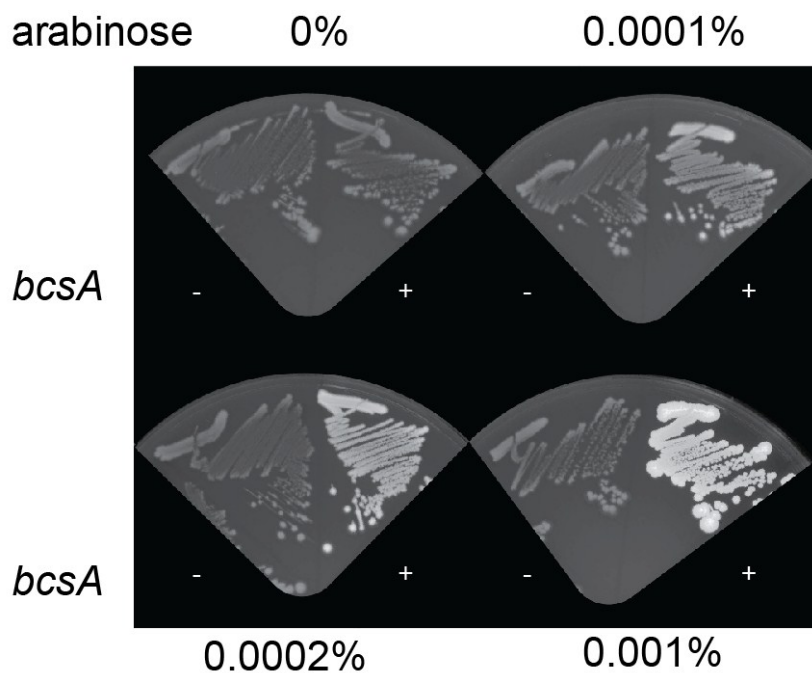


Figure 4.5: A *S. Typhimurium* strain harboring a chromosomal arabinose-inducible DGC generates cellulose in the presence of arabinose. Cellulose production on calcofluor-agar plates with the indicated concentrations of arabinose for *S. Typhimurium ara::DGC*, or *S. Typhimurium ara::DGC* in which the *bcsA* gene has been deleted. As the concentration of arabinose is increased, calcofluor fluorescence is also increased.

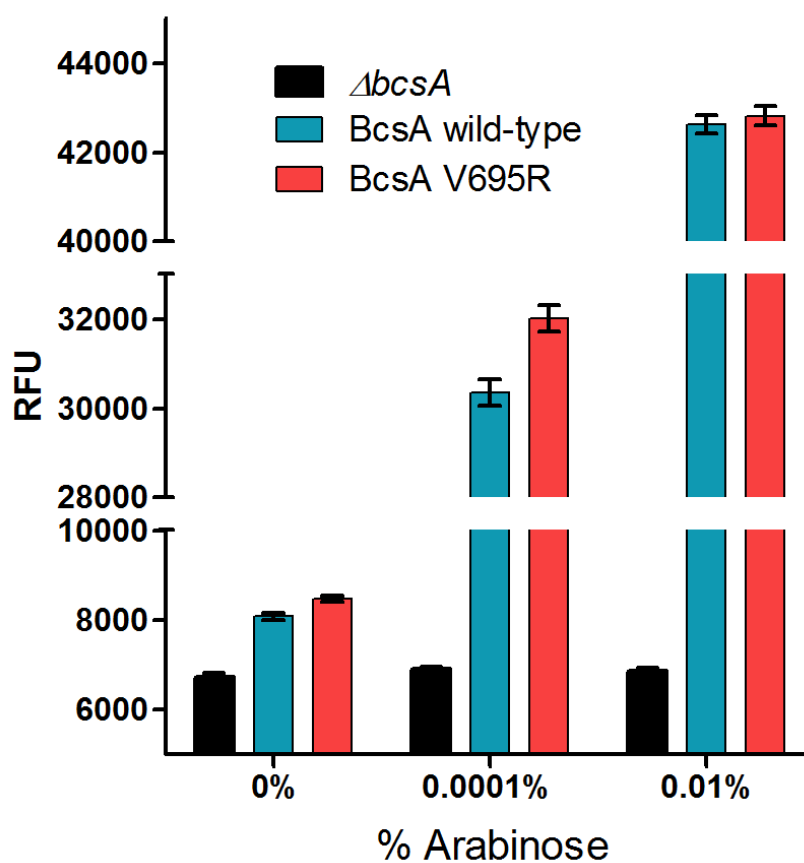


Figure 4.6: A *S. Typhimurium* strain harboring the higher-affinity *bcsA-V695R* mutation produces more cellulose at low levels of c-di-GMP than a *bcsA* wild-type strain. Calcofluor fluorescence at different concentrations of arabinose for *S. Typhimurium ara::DGC* (BcsA wild-type), or *S. Typhimurium ara::DGC* in which the *bcsA* gene has either been deleted ($\Delta bcsA$) or mutated (*bcsA-V695R*). Shown is the average fluorescence emission intensity at 420 nm, after excitation at 365 nm. n.s. = not significant.

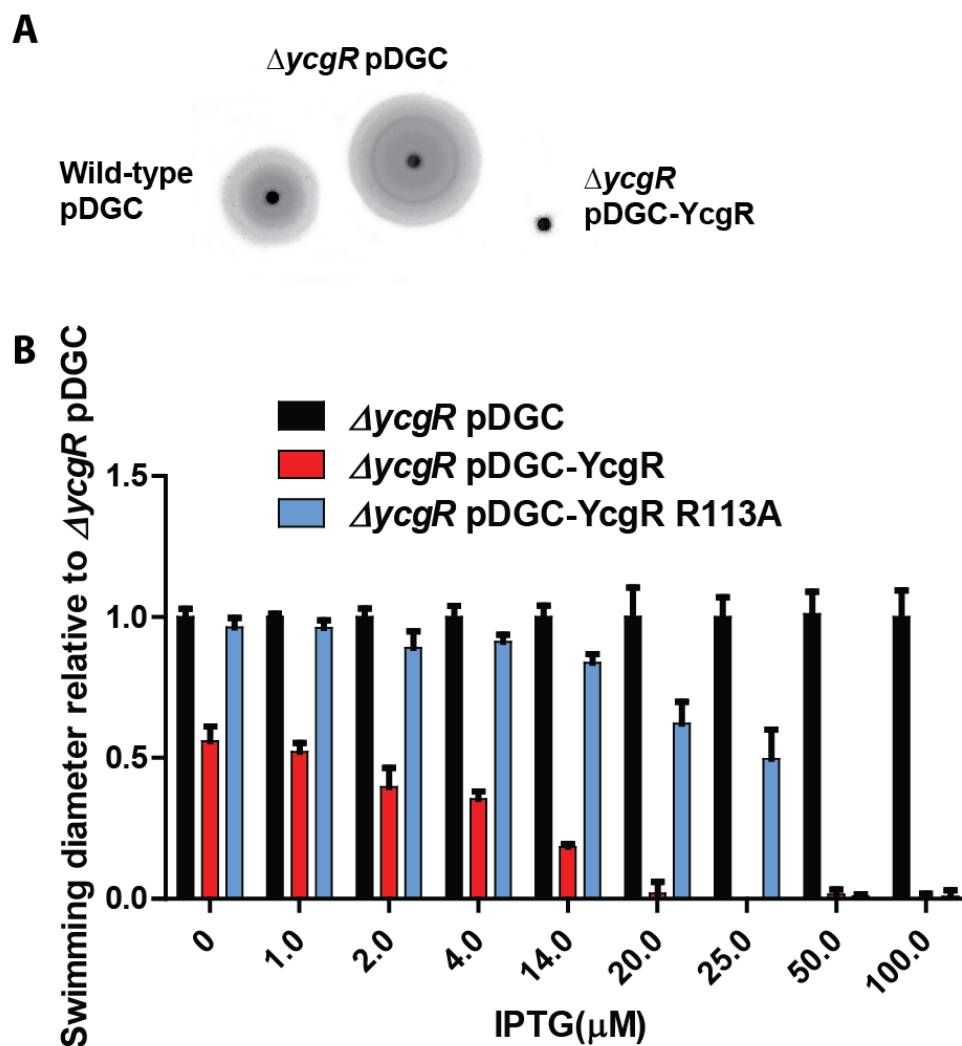


Figure 4.7: The YcgR R113A mutation increases the amount of c-di-GMP needed for YcgR to inhibit motility in *S. Typhimurium*. (a) Motility assay on soft-agar plates with 25 μ M IPTG of *S. Typhimurium* strains harboring pDGC or pDGC-YcgR at 37°C for 12 hours. A wild-type strain without exogenous DGC was not shown since the swimming diameter of this strain is much larger than that of strains harboring pDGC even in the absence of YcgR. (b) Swimming diameters of *S. Typhimurium* $\Delta ycgR$ harboring either pDGC-YcgR or pDGC-YcgR R113A, relative to the swimming diameter of the uncomplemented *S. Typhimurium* $\Delta ycgR$ strain, at indicated levels of IPTG at 37°C. Both YcgR and YcgR R113A effect a decrease in motility at increasing IPTG levels, but the YcgR R113A mutant protein requires a higher concentration of IPTG to inhibit motility than the wild-type YcgR protein.

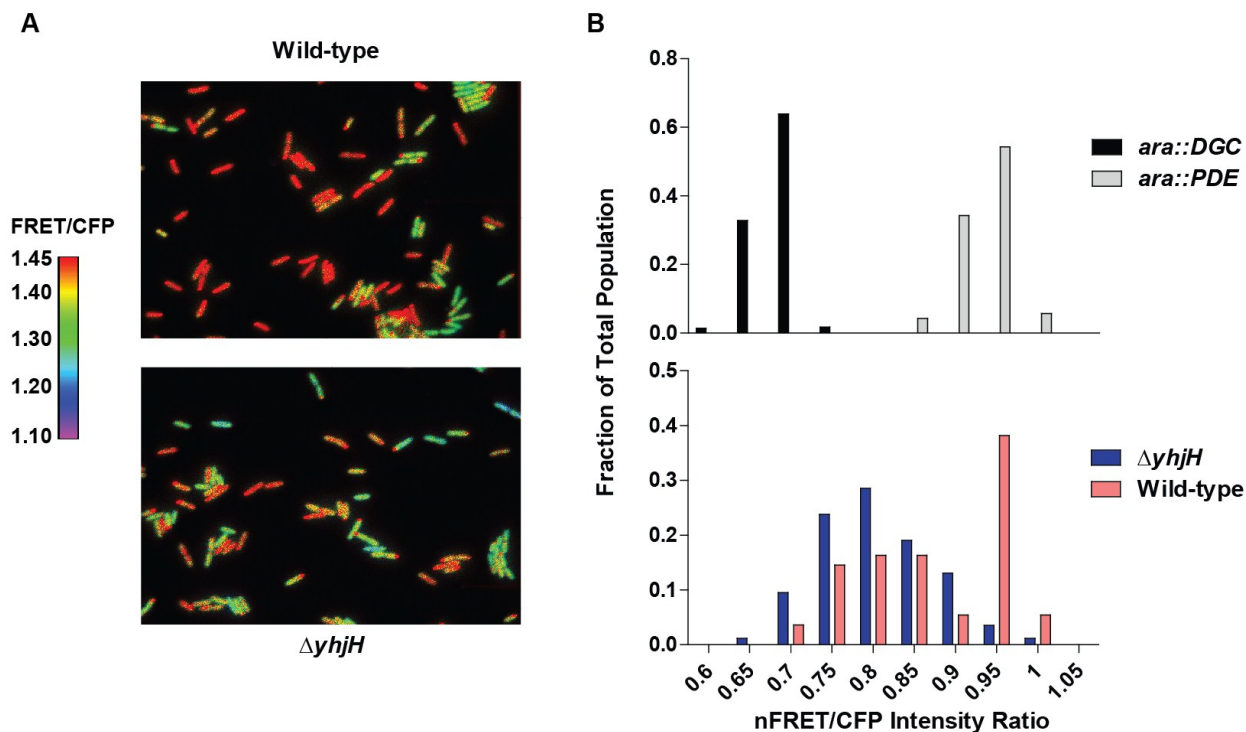


Figure 4.8: A *S. Typhimurium* strain harboring a *yhjH* mutation demonstrates a larger proportion of cells with c-di-GMP bound to YcgR than the wild-type strain. (a) Dual-emission ratio microscopic images (FRET/CFP) of *S. Typhimurium* (above) or a *yhjH* mutant (below) expressing pYcgR-Spy (see Chapter 5). Pseudocolors represent emission ratios (527/480 nm) of the FRET-based biosensor as indicated by the figure legend to the left. (b) Histogram showing the fraction of cells that demonstrate the indicated average nFRET/CFP ratios for either control strains expressing a DGC or a PDE off of an arabinose-inducible promoter (top), or for wild-type or *yhjH* mutant strains (bottom). nFRET/CFP ratios differ from FRET/CFP ratios since nFRET intensities have been corrected for bleedthrough and fluorescence in the YFP channel. The difference between the wild-type and $\Delta yhjH$ strains is highly significant ($P < 0.0001$). nFRET: net FRET intensity, calculated by subtracting bleedthrough coefficients and intensity of the YFP channel as detailed in Materials and Methods. All analyses were performed at 37°C.

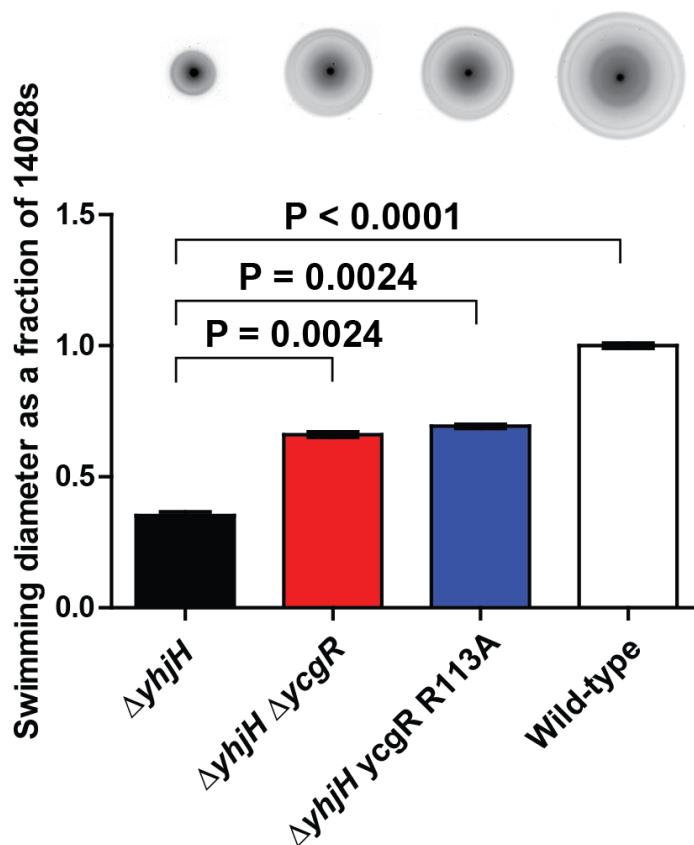


Figure 4.9: *S. Typhimurium* strain harboring the lower-affinity *ycgR-R113A* mutation does not demonstrate YcgR-dependent motility inhibition in a $\Delta yhjH$ mutant. Above: swimming diameters (from left to right) of $\Delta yhjH$, $\Delta yhjH \Delta ycgR$, $\Delta yhjH ycgR-R113A$, and wild-type *S. Typhimurium* strains, on soft-agar plates incubated at 37°C for 9 hours. Below: quantitation of the swimming diameters of indicated *S. Typhimurium* $\Delta yhjH$ mutant strains compared to the wild-type strain. Statistical significance is indicated. The $\Delta yhjH \Delta ycgR$ and $\Delta yhjH ycgR-R113A$ mutant strains demonstrated the same level of statistical significance compared to the $\Delta yhjH$ mutant strain.

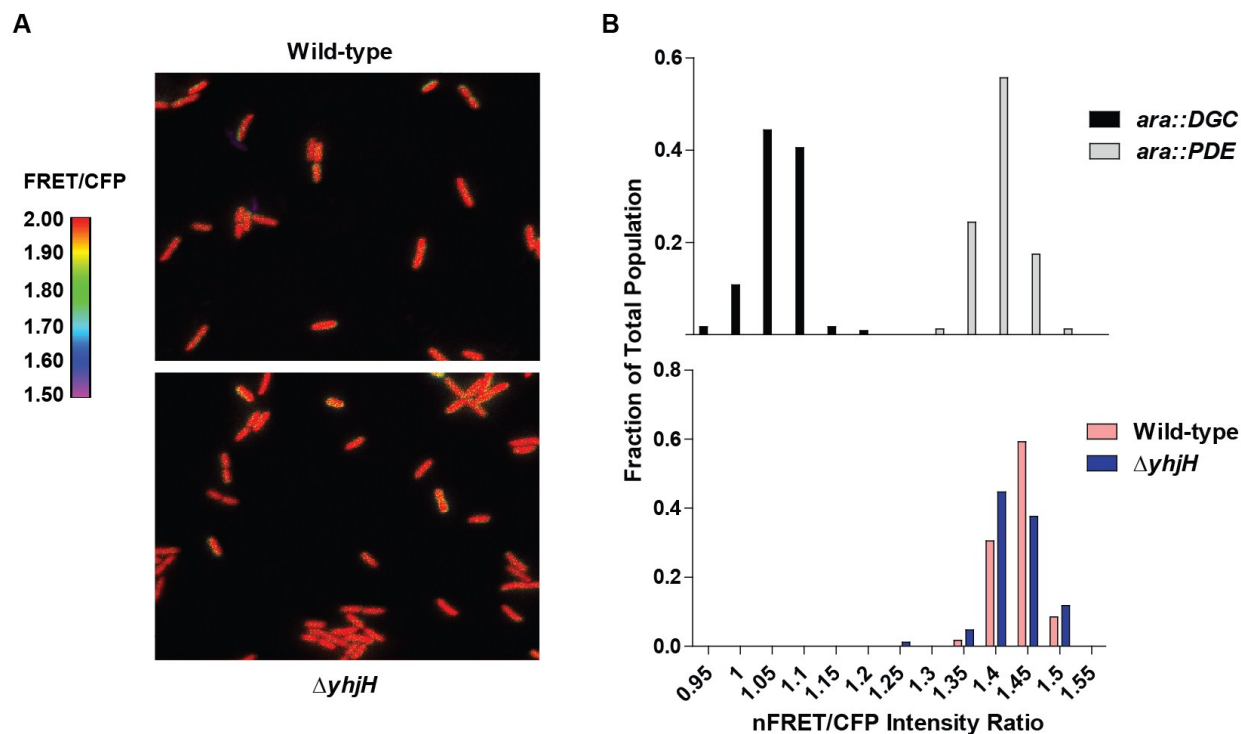


Figure 4.10: A *S. Typhimurium* $\Delta yhjH$ mutant strain does not demonstrate a difference in c-di-GMP binding to the BcsA PilZ domain as compared to the wild-type strain. (a) Dual-emission ratio microscopic images (FRET/CFP) of wild-type (top) or $\Delta yhjH$ mutant (bottom) *S. Typhimurium* expressing pBcsA-Spy (see Chapter 5). Pseudocolors represent emission ratios (527/480 nm) of the FRET-based biosensor as indicated by the figure legend to the left. (b) Histogram showing the fraction of cells that demonstrate the indicated nFRET/CFP ratios for control strains expressing a DGC or a PDE off of an arabinose-inducible promoter (top) and either wild-type or $\Delta yhjH$ mutant strains (bottom). nFRET/CFP ratios are different than FRET/CFP ratios since nFRET intensities have been corrected for bleedthrough and fluorescence in the YFP channel. nFRET: net FRET intensity, calculated by subtracting bleedthrough coefficients and intensity of the YFP channel as detailed in Materials and Methods. The difference in nFRET/CFP ratios between the wild-type and the $\Delta yhjH$ is not significant ($P > 0.05$). All analyses were performed at 37°C.

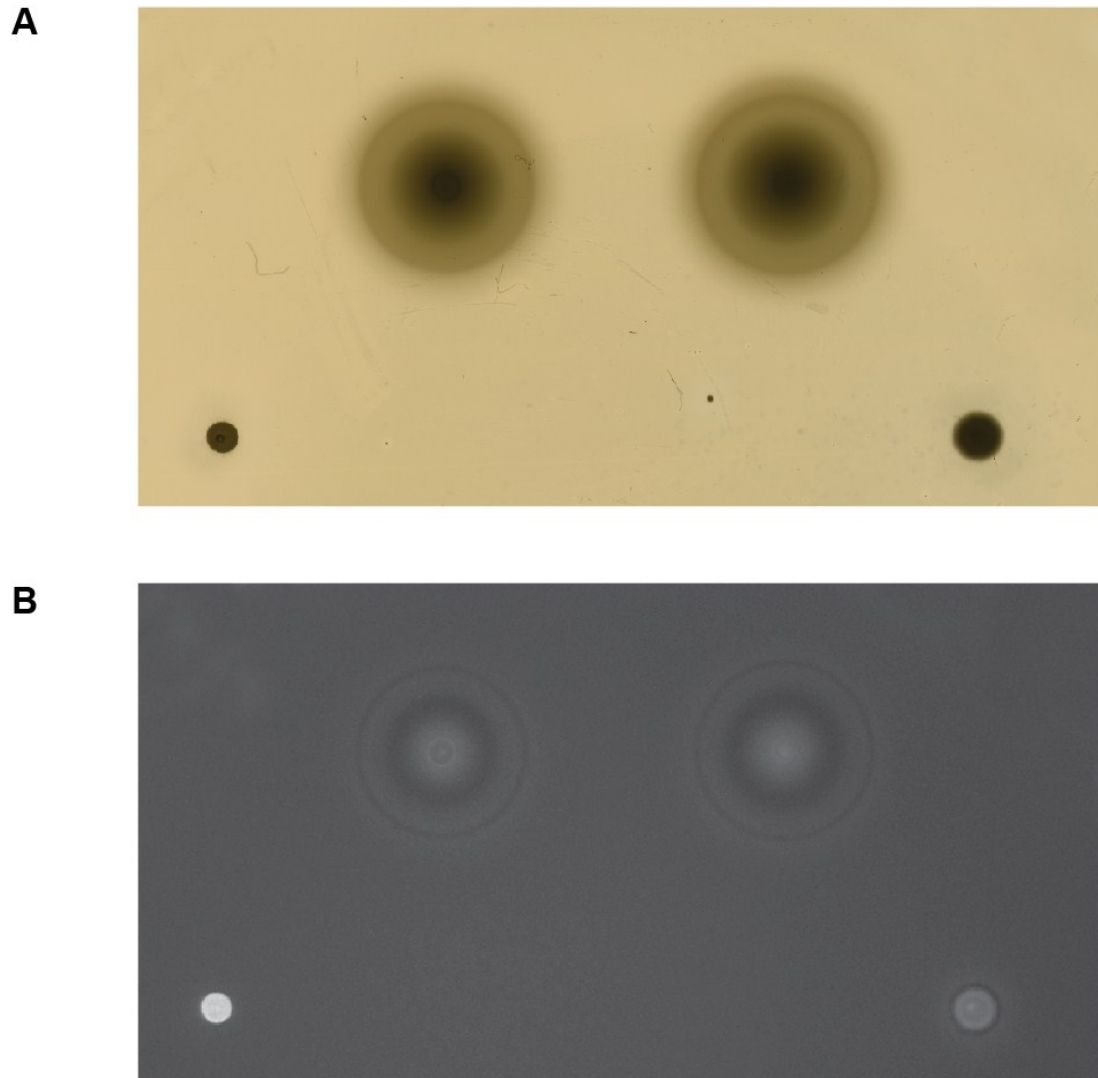


Figure 4.11: A *S. Typhimurium* $\Delta yhjH$ mutant strain does not produce cellulose on a soft-agar motility plate. (a) Visible light and (b) UV images of strains of *S. Typhimurium* on soft-agar motility plates with calcofluor, incubated at 37°C for 12 hours. From left: *S. Typhimurium* pDGC, $\Delta yhjH$, $\Delta yhjH \Delta bcsA$, $\Delta bcsA$ pDGC.

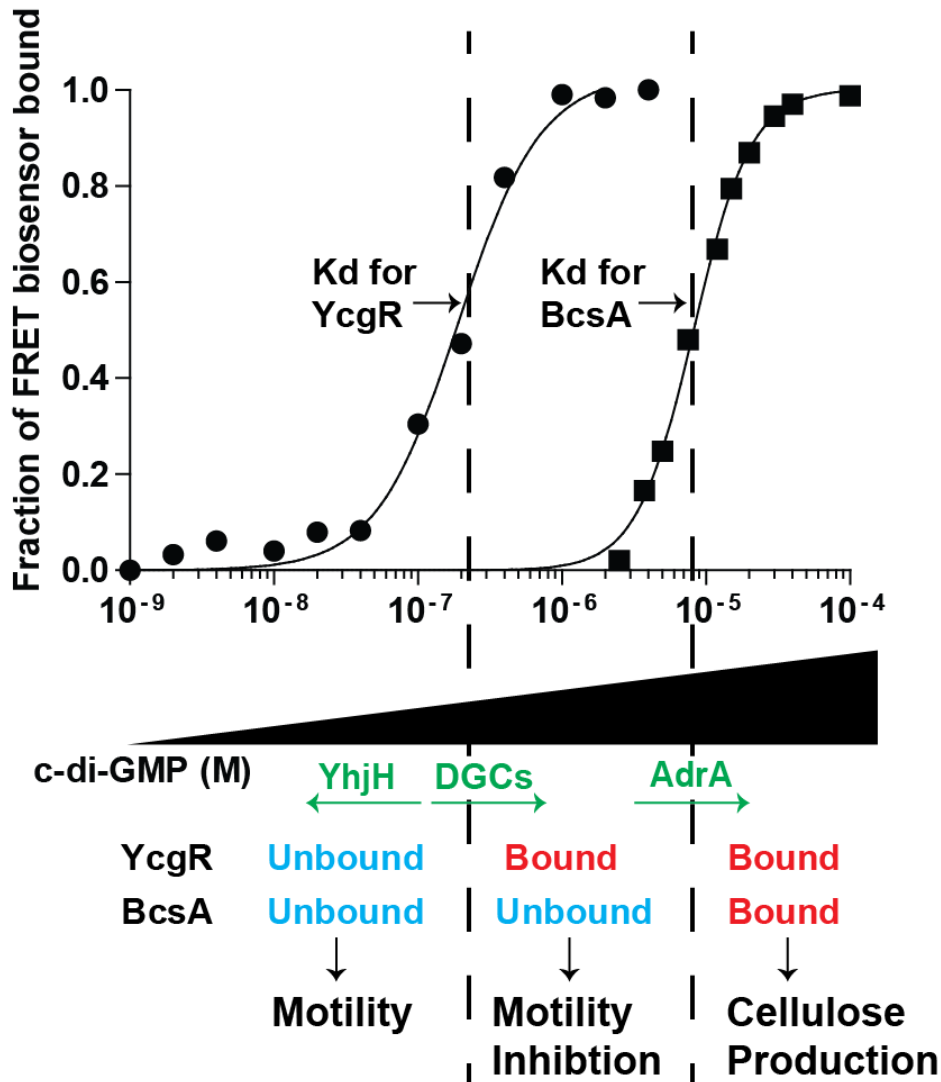


Figure 4.12: The binding affinities of YcgR and BcsA for c-di-GMP determine cellular phenotypes. When cellular c-di-GMP levels are kept low by PDEs such as YhjH, neither PilZ domain protein is bound to c-di-GMP, resulting in a motile cell that does not produce cellulose. As cellular DGCs increase the concentration of c-di-GMP past the K_d for YcgR, YcgR becomes bound to c-di-GMP and thus inhibits motility, even at levels of c-di-GMP that are not high enough to bind BcsA. Activation of AdrA expression results in enough c-di-GMP being produced to bind to BcsA, and cellulose synthesis occurs.

Table 4.1: Survival of mice inoculated with PilZ domain protein deletion mutant strains of *S. Typhimurium*

Inoculum size: 100 cells

Strain	# of mice surviving (n=4)		
	Day 0	Day 4	Day 5
14028s	4	4	0
$\Delta bcsA$	4	1	0
$\Delta ycgR$	4	3	1
$\Delta bcsA \Delta ycgR$	4	4	0

Inoculum size: 10 cells

Strain	# of mice surviving (n=4)			
	Day 0	Day 4	Day 5	Day 6
14028s	4	3	3	3
$\Delta bcsA$	4	3	1	1
$\Delta ycgR$	4	3	2	0
$\Delta bcsA \Delta ycgR$	4	4	1	1

CHAPTER 5: BIOSENSORS WITH ALTERED AFFINITIES FOR C-DI-GMP EXPAND THE MEASURABLE RANGE OF C-DI-GMP *IN VIVO*

Summary

Many important questions in the c-di-GMP signaling field can only be answered by measuring free c-di-GMP concentrations in live, individual cells *in vivo*. This type of measurement can be achieved by expressing FRET-based c-di-GMP biosensors in live cells that report on the concentration of c-di-GMP available to the receptor in real time. Here we present the construction of three new FRET-based *in vivo* biosensors, using c-di-GMP binding receptors that vary in their affinities for c-di-GMP. These receptors are capable of separating populations of cells based on their c-di-GMP concentrations. Correlation of specific FRET/CFP ratios observed *in vivo* to particular c-di-GMP concentrations will allow for the accurate determination of the free c-di-GMP concentration from the nanomolar to the micromolar range in live individual cells.

Introduction

The work presented in the previous two chapters provides evidence that many different c-di-GMP concentrations, including intermediate levels, can have diverse effects on cellular behavior, and that even small alterations in c-di-GMP levels can lead to significant physiological

changes (Table 1.1, Figure 4.7, Figure 4.8). The ability to accurately measure c-di-GMP concentrations *in vivo* under different environmental conditions, and to correlate these levels to cellular behavior, is thus essential to answering many questions about c-di-GMP signaling.

Several techniques exist for measuring the intracellular concentration of c-di-GMP (Chapter 1, Section iv). Chromatographic methods coupled to mass spectrometry, which determine the concentration of c-di-GMP in batch culture, are most frequently used to measure cytoplasmic c-di-GMP concentrations (10, 114, 119). However, these methods have several inherent limitations. First, chromatographic methods are capable of measuring the average c-di-GMP concentration for a large number of cells, but they are not informative regarding cell-cell heterogeneity in second messenger concentration within a population. It is now clear that even planktonic cells grown under the same environmental conditions demonstrate large differences in c-di-GMP concentrations (23) (Figure 4.8). Second, these methods measure the total c-di-GMP present in the cell; however, much of the intracellular c-di-GMP may actually exist in the bound state (139), and it is the free cytoplasmic level of c-di-GMP that determines its binding to downstream receptors. Finally, chromatographic methods represent endpoint measurements, in which cells are destroyed and nucleotides are extracted using extensive extraction protocols (114, 119). These assays are thus not conducive to monitoring fluctuations of second messenger concentrations. Since c-di-GMP can be rapidly created and degraded by cellular DGCs and PDEs (Chapter 1), it would be beneficial to be able to monitor the fluctuating levels of c-di-GMP in response to environmental stimuli during dynamic cellular processes.

To overcome these limitations, Christen *et al* constructed a genetically-encoded c-di-GMP biosensor by fusing the FRET pair mCyPet and mYPet to the c-di-GMP-binding protein YcgR (23). mCyPet and mYPet are fluorescent proteins that have been evolutionarily optimized

for FRET (81). FRET-based biosensors have been used in eukaryotic cells to monitor the concentrations of many small molecules such as cGMP and calcium (27, 78, 84, 87, 107, 130, 147). With these biosensors, the FRET/CFP ratio is used as a readout for the binding state of the biosensor inside of live cells, which in turn can be correlated to a specific c-di-GMP concentration based on the affinity of the biosensor for c-di-GMP (23). The YcgR-based c-di-GMP biosensor is the first construct that applies this method to the analysis of small molecule concentrations inside of bacterial cells. Measuring intracellular c-di-GMP *in vivo* using the FRET-based YcgR biosensor has several advantages over chromatographic methods. Binding of this biosensor to c-di-GMP can be visualized in individual cells using fluorescence microscopy, allowing the measurement of variability in c-di-GMP concentrations within a population. Since this technique measures only the c-di-GMP that is available to the biosensor, it measures the free cytoplasmic concentration of c-di-GMP, not the total amount. Also, since the YcgR biosensor binds to c-di-GMP both rapidly and reversibly, it can be utilized to monitor rapid c-di-GMP fluctuations during dynamic cellular processes. Additionally, this technique does not require the addition of any exogenous reagents. Thus this method is capable of measuring the biologically effective cellular concentrations of c-di-GMP in individual live cells in real time.

However, estimating c-di-GMP concentrations using this FRET-based technique has an important limitation. The YcgR-based c-di-GMP biosensor can only accurately measure c-di-GMP concentrations between approximately 50 and 700 nM at 25°C, since its range of measurement is limited by the binding affinity of YcgR for c-di-GMP. Resolution of c-di-GMP concentrations beyond this range is impossible using this biosensor. Examinations of binding affinities of c-di-GMP-binding receptors indicate that c-di-GMP levels are likely capable of spanning a large concentration range even within the same organism (Table 1.1). Measuring c-

di-GMP concentrations using the YcgR biosensor alone would not be sensitive to differences in concentration at these higher levels of c-di-GMP. In the following work, we introduce a panel of biosensors based on PilZ domain proteins that have lower affinities for c-di-GMP than YcgR, thus expanding the range of c-di-GMP concentrations that can be measured using this technique.

FRET-based biosensors that demonstrate different binding affinities for c-di-GMP expand the measurable concentration range of c-di-GMP *in vitro*

In the work presented above, we generated c-di-GMP-binding FRET constructs using either the BcsA PilZ domain, or a mutant YcgR R113A protein, that demonstrate lower affinities for c-di-GMP than the YcgR FRET construct (Figure 3.1, Figure 4.3). These biosensors are capable of accurately reporting on second messenger concentrations that fall within the linear portion of their binding curves based on their FRET/CFP emission ratios. The linear region of the binding curve encompasses approximately 10% to 90% total bound biosensor in solution (Figure 5.1). Thus, the specific concentration range of measurable c-di-GMP is based on the binding affinities of these receptors. The measurable range of c-di-GMP for the YcgR wild-type, YcgR R113A mutant, and BcsA PilZ domain FRET constructs are 50-700, 1300-9000, and 3000-22000 nM, respectively, at 25°C (Figure 5.1, Table 5.1). Comparison of these c-di-GMP concentration ranges revealed that the c-di-GMP concentration range between 700-1300 nM could not be accurately measured by an existing biosensor, since at this concentration range, over 90% of the YcgR wild-type biosensor is bound to c-di-GMP, but less than 10% of the YcgR R113A biosensor is bound to c-di-GMP. An additional biosensor with an intermediate affinity for c-di-GMP was needed to cover this range.

In order to generate a biosensor with an intermediate affinity for c-di-GMP, we focused on the conserved PilZ motif DxSxxG in the wild-type YcgR protein as a potential target for affinity alteration by site-directed mutagenesis. In the *P. putida* YcgR homologue, PP4397, mutation of the serine in this motif to an alanine was shown to decrease the binding affinity of PP4397 for c-di-GMP by approximately 4.5-fold (58). Thus, we generated a S147A YcgR variant using site-directed mutagenesis of the wild-type YcgR FRET construct, and analyzed its binding to c-di-GMP. Like the wild-type YcgR FRET construct, this S147A mutant biosensor demonstrated a decrease in FRET upon the addition of c-di-GMP (Figure 5.1). The binding affinity of the YcgR S147A FRET construct for c-di-GMP was then measured by increasing c-di-GMP into a solution containing purified YcgR S147A biosensor and monitoring the corresponding decrease in FRET. The S147A mutant was found to bind c-di-GMP with an affinity of 478 ± 38 nM at 25°C, representing a 2.7-fold decrease in affinity from the wild-type YcgR protein (Figure 5.2). The Hill coefficient for binding was approximately 1.6 ± 0.2 . Based on the linear range of the binding curve, this protein is capable of accurately measuring the c-di-GMP concentration from 120-2100 nM at 25°C. Thus, by constructing this YcgR S147A mutant, we completed a panel of biosensors that expands the measurable range of c-di-GMP concentrations from 50 nM to 22 μ M at 25°C, over two orders of magnitude (Table 5.1).

FRET- based biosensors with different affinities for c-di-GMP distinguish between populations of cells with high and low c-di-GMP levels *in vivo*

In order to measure the concentration of c-di-GMP *in vivo*, these biosensors must demonstrate a different FRET/CFP ratio when bound or unbound to c-di-GMP inside of live cells. To test this, we examined the ability of these biosensors to distinguish between two populations of cells in which the level of c-di-GMP had been artificially manipulated to be either very high or very low. This was done by expressing the biosensors in two separate strains of *S. Typhimurium* that harbored either a strong DGC or a strong PDE expressed off of the native chromosomal arabinose-inducible promoter (Figure 4.5, these strains were used as controls in Figure 4.8 and in Figure 4.10). The addition of arabinose into the growth media of the *ara::DGC* or *ara::PDE* strains results in the generation of large amounts of intracellular c-di-GMP, or its degradation, respectively, as determined by effects on cellular phenotypes (Figure 4.1 and data not shown). Thus, these strains represent a model system in which the ability of FRET-based c-di-GMP biosensors to discriminate between populations of high and low c-di-GMP levels can be tested.

The YcgR R113A and BcsA PilZ *in vivo* biosensor plasmids were constructed in the same IPTG-inducible expression vector as the wild-type YcgR biosensor plasmid (23). The YcgR S147A *in vivo* expression construct is currently in progress. The YcgR R113A and BcsA PilZ biosensor plasmids were transformed into the *ara::DGC* strain and the *ara::PDE* strain. Transformed cells were grown in modified M9 media to exponential phase in the presence of IPTG and arabinose. Cells were then immobilized on agar pads, and the FRET and CFP emission intensities upon excitation at 425 nm for each individual cell were measured using a fluorescence microscope coupled to a sensitive EMCCD camera. The wild-type YcgR biosensor, which had already been shown to discriminate between cells containing high and low levels of c-di-GMP (23), was able to clearly distinguish between these strains based on their

FRET/CFP ratios (Figure 5.3). Similarly, expression of either the YcgR R113A or BcsA PilZ biosensors also demonstrated clear separation of the *ara::DGC* and *ara::PDE* strains into two distinct populations based on their FRET/CFP ratios (Figure 5.4, 5.5). The *ara::DGC* and *ara::PDE* populations demonstrated different trajectories when the nFRET values were plotted against the CFP intensity values (Figures 5.3B, 5.4B, 5.5B), suggesting that these biosensors could be used to measure intermediate FRET/CFP ratios. This demonstrates the utility of these biosensors for measuring c-di-GMP concentrations *in vivo*.

Discussion

This work characterizes three new c-di-GMP biosensors that show promise for the accurate measurement of c-di-GMP inside of live cells over a large range of concentrations. Although the S147A YcgR biosensor remains to be tested *in vivo*, the YcgR R113A and BcsA PilZ biosensors are able to distinguish between populations of high and low c-di-GMP levels without overlap, based on their FRET/CFP ratios. Several key experiments remain before these biosensors can be applied to measure specific concentrations of c-di-GMP in live cells. An important control experiment is to express a FRET construct that does not bind c-di-GMP in strains in which c-di-GMP is artificially modulated, to verify that the expression of a DGC or PDE does not induce the production of some other factor that alters the FRET/CFP ratio. In addition, to correlate *in vivo* FRET/CFP ratios of these biosensors to specific c-di-GMP concentrations, the FRET/CFP ratios of purified biosensors should be determined *in vitro* using the same microscope settings and conditions as for *in vivo* FRET/CFP ratio measurements. One

way to accomplish this is by analyzing the FRET/CFP ratios of purified, His-tagged biosensor immobilized to Ni-NTA silica beads in the presence of different concentrations of c-di-GMP (Figure 5.6). Since PilZ domain protein binding affinities vary with temperature (Figure 3.3), this analysis should be performed at every temperature at which *in vivo* measurements are performed. This will allow for the assignment of specific *in vivo* FRET ratios for each biosensor to particular c-di-GMP concentrations.

Using these biosensors as a molecular scale for c-di-GMP has many potential applications. One of these is analyzing the effects of inactivation of various DGCs or PDEs (Figure 4.8, Figure 4.10). These biosensors may also be used to compare the relative activities of overexpressed DGCs or PDEs *in vivo*: some of these c-di-GMP-metabolizing enzymes may affect intracellular c-di-GMP concentrations to a significantly larger extent than others, due to factors such as feedback inhibition. Expressing biosensors with altered affinities for c-di-GMP will also provide insight into the extent of the heterogeneity of c-di-GMP concentrations in populations where environmental conditions are kept constant, such as growth in broth culture. Another application is determining how environmental conditions contribute to fluctuating c-di-GMP levels during various cellular processes, such as the cell cycle (23). Finally, computational methods that allow for the deconvolution of two or more FRET signals expressed simultaneously will allow expression of multiple FRET-based c-di-GMP biosensors in the same cell (1, 41, 82).

Tables and Figures

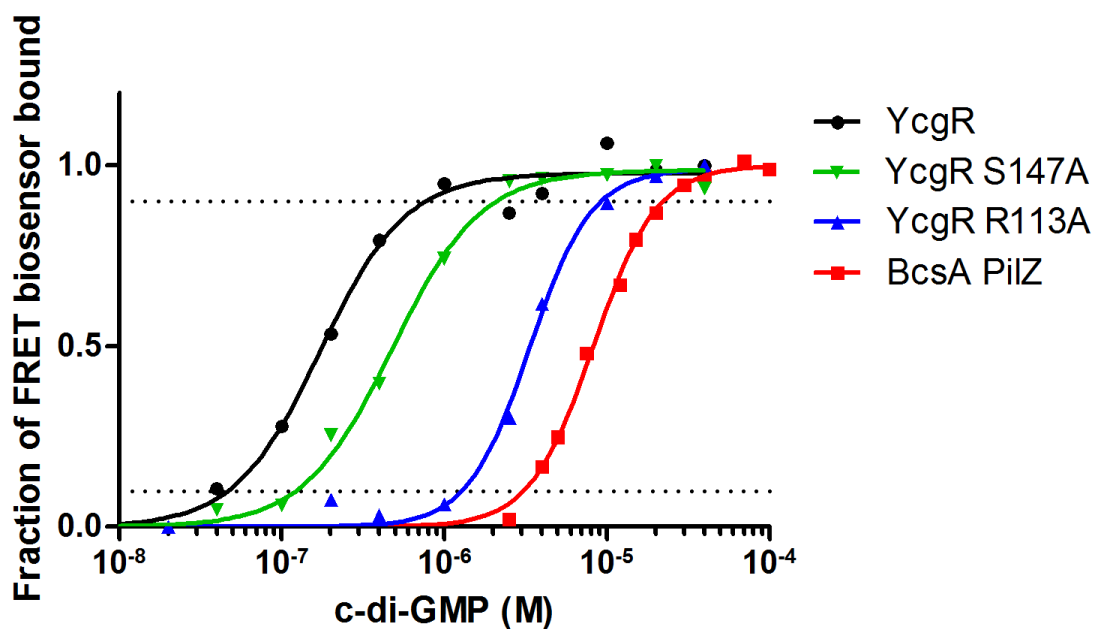


Figure 5.1: c-di-GMP binding curves of FRET-based biosensors used in this study. For each biosensor, the fraction of FRET biosensor bound to c-di-GMP was calculated by measuring the FRET/CFP ratio at each indicated c-di-GMP concentration, subtracting the unbound FRET/CFP ratio, and dividing this number by the difference between the bound and unbound FRET ratios. A number of 0 indicates that the FRET biosensor is completely unbound to c-di-GMP, and a number of 1 indicates that the FRET biosensor is completely bound to c-di-GMP. ● YcgR; ▼ YcgR S147A; ▲ YcgR R113A; ■ BcsA PilZ. Dotted lines indicate the FRET/CFP ratios at which 10% or 90% of the total FRET biosensor is bound.

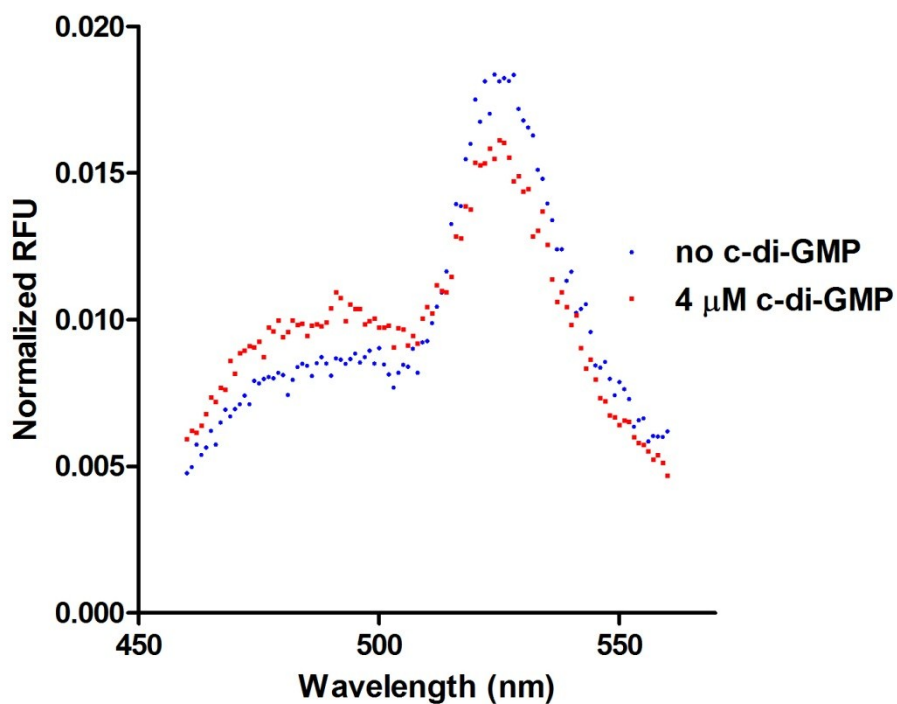


Figure 5.2: Fluorescence emission spectra of the YcgR S147A biosensor. 100 nM YcgR S147A biosensor was excited at 425 nm at 25°C, in the presence and absence of c-di-GMP, and the emission spectra were recorded. Addition of c-di-GMP to the YcgR S147A biosensor results in a decrease in the YFP to CFP emission ratios (525/480).

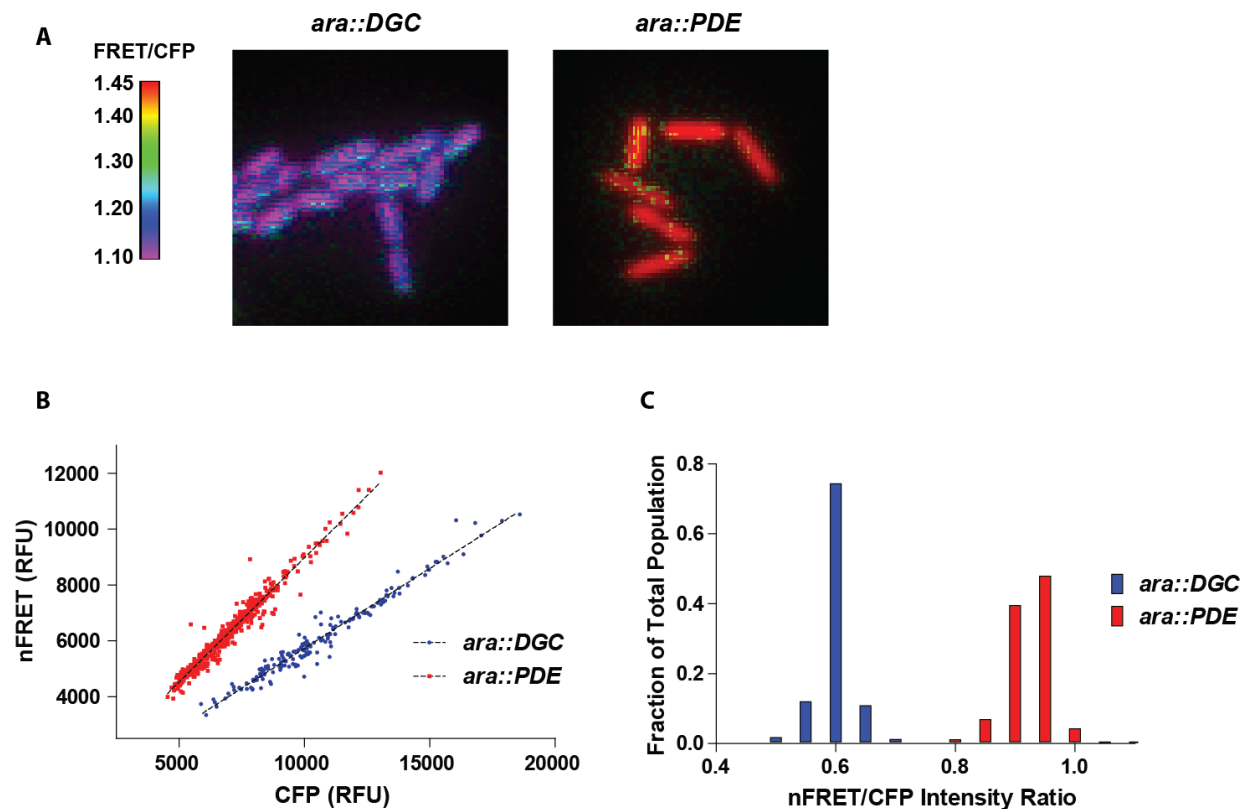


Figure 5.3: Expression of the YcgR biosensor differentiates between cells overexpressing a DGC and cells overexpressing a PDE. (a) Dual-emission ratio microscopic images (FRET/CFP) of cells expressing a DGC (*ara::DGC*) or a PDE (*ara::PDE*) and the YcgR biosensor. Pseudocolors represent emission ratios (527/480 nm) of the FRET-based biosensor as indicated by the figure legend to the left. (b) Dot plot illustrating the FRET/CFP ratios of cells expressing either a DGC or a PDE in addition to the YcgR biosensor. Each dot represents the FRET and CFP emission intensities of an individual cell. Expression of the biosensor separates the strains into two distinct populations based on their FRET/CFP ratios. (c) Histogram showing the fraction of cells that demonstrate the indicated nFRET/CFP ratios for strains expressing either a DGC or a PDE. nFRET: net FRET intensity, calculated by subtracting bleedthrough coefficients and intensity of the YFP channel as detailed in Materials and Methods. All analyses were performed at 30°C.

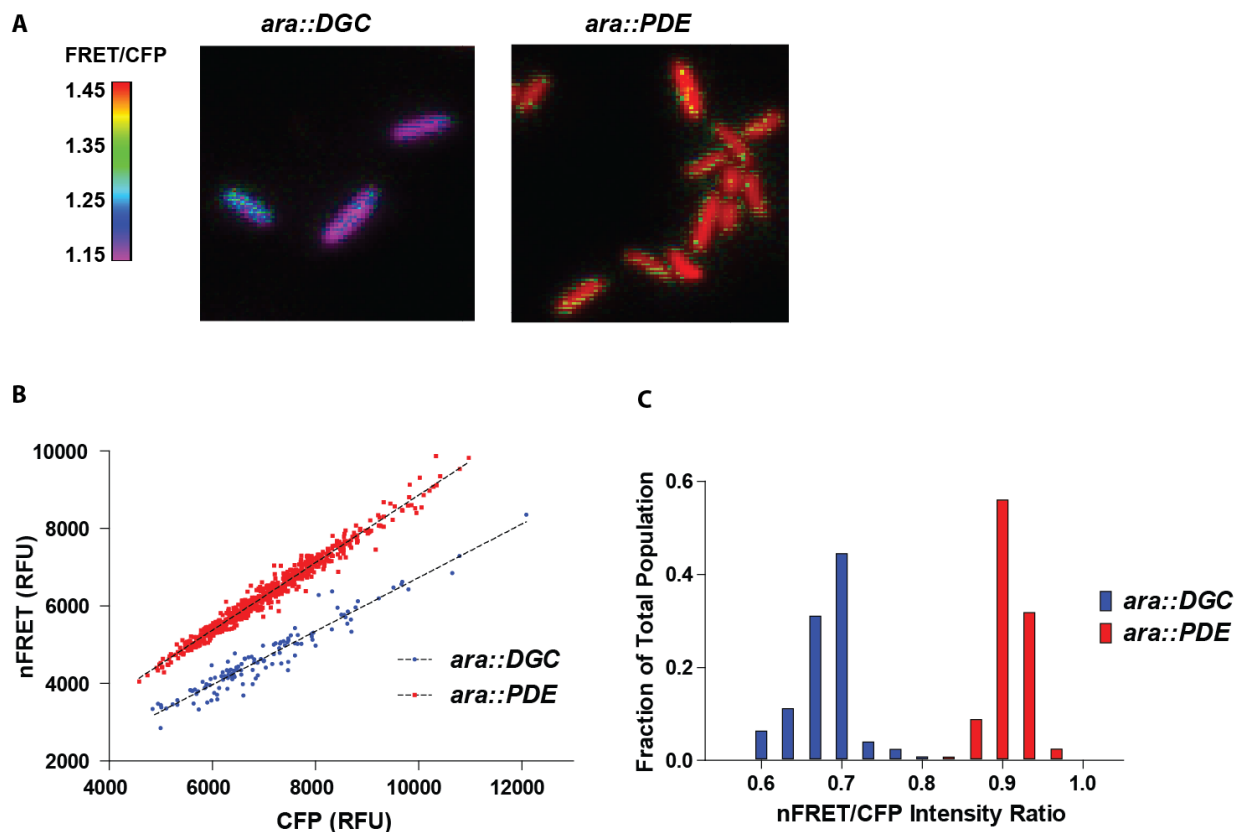


Figure 5.4: Expression of the YcgR R113A biosensor differentiates between cells overexpressing a DGC and cells overexpressing a PDE. (a) Dual-emission ratio microscopic images (FRET/CFP) of cells expressing a DGC (*ara::DGC*) or a PDE (*ara::PDE*) and the YcgR R113A biosensor. Pseudocolors represent emission ratios (527/480 nm) of the FRET-based biosensor as indicated by the figure legend to the left. (b) Dot plot illustrating FRET/CFP ratios of cells expressing either a DGC or a PDE, in addition to the YcgR R113A biosensor. Each dot represents the FRET and CFP emission intensities of an individual cell. Expression of the biosensor separates the strains into two distinct populations based on their FRET/CFP ratios. (c) Histogram showing the fraction of cells that demonstrate the indicated FRET/CFP ratios for strains expressing either a DGC or a PDE. nFRET: net FRET intensity, calculated by subtracting bleedthrough coefficients and intensity of the YFP channel as detailed in Materials and Methods. All analyses were performed at 30°C.

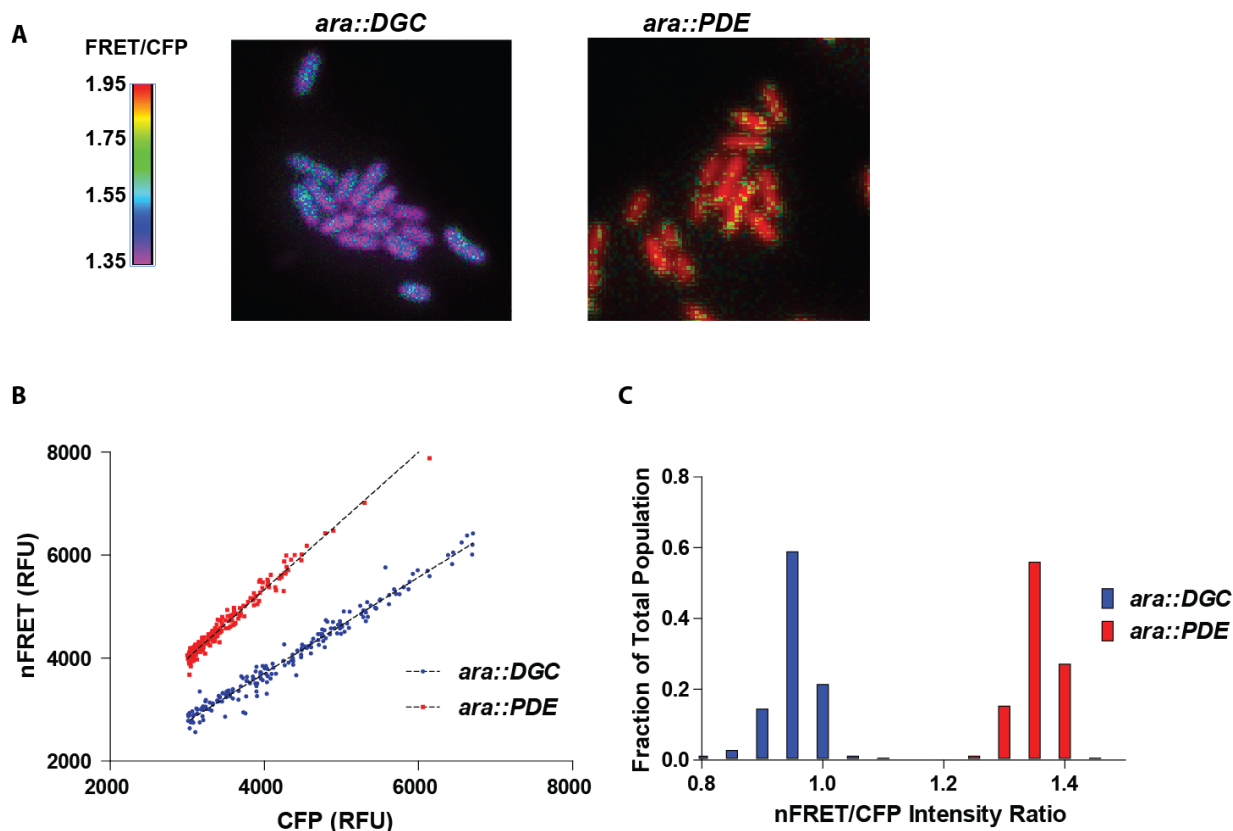


Figure 5.5: Expression of the BcsA PilZ biosensor differentiates between cells overexpressing a DGC and cells overexpressing a PDE. (a) Dual-emission ratio microscopic images (FRET/CFP) of cells expressing a DGC (*ara::DGC*) or a PDE (*ara::PDE*) and the BcsA PilZ biosensor. Pseudocolors represent emission ratios (527/480 nm) of the FRET-based biosensor as indicated by the figure legend to the left. (b) Dot plot illustrating FRET/CFP ratios of cells expressing either a DGC or a PDE, in addition to the BcsA PilZ biosensor. Each dot represents the FRET and CFP emission intensities of an individual cell. Expression of the biosensor separates the strains into two distinct populations based on their FRET/CFP ratios. (c) Histogram showing the fraction of cells that demonstrate the indicated FRET/CFP ratios for strains expressing either a DGC or a PDE. nFRET: net FRET intensity, calculated by subtracting bleedthrough coefficients and intensity of the YFP channel as detailed in Materials and Methods. All analyses were performed at 30°C.

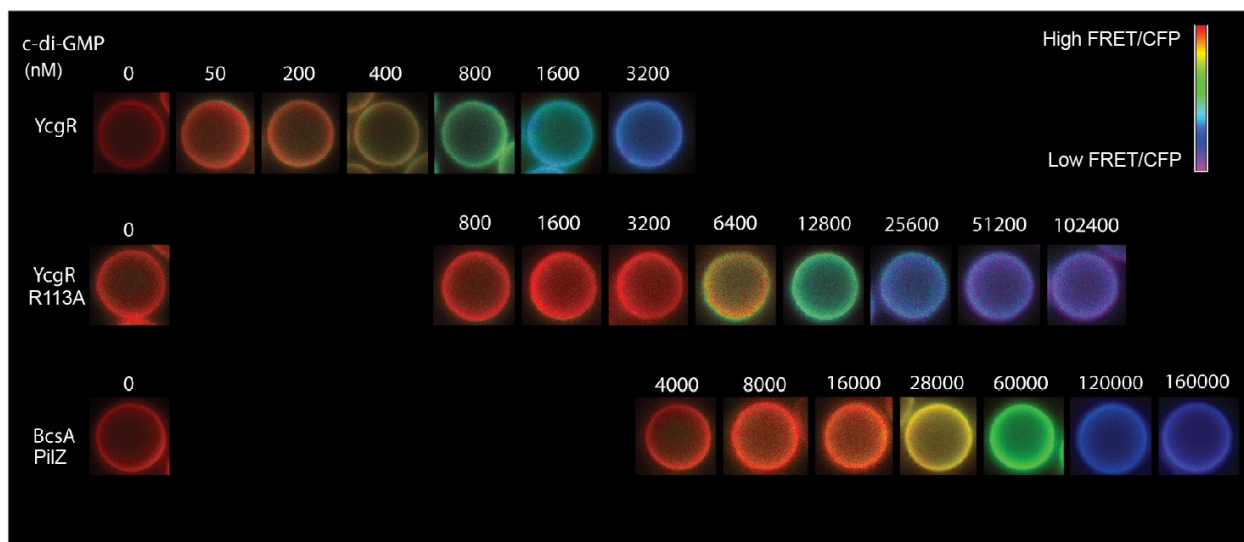


Figure 5.6: FRET/CFP ratios of purified biosensors immobilized on Ni-NTA silica beads. For each biosensor, shown is a representative image of a single bead in the presence of the indicated c-di-GMP concentration. YcgR, 12.5 nM; YcgR R113A, 12.5 nM; BcsA PilZ, 50 nM. Pseudocolors represent FRET/CFP ratios as indicated by the legend at right. Individual FRET/CFP ratios were: YcgR, 1.5-2.3; YcgR R113A, 1.15-1.65; BcsA PilZ 2-4.7. The higher FRET ratios as determined in this experiment compared to those of the *in vivo* measurements are due to differences in optical configurations used for imaging (see Materials and Methods), and also may be affected by intermolecular FRET of individual biosensor molecules loaded adjacent to each other on the bead. This experiment was performed at 30°C.

Table 5.1: Measureable range of c-di-GMP concentrations for biosensors used in this study

Biosensor	Kd (nM) ¹	Measurement Range (nM) ²
YcgR	174 ± 14	50-700
YcgR S147A	478 ± 38	120-2100
YcgR R113A	3352 ± 280	1300-9000
BcsA PilZ	8267 ± 249	3000-22000

¹Binding affinities were measured at 25°C

²Measurement range is based on the c-di-GMP concentrations at which ~10-90% FRET biosensor is bound to c-di-GMP

CHAPTER 6: CONCLUSIONS AND FUTURE DIRECTIONS

c-di-GMP is a second messenger that is used by many bacterial species to integrate environmental information from different cellular inputs in order to direct cellular behavior. Because many GGDEF and EAL domains are physically linked to putative environmental sensing domains, the precise level of c-di-GMP in the cell is likely tightly controlled by multiple environmental signals (77). Although every DGC produces the same small, diffusible second messenger molecule, many of these enzymes can be specifically linked to a particular downstream c-di-GMP-regulated process (12, 37, 55, 112, 113). In the work above, we present evidence that one mechanism by which this signaling specificity can occur is through the selective activation of c-di-GMP receptors based on their affinities for the second messenger.

In Chapter 3, we found that the downstream targets for c-di-GMP, PilZ domain proteins, differ greatly in their affinities for c-di-GMP even within the same organism. To measure the binding affinities of PilZ domain proteins, we employed a FRET-based method in which individual PilZ domain proteins are expressed as fusion proteins with a FRET pair of fluorophores. Binding to c-di-GMP can then be assessed by monitoring the amount of FRET in these constructs, which is sensitive to small changes in protein structure. We found that the PilZ domain proteins in *S. Typhimurium* differed by 43-fold in their affinities for c-di-GMP, and the PilZ domain proteins in *P. aeruginosa* differed by 145-fold. The striking variability in c-di-GMP-binding affinities of PilZ domain proteins suggests that binding affinities may be important for the biological phenotypes of these proteins.

In Chapter 4, we take this work a step further and determine the effects of binding affinities on the biological phenotypes that have been attributed to the two PilZ domain proteins in *S. Typhimurium*, BcsA and YcgR. Increasing the binding affinity of BcsA for c-di-GMP increased the amount of cellulose that this enzyme produced at lower levels of c-di-GMP than for the wild-type enzyme. Decreasing the binding affinity of YcgR for c-di-GMP increased the amount of c-di-GMP needed for this protein to inhibit cellular motility. This decrease in binding affinity abolished the phenotype typically ascribed to YcgR; namely, its ability to inhibit cellular motility in a $\Delta yhjH$ mutant, which encodes an EAL domain protein. During the course of this work, we also determined that in this $\Delta yhjH$ mutant, there is an increase in the fraction of the cellular population that demonstrates levels of c-di-GMP that are high enough to bind to the high-affinity YcgR; however, this increase in intracellular c-di-GMP levels does not appear to be high enough to bind to the low-affinity BcsA PilZ domain. Accordingly, $\Delta yhjH$ mutation does not stimulate the production of cellulose. This indicates that the affinities of YcgR and BcsA are important for their biological phenotypes, and that their disparities in binding affinities for c-di-GMP may allow them to be selectively targeted by cellular c-di-GMP-metabolizing enzymes.

Finally, in Chapter 5, we introduced three new FRET-based constructs as *in vivo*, genetically encoded biosensors for the estimation of c-di-GMP concentrations inside of live, individual cells. These constructs are based on PilZ domain proteins used in Chapter 4, and demonstrate significantly lower binding affinities than the established FRET-based *in vivo* biosensor, which is based on the YcgR protein. Two of these three biosensors are characterized in Chapter 5, and shown to clearly distinguish between cellular populations that have artificially raised, or artificially lowered, c-di-GMP levels. Further development and use of these biosensors

will result in the accurate measurement of free c-di-GMP levels in individual live cells from the nanomolar to the micromolar range.

Does c-di-GMP signaling specificity also occur by the generation of local c-di-GMP pools?

Observations of specificity in c-di-GMP signaling indicate that c-di-GMP signaling can be functionally compartmentalized (45, 55, 62, 77, 92, 138). This work provides support to the hypothesis that specific targeting of c-di-GMP receptors occurs through the affinity of receptors for c-di-GMP. However, an alternative hypothesis for how signaling specificity can be achieved, based on the generation of localized pools of c-di-GMP, has been proposed (72, 76, 113). In this hypothesis, c-di-GMP metabolizing enzymes would be localized in the cell cytoplasm close to their target receptors, and thus would achieve specificity for these receptors by affecting the c-di-GMP concentration only within the immediate vicinity.

It is difficult to envision how the maintenance of local pools of a small, freely diffusible molecule would be achieved in the bacterial cell in the absence of some compartmentalizing physical structure such as a phospholipid membrane. In eukaryotic cells, individual pools of the second messenger cAMP have been observed with a diameter as small as 1 μm (147). Like c-di-GMP, cAMP is a hydrophilic second messenger that would also be freely diffusible. One hypothesis regarding how these microdomains are maintained involves PDEs that are specifically localized in subcellular compartments that act to decrease the concentration of cAMP in a spatially restricted manner, thereby generating these local pools (146). However, a small molecule takes approximately 1000 times longer to diffuse across a eukaryotic cell than a

bacterial cell (79). Given the viscosity of the bacterial cytoplasm, and the experimentally-determined average radius of c-di-GMP, this small molecule would achieve equilibrium in the bacterial cell in less than 30 milliseconds (38, 79, 134). Thus, any physiological difference in local concentrations of c-di-GMP in the bacterial cell would be dissipated due to diffusion. This is supported by observations of c-di-GMP levels in individual cells during imaging of cells expressing c-di-GMP biosensors. Although heterogeneity in c-di-GMP concentrations was readily observed between adjacent individual cells, no evidence for separate pools of c-di-GMP was observed in the thousands of *S. Typhimurium* cells analyzed during the course of this work. This has also been observed by Christen *et al*, who used this FRET-based biosensor method and found that the level of c-di-GMP in a mother cell of *C. crescentus* is homogeneous throughout the cell cytoplasm before division; individual daughter cells demonstrate differences in cellular c-di-GMP levels only when the plasma membrane forms between daughter cells and effectively separates their individual cytoplasms (23) (personal communication). In addition, generation of local pools as a mechanism to achieve signaling specificity has been hypothesized to explain the observation that inactivation of some DGCs and PDEs, which are known to affect cellular behavior in a c-di-GMP dependent manner, do not demonstrate a change in the total amount of c-di-GMP in the cell (76, 112). However, we have found that even small changes in c-di-GMP concentrations that occur upon DGC or PDE inactivation can result in a shift in the bound state of downstream receptors. Thus, failure to observe gross changes in total c-di-GMP concentrations does not necessarily indicate that the mutation has no effect on free intracellular c-di-GMP levels, or that its effect is due to localized pools of c-di-GMP.

The work presented here favors a mode of regulation in c-di-GMP signaling that depends upon the total level of cytoplasmic c-di-GMP; however, this mechanism of regulation is by no

means mutually exclusive with other mechanisms. Although this work is supported by the work of others that suggest that regulation of downstream effectors occurs through total intracellular levels of c-di-GMP in *Salmonella* (116), the mechanisms of regulation may differ between organisms. Indeed, recent work has elegantly demonstrated that the level of c-di-GMP inside of *V. cholerae* only correlates slightly with the phenotypic output of biofilm formation, although the correlation between the c-di-GMP produced by individual DGCs and the production of biofilm is much more robust (72). It is possible that other mechanisms are at work in the c-di-GMP signaling network of *V. cholerae* that remain to be determined. It has also been suggested that different mechanisms for achieving signaling specificity may occur even within the same organism (92, 113).

Do the enzymatic activities of c-di-GMP metabolizing enzymes determine their abilities to affect different downstream receptors?

Future work in c-di-GMP signaling should further unravel the biochemical basis by which different DGCs and PDEs are able to communicate with specific downstream receptors. The hypothesis presented here predicts that different DGCs and PDEs demonstrate variability in the amount of c-di-GMP inside of the cell that they can metabolize. In DGCs, this variability could result from differences in catalytic activities, such as variability in the affinity for the GTP substrate or the velocity of the reaction, and also from the presence of inhibitory I-sites, which would limit the synthesis of c-di-GMP to particular concentrations that are defined by the affinity of the I-site for the second messenger. In this way, DGCs would be able to communicate with

certain downstream receptors based on the combination of c-di-GMP production ability and the binding affinities of the downstream receptors. For example, the work presented in previous chapters suggests that the DGC AdrA in *S. Typhimurium* is much more active than other DGCs in this organism, and for this reason it is capable of stimulating BcsA activity whereas other DGCs are incapable of doing so. Altering the ability of c-di-GMP metabolizing enzymes in *S. Typhimurium*, and then monitoring the ability of these enzymes to communicate with specific downstream receptors, is a next step in exploring this hypothesis. FRET-based biosensors will be useful in these types of studies, as they can provide a readout for the bound state of specific c-di-GMP receptors. Association of all c-di-GMP metabolizing enzymes encoded in bacterial genomes with the downstream receptors that they regulate will involve a systems biology approach to the study of c-di-GMP signaling. Although this is a daunting task, the association of the activities of c-di-GMP-metabolizing enzymes with particular downstream receptors will add greatly to our understanding of c-di-GMP signaling networks.

What is the significance of heterogeneity of c-di-GMP concentrations within a population?

Another theme that warrants further study in c-di-GMP signaling is observed heterogeneity of c-di-GMP concentrations within populations of cells (Figure 4.8) (23). Diversifying cellular behaviors through maintaining different c-di-GMP levels may result in beneficial properties for the bacterial population (23). It is possible that heterogeneity of c-di-GMP concentrations exists in many different environmental situations. For example, during the course of this work, we observed that overexpression of a DGC in *S. Typhimurium* on LB-calcofluor agar plates results in much more calcofluor binding than growth of the wild-type

strain at a temperature permissible for cellulose production (Figure 4.1). This could be because the level of c-di-GMP produced inside of wild-type cells is not high enough to fully saturate the BcsA enzyme, or it could be due to heterogeneity of c-di-GMP concentrations in the wild-type strain in which some bacteria provide cellulose for the entire colony, while in the DGC-overexpressing strain, all of the bacteria have c-di-GMP levels that are high enough to produce the polysaccharide, and thus copious amounts of cellulose is produced. Expressing *in vivo* c-di-GMP biosensors will assist in determining the extent of c-di-GMP heterogeneity in this situation and in others.

In conclusion, our data suggest that c-di-GMP signaling specificity may be achieved through the affinities of downstream receptors. This theory is consistent with environmental signal integration by DGCs and PDEs resulting in the generation of a specific free level of c-di-GMP. The fascinatingly complex regulation of c-di-GMP signaling likely involves many different, ingenious strategies, which will be unraveled by future studies into the c-di-GMP signaling networks of many different bacteria.

REFERENCES

1. Ai, H. W., K. L. Hazelwood, M. W. Davidson, and R. E. Campbell. 2008. Fluorescent protein FRET pairs for ratiometric imaging of dual biosensors. *Nat Methods* 5:401-403.
2. Amikam, D., and M. Y. Galperin. 2006. PilZ domain is part of the bacterial c-di-GMP binding protein. *Bioinformatics* 22:3-6.
3. Amikam, D., O. Steinberger, T. Shkolnik, and Z. Ben-Ishai. 1995. The novel cyclic dinucleotide 3'-5' cyclic diguanylic acid binds to p21ras and enhances DNA synthesis but not cell replication in the Molt 4 cell line. *Biochem J* 311 (Pt 3):921-927.
4. Ausmees, N., R. Mayer, H. Weinhouse, G. Volman, D. Amikam, M. Benziman, and M. Lindberg. 2001. Genetic data indicate that proteins containing the GGDEF domain possess diguanylate cyclase activity. *FEMS Microbiol Lett* 204:163-167.
5. Baraquet, C., K. Murakami, M. R. Parsek, and C. S. Harwood. 2012. The FleQ protein from *Pseudomonas aeruginosa* functions as both a repressor and an activator to control gene expression from the pel operon promoter in response to c-di-GMP. *Nucleic Acids Res.*
6. Benach, J., S. S. Swaminathan, R. Tamayo, S. K. Handelman, E. Folta-Stogniew, J. E. Ramos, F. Forouhar, H. Neely, J. Seetharaman, A. Camilli, and J. F. Hunt. 2007. The structural basis of cyclic diguanylate signal transduction by PilZ domains. *EMBO J* 26:5153-5166.
7. Berg, H. C. 2003. The rotary motor of bacterial flagella. *Annu Rev Biochem* 72:19-54.
8. Beyhan, S., and F. H. Yildiz. 2007. Smooth to rugose phase variation in *Vibrio cholerae* can be mediated by a single nucleotide change that targets c-di-GMP signalling pathway. *Mol Microbiol* 63:995-1007.
9. Bobrov, A. G., O. Kirillina, and R. D. Perry. 2007. Regulation of biofilm formation in *Yersinia pestis*. *Adv Exp Med Biol* 603:201-210.
10. Bochner, B. R., and B. N. Ames. 1982. Complete analysis of cellular nucleotides by two-dimensional thin layer chromatography. *J Biol Chem* 257:9759-9769.
11. Bochner, B. R., H. C. Huang, G. L. Schieven, and B. N. Ames. 1980. Positive selection for loss of tetracycline resistance. *J Bacteriol* 143:926-933.
12. Boehm, A., M. Kaiser, H. Li, C. Spangler, C. A. Kasper, M. Ackermann, V. Kaefer, V. Sourjik, V. Roth, and U. Jenal. 2010. Second messenger-mediated adjustment of bacterial swimming velocity. *Cell* 141:107-116.
13. Bordeleau, E., L. C. Fortier, F. Malouin, and V. Burrus. 2011. c-di-GMP Turn-Over in *Clostridium difficile* Is Controlled by a Plethora of Diguanylate Cyclases and Phosphodiesterases. *PLoS Genet* 7:e1002039.
14. Botsford, J. L., and J. G. Harman. 1992. Cyclic AMP in prokaryotes. *Microbiol Rev* 56:100-122.
15. Brown, P. K., C. M. Dozois, C. A. Nickerson, A. Zuppardo, J. Terlonge, and R. Curtiss, 3rd. 2001. MlrA, a novel regulator of curli (AgF) and extracellular matrix synthesis by *Escherichia coli* and *Salmonella enterica* serovar Typhimurium. *Mol Microbiol* 41:349-363.

16. Burdette, D. L., K. M. Monroe, K. Sotelo-Troha, J. S. Iwig, B. Eckert, M. Hyodo, Y. Hayakawa, and R. E. Vance. 2011. STING is a direct innate immune sensor of cyclic di-GMP. *Nature* 478:515-518.
17. Cashel, M., and B. Kalbacher. 1970. The control of ribonucleic acid synthesis in *Escherichia coli*. V. Characterization of a nucleotide associated with the stringent response. *J Biol Chem* 245:2309-2318.
18. Chan, C., R. Paul, D. Samoray, N. C. Amiot, B. Giese, U. Jenal, and T. Schirmer. 2004. Structural basis of activity and allosteric control of diguanylate cyclase. *Proc Natl Acad Sci USA* 101:17084-17089.
19. Chin, K. H., Y. C. Lee, Z. L. Tu, C. H. Chen, Y. H. Tseng, J. M. Yang, R. P. Ryan, Y. McCarthy, J. M. Dow, A. H. Wang, and S. H. Chou. 2010. The cAMP receptor-like protein CLP is a novel c-di-GMP receptor linking cell-cell signaling to virulence gene expression in *Xanthomonas campestris*. *J Mol Biol* 396:646-662.
20. Christen, B., M. Christen, R. Paul, F. Schmid, M. Folcher, P. Jenoe, M. Meuwly, and U. Jenal. 2006. Allosteric control of cyclic di-GMP signaling. *J Biol Chem* 281:32015-32024.
21. Christen, M., B. Christen, M. G. Allan, M. Folcher, P. Jenoe, S. Grzesiek, and U. Jenal. 2007. DgrA is a member of a new family of cyclic diguanosine monophosphate receptors and controls flagellar motor function in *Caulobacter crescentus*. *Proc Natl Acad Sci U S A* 104:4112-4117.
22. Christen, M., B. Christen, M. Folcher, A. Schauerte, and U. Jenal. 2005. Identification and characterization of a cyclic di-GMP-specific phosphodiesterase and its allosteric control by GTP. *J Biol Chem* 280:30829-30837.
23. Christen, M., H. D. Kulasekara, B. Christen, B. R. Kulasekara, L. R. Hoffman, and S. I. Miller. 2010. Asymmetrical distribution of the second messenger c-di-GMP upon bacterial cell division. *Science* 328:1295-1297.
24. Colvin, K. M., V. D. Gordon, K. Murakami, B. R. Borlee, D. J. Wozniak, G. C. Wong, and M. R. Parsek. 2011. The pel polysaccharide can serve a structural and protective role in the biofilm matrix of *Pseudomonas aeruginosa*. *PLoS Pathog* 7:e1001264.
25. Datsenko, K. A., and B. L. Wanner. 2000. One-step inactivation of chromosomal genes in *Escherichia coli* K-12 using PCR products. *Proc Natl Acad Sci U S A* 97:6640-6645.
26. Davies, B. W., R. W. Bogard, T. S. Young, and J. J. Mekalanos. 2012. Coordinated regulation of accessory genetic elements produces cyclic di-nucleotides for *V. cholerae* virulence. *Cell* 149:358-370.
27. DiPilato, L. M., X. Cheng, and J. Zhang. 2004. Fluorescent indicators of cAMP and Epac activation reveal differential dynamics of cAMP signaling within discrete subcellular compartments. *Proc Natl Acad Sci U S A* 101:16513-16518.
28. Duerig, A., S. Abel, M. Folcher, M. Nicollier, T. Schwede, N. Amiot, B. Giese, and U. Jenal. 2009. Second messenger-mediated spatiotemporal control of protein degradation regulates bacterial cell cycle progression. *Genes Dev* 23:93-104.
29. Duvel, J., D. Bertinetti, S. Moller, F. Schwede, M. Morr, J. Wissing, L. Radamm, B. Zimmermann, H. G. Genieser, L. Jansch, F. W. Herberg, and S. Haussler. 2012. A chemical proteomics approach to identify c-di-GMP binding proteins in *Pseudomonas aeruginosa*. *J Microbiol Methods* 88:229-236.

30. Fang, X., and M. Gomelsky. 2010. A post-translational, c-di-GMP-dependent mechanism regulating flagellar motility. *Mol Microbiol* 76:1295-1305.
31. Frey, J., and H. M. Krisch. 1985. Omega mutagenesis in gram-negative bacteria: a selectable interposon which is strongly polar in a wide range of bacterial species. *Gene* 36:143-150.
32. Friedman, L., and R. Kolter. 2004. Two genetic loci produce distinct carbohydrate-rich structural components of the *Pseudomonas aeruginosa* biofilm matrix. *J Bacteriol* 186:4457-4465.
33. Frye, J., J. E. Karlinsey, H. R. Felise, B. Marzolf, N. Dowidar, M. McClelland, and K. T. Hughes. 2006. Identification of new flagellar genes of *Salmonella enterica* serovar Typhimurium. *J Bacteriol* 188:2233-2243.
34. Furste, J. P., W. Pansegrau, R. Frank, H. Blocker, P. Scholz, M. Bagdasarian, and E. Lanka. 1986. Molecular cloning of the plasmid RP4 primase region in a multi-host-range tacP expression vector. *Gene* 48:119-131.
35. Galperin, M. Y. 2006. Structural classification of bacterial response regulators: diversity of output domains and domain combinations. *J Bacteriol* 188:4169-4182.
36. Galperin, M. Y., A. N. Nikolskaya, and E. V. Koonin. 2001. Novel domains of the prokaryotic two-component signal transduction systems. *FEMS Microbiol Lett* 203:11-21.
37. Garcia, B., C. Latasa, C. Solano, F. Garcia-del Portillo, C. Gamazo, and I. Lasa. 2004. Role of the GGDEF protein family in *Salmonella* cellulose biosynthesis and biofilm formation. *Mol Microbiol* 54:264-277.
38. Gentner, M., M. G. Allan, F. Zaehring, T. Schirmer, and S. Grzesiek. 2012. Oligomer formation of the bacterial second messenger c-di-GMP: reaction rates and equilibrium constants indicate a monomeric state at physiological concentrations. *J Am Chem Soc* 134:1019-1029.
39. Gerstel, U., C. Park, and U. Romling. 2003. Complex regulation of csgD promoter activity by global regulatory proteins. *Mol Microbiol* 49:639-654.
40. Girgis, H. S., Y. Liu, W. S. Ryu, and S. Tavazoie. 2007. A comprehensive genetic characterization of bacterial motility. *PLoS Genet* 3:1644-1660.
41. Grant, D. M., W. Zhang, E. J. McGhee, T. D. Bunney, C. B. Talbot, S. Kumar, I. Munro, C. Dunsby, M. A. Neil, M. Katan, and P. M. French. 2008. Multiplexed FRET to image multiple signaling events in live cells. *Biophys J* 95:L69-71.
42. Gualdi, L., L. Tagliabue, S. Bertagnoli, T. Ierano, C. De Castro, and P. Landini. 2008. Cellulose modulates biofilm formation by counteracting curli-mediated colonization of solid surfaces in *Escherichia coli*. *Microbiology* 154:2017-2024.
43. Guvener, Z. T., and C. S. Harwood. 2007. Subcellular location characteristics of the *Pseudomonas aeruginosa* GGDEF protein, WspR, indicate that it produces cyclic-di-GMP in response to growth on surfaces. *Mol Microbiol* 66:1459-1473.
44. Habazettl, J., M. G. Allan, U. Jenal, and S. Grzesiek. 2011. Solution structure of the PilZ domain protein PA4608 complex with c-di-GMP identifies charge clustering as molecular readout. *J Biol Chem* 286:14304-14314.
45. Hengge, R. 2009. Principles of c-di-GMP signalling in bacteria. *Nat Rev Microbiol* 7:263-273.

46. Hickman, J. W., and C. S. Harwood. 2008. Identification of FleQ from *Pseudomonas aeruginosa* as a c-di-GMP-responsive transcription factor. *Mol Microbiol* 69:376-389.
47. Hickman, J. W., D. F. Tifrea, and C. S. Harwood. 2005. A chemosensory system that regulates biofilm formation through modulation of cyclic diguanylate levels. *Proc Natl Acad Sci U S A* 102:14422-14427.
48. Hisert, K. B., M. MacCoss, M. U. Shiloh, K. H. Darwin, S. Singh, R. A. Jones, S. Ehrt, Z. Zhang, B. L. Gaffney, S. Gandotra, D. W. Holden, D. Murray, and C. Nathan. 2005. A glutamate-alanine-leucine (EAL) domain protein of *Salmonella* controls bacterial survival in mice, antioxidant defence and killing of macrophages: role of cyclic diGMP. *Mol Microbiol* 56:1234-1245.
49. Hoffman, L. R., D. A. D'Argenio, M. J. MacCoss, Z. Zhang, R. A. Jones, and S. I. Miller. 2005. Aminoglycoside antibiotics induce bacterial biofilm formation. *Nature* 436:1171-1175.
50. Huang, B., C. B. Whitchurch, and J. S. Mattick. 2003. FimX, a multidomain protein connecting environmental signals to twitching motility in *Pseudomonas aeruginosa*. *J Bacteriol* 185:7068-7076.
51. Jager, R., C. Russwurm, F. Schwede, H. G. Genieser, D. Koesling, and M. Russwurm. 2012. Activation of PDE10 and PDE11 Phosphodiesterases. *J Biol Chem* 287:1210-1219.
52. Jares-Erijman, E. A., and T. M. Jovin. 2003. FRET imaging. *Nat Biotechnol* 21:1387-1395.
53. Jarvik, T., C. Smillie, E. A. Groisman, and H. Ochman. 2010. Short-term signatures of evolutionary change in the *Salmonella enterica* serovar typhimurium 14028 genome. *J Bacteriol* 192:560-567.
54. Jenal, U., and J. Malone. 2006. Mechanisms of cyclic-di-GMP signaling in bacteria. *Annu Rev Genet* 40:385-407.
55. Kader, A., R. Simm, U. Gerstel, M. Morr, and U. Romling. 2006. Hierarchical involvement of various GGDEF domain proteins in rdar morphotype development of *Salmonella enterica* serovar Typhimurium. *Mol Microbiol* 60:602-616.
56. Karaolis, D. K., T. K. Means, D. Yang, M. Takahashi, T. Yoshimura, E. Muraille, D. Philpott, J. T. Schroeder, M. Hyodo, Y. Hayakawa, B. G. Talbot, E. Brouillette, and F. Malouin. 2007. Bacterial c-di-GMP is an immunostimulatory molecule. *J Immunol* 178:2171-2181.
57. Karaolis, D. K., M. W. Newstead, X. Zeng, M. Hyodo, Y. Hayakawa, U. Bhan, H. Liang, and T. J. Standiford. 2007. Cyclic di-GMP stimulates protective innate immunity in bacterial pneumonia. *Infect Immun* 75:4942-4950.
58. Ko, J., K. S. Ryu, H. Kim, J. S. Shin, J. O. Lee, C. Cheong, and B. S. Choi. 2010. Structure of PP4397 reveals the molecular basis for different c-di-GMP binding modes by Pilz domain proteins. *J Mol Biol* 398:97-110.
59. Ko, M., and C. Park. 2000. Two novel flagellar components and H-NS are involved in the motor function of *Escherichia coli*. *J Mol Biol* 303:371-382.
60. Kozlova, E. V., B. K. Khajanchi, J. Sha, and A. K. Chopra. 2011. Quorum sensing and c-di-GMP-dependent alterations in gene transcripts and virulence-associated phenotypes in a clinical isolate of *Aeromonas hydrophila*. *Microb Pathog* 50:213-223.

61. Krasteva, P. V., J. C. Fong, N. J. Shikuma, S. Beyhan, M. V. Navarro, F. H. Yildiz, and H. Sondermann. 2010. *Vibrio cholerae* VpsT regulates matrix production and motility by directly sensing cyclic di-GMP. *Science* 327:866-868.
62. Kulasakara, H., V. Lee, A. Brencic, N. Liberati, J. Urbach, S. Miyata, D. G. Lee, A. N. Neely, M. Hyodo, Y. Hayakawa, F. M. Ausubel, and S. Lory. 2006. Analysis of *Pseudomonas aeruginosa* diguanylate cyclases and phosphodiesterases reveals a role for bis-(3'-5')-cyclic-GMP in virulence. *Proc Natl Acad Sci U S A* 103:2839-2844.
63. Lamprokostopoulou, A., C. Monteiro, M. Rhen, and U. Romling. 2010. Cyclic di-GMP signalling controls virulence properties of *Salmonella enterica* serovar Typhimurium at the mucosal lining. *Environ Microbiol* 12:40-53.
64. Lapidot, A., and S. Yaron. 2009. Transfer of *Salmonella enterica* serovar Typhimurium from contaminated irrigation water to parsley is dependent on curli and cellulose, the biofilm matrix components. *J Food Prot* 72:618-623.
65. Le Quere, B., and J. M. Ghigo. 2009. BcsQ is an essential component of the *Escherichia coli* cellulose biosynthesis apparatus that localizes at the bacterial cell pole. *Mol Microbiol* 72:724-740.
66. Ledebor, N. A., and B. D. Jones. 2005. Exopolysaccharide sugars contribute to biofilm formation by *Salmonella enterica* serovar typhimurium on HEp-2 cells and chicken intestinal epithelium. *J Bacteriol* 187:3214-3226.
67. Lee, E. R., J. L. Baker, Z. Weinberg, N. Sudarsan, and R. R. Breaker. 2010. An allosteric self-splicing ribozyme triggered by a bacterial second messenger. *Science* 329:845-848.
68. Lee, V. T., J. M. Matewish, J. L. Kessler, M. Hyodo, Y. Hayakawa, and S. Lory. 2007. A cyclic-di-GMP receptor required for bacterial exopolysaccharide production. *Mol Microbiol* 65:1474-1484.
69. Ma, Q., Z. Yang, M. Pu, W. Peti, and T. K. Wood. 2011. Engineering a novel c-di-GMP-binding protein for biofilm dispersal. *Environ Microbiol* 13:631-642.
70. Marden, J. N., Q. Dong, S. Roychowdhury, J. E. Berleman, and C. E. Bauer. 2011. Cyclic GMP controls *Rhodospirillum centenum* cyst development. *Mol Microbiol* 79:600-615.
71. Martinez-Wilson, H. F., R. Tamayo, A. D. Tischler, D. W. Lazinski, and A. Camilli. 2008. The *vibrio cholerae* hybrid sensor kinase VieS contributes to motility and biofilm regulation by altering the cyclic diguanylate level. *J Bacteriol* 190:6439-6447.
72. Massie, J. P., E. L. Reynolds, B. J. Koestler, J. P. Cong, M. Agostoni, and C. M. Waters. 2012. Quantification of high-specificity cyclic diguanylate signaling. *Proc Natl Acad Sci U S A*.
73. McClelland, M., K. E. Sanderson, J. Spieth, S. W. Clifton, P. Latreille, L. Courtney, S. Porwollik, J. Ali, M. Dante, F. Du, S. Hou, D. Layman, S. Leonard, C. Nguyen, K. Scott, A. Holmes, N. Grewal, E. Mulvaney, E. Ryan, H. Sun, L. Florea, W. Miller, T. Stoneking, M. Nhan, R. Waterston, and R. K. Wilson. 2001. Complete genome sequence of *Salmonella enterica* serovar Typhimurium LT2. *Nature* 413:852-856.
74. Mendez-Ortiz, M. M., M. Hyodo, Y. Hayakawa, and J. Membrillo-Hernandez. 2006. Genome-wide transcriptional profile of *Escherichia coli* in response to high levels of the second messenger 3',5'-cyclic diguanylic acid. *J Biol Chem* 281:8090-8099.

75. Merighi, M., V. T. Lee, M. Hyodo, Y. Hayakawa, and S. Lory. 2007. The second messenger bis-(3'-5')-cyclic-GMP and its PilZ domain-containing receptor Alg44 are required for alginate biosynthesis in *Pseudomonas aeruginosa*. *Mol Microbiol* 65:876-895.
76. Merritt, J. H., D. G. Ha, K. N. Cowles, W. Lu, D. K. Morales, J. Rabinowitz, Z. Gitai, and G. A. O'Toole. 2010. Specific control of *Pseudomonas aeruginosa* surface-associated behaviors by two c-di-GMP diguanylate cyclases. *MBio* 1.
77. Mills, E., I. S. Pultz, H. D. Kulasekara, and S. I. Miller. 2011. The bacterial second messenger c-di-GMP: mechanisms of signalling. *Cell Microbiol* 13:1122-1129.
78. Miyawaki, A., J. Llopis, R. Heim, J. M. McCaffery, J. A. Adams, M. Ikura, and R. Y. Tsien. 1997. Fluorescent indicators for Ca²⁺ based on green fluorescent proteins and calmodulin. *Nature* 388:882-887.
79. Moran, U., R. Phillips, and R. Milo. 2010. SnapShot: key numbers in biology. *Cell* 141:1262-1262 e1261.
80. Navarro, M. V., N. De, N. Bae, Q. Wang, and H. Sondermann. 2009. Structural analysis of the GGDEF-EAL domain-containing c-di-GMP receptor FimX. *Structure* 17:1104-1116.
81. Nguyen, A. W., and P. S. Daugherty. 2005. Evolutionary optimization of fluorescent proteins for intracellular FRET. *Nat Biotechnol* 23:355-360.
82. Niino, Y., K. Hotta, and K. Oka. 2009. Simultaneous live cell imaging using dual FRET sensors with a single excitation light. *PLoS One* 4:e6036.
83. Nikolaev, V. O., S. Gambaryan, and M. J. Lohse. 2006. Fluorescent sensors for rapid monitoring of intracellular cGMP. *Nat Methods* 3:23-25.
84. Nikolaev, V. O., and M. J. Lohse. 2006. Monitoring of cAMP synthesis and degradation in living cells. *Physiology (Bethesda)* 21:86-92.
85. Ogasawara, H., K. Yamada, A. Kori, K. Yamamoto, and A. Ishihama. 2010. Regulation of the *Escherichia coli* *csgD* promoter: interplay between five transcription factors. *Microbiology* 156:2470-2483.
86. Ogasawara, H., K. Yamamoto, and A. Ishihama. 2011. Role of the biofilm master regulator CsgD in cross-regulation between biofilm formation and flagellar synthesis. *J Bacteriol* 193:2587-2597.
87. Ohashi, T., S. D. Galiacy, G. Briscoe, and H. P. Erickson. 2007. An experimental study of GFP-based FRET, with application to intrinsically unstructured proteins. *Protein Sci* 16:1429-1438.
88. Ohl, M. E., and S. I. Miller. 2001. *Salmonella*: a model for bacterial pathogenesis. *Annu Rev Med* 52:259-274.
89. Paul, K., V. Nieto, W. C. Carlquist, D. F. Blair, and R. M. Harshey. 2010. The c-di-GMP binding protein YcgR controls flagellar motor direction and speed to affect chemotaxis by a "backstop brake" mechanism. *Mol Cell* 38:128-139.
90. Paul, R., S. Weiser, N. C. Amiot, C. Chan, T. Schirmer, B. Giese, and U. Jenal. 2004. Cell cycle-dependent dynamic localization of a bacterial response regulator with a novel di-guanylate cyclase output domain. *Genes Dev* 18:715-727.
91. Perlman, R. L., and I. Pastan. 1968. Regulation of beta-galactosidase synthesis in *Escherichia coli* by cyclic adenosine 3',5'-monophosphate. *J Biol Chem* 243:5420-5427.

92. Pesavento, C., G. Becker, N. Sommerfeldt, A. Possling, N. Tschowri, A. Mehlis, and R. Hengge. 2008. Inverse regulatory coordination of motility and curli-mediated adhesion in *Escherichia coli*. *Genes Dev* 22:2434-2446.
93. Pitzer, J. E., S. Z. Sultan, Y. Hayakawa, G. Hobbs, M. R. Miller, and M. A. Motaleb. 2011. Analysis of the *Borrelia burgdorferi* cyclic-di-GMP binding protein PlzA reveals a role in motility and virulence. *Infect Immun*.
94. Povolotsky, T. L., and R. Hengge. 2011. 'Life-style' control networks in *Escherichia coli*: Signaling by the second messenger c-di-GMP. *J Biotechnol*.
95. Pratt, J. T., R. Tamayo, A. D. Tischler, and A. Camilli. 2007. PilZ domain proteins bind cyclic diguanylate and regulate diverse processes in *Vibrio cholerae*. *J Biol Chem* 282:12860-12870.
96. Quon, K. C., B. Yang, I. J. Domian, L. Shapiro, and G. T. Marczynski. 1998. Negative control of bacterial DNA replication by a cell cycle regulatory protein that binds at the chromosome origin. *Proc Natl Acad Sci U S A* 95:120-125.
97. Ramelot, T. A., A. Yee, J. R. Cort, A. Semesi, C. H. Arrowsmith, and M. A. Kennedy. 2007. NMR structure and binding studies confirm that PA4608 from *Pseudomonas aeruginosa* is a PilZ domain and a c-di-GMP binding protein. *Proteins* 66:266-271.
98. Rehm, H. 2006. *Protein Biochemistry and Proteomics*, 6th ed. Elsevier.
99. Robbe-Saule, V., V. Jaumouille, M. C. Prevost, S. Guadagnini, C. Talhouarne, H. Mathout, A. Kolb, and F. Norel. 2006. Crl activates transcription initiation of RpoS-regulated genes involved in the multicellular behavior of *Salmonella enterica* serovar Typhimurium. *J Bacteriol* 188:3983-3994.
100. Romling, U. 2005. Characterization of the rdar morphotype, a multicellular behaviour in *Enterobacteriaceae*. *Cell Mol Life Sci* 62:1234-1246.
101. Romling, U., Z. Bian, M. Hammar, W. D. Sierralta, and S. Normark. 1998. Curli fibers are highly conserved between *Salmonella typhimurium* and *Escherichia coli* with respect to operon structure and regulation. *J Bacteriol* 180:722-731.
102. Romling, U., M. Rohde, A. Olsen, S. Normark, and J. Reinkoster. 2000. AgfD, the checkpoint of multicellular and aggregative behaviour in *Salmonella typhimurium* regulates at least two independent pathways. *Mol Microbiol* 36:10-23.
103. Romling, U., W. D. Sierralta, K. Eriksson, and S. Normark. 1998. Multicellular and aggregative behaviour of *Salmonella typhimurium* strains is controlled by mutations in the agfD promoter. *Mol Microbiol* 28:249-264.
104. Ross, P., Y. Aloni, H. Weinhouse, D. Michaeli, P. Weinberger-Ohana, R. Mayer, and M. Benziman. 1986. Control of cellulose synthesis in *Acetobacter xylinum* – a unique guanyl oligonucleotide is the immediate activator of the cellulose synthase. *Carbohydr Res* 149:101-117.
105. Ross, P., H. Weinhouse, Y. Aloni, D. Michaeli, P. Weinberger-Ohana, R. Mayer, S. Braun, E. de Vroom, G. A. van der Marel, J. H. van Boom, and M. Benziman. 1987. Regulation of cellulose synthesis in *Acetobacter xylinum* by cyclic diguanylic acid. *Nature* 325:279-281.
106. Roy, R., S. Hohng, and T. Ha. 2008. A practical guide to single-molecule FRET. *Nat Methods* 5:507-516.

107. Russwurm, M., F. Mullershausen, A. Friebe, R. Jager, C. Russwurm, and D. Koesling. 2007. Design of fluorescence resonance energy transfer (FRET)-based cGMP indicators: a systematic approach. *Biochem J* 407:69-77.
108. Ryjenkov, D. A., R. Simm, U. Romling, and M. Gomelsky. 2006. The PilZ domain is a receptor for the second messenger c-di-GMP: the PilZ domain protein YcgR controls motility in enterobacteria. *J Biol Chem* 281:30310-30314.
109. Sanchez-Torres, V., H. Hu, and T. K. Wood. 2011. GGDEF proteins YeaI, YedQ, and YfiN reduce early biofilm formation and swimming motility in *Escherichia coli*. *Appl Microbiol Biotechnol* 90:651-658.
110. Schmidt, A. J., D. A. Ryjenkov, and M. Gomelsky. 2005. The ubiquitous protein domain EAL is a cyclic diguanylate-specific phosphodiesterase: enzymatically active and inactive EAL domains. *J Bacteriol* 187:4774-4781.
111. Shin, J. S., K. S. Ryu, J. Ko, A. Lee, and B. S. Choi. 2011. Structural characterization reveals that a PilZ domain protein undergoes substantial conformational change upon binding to cyclic dimeric guanosine monophosphate. *Protein Sci* 20:270-277.
112. Simm, R., A. Lusch, A. Kader, M. Andersson, and U. Romling. 2007. Role of EAL-containing proteins in multicellular behavior of *Salmonella enterica* serovar Typhimurium. *J Bacteriol* 189:3613-3623.
113. Simm, R., M. Morr, A. Kader, M. Nimtz, and U. Romling. 2004. GGDEF and EAL domains inversely regulate cyclic di-GMP levels and transition from sessility to motility. *Mol Microbiol* 53:1123-1134.
114. Simm, R., M. Morr, U. Remminghorst, M. Andersson, and U. Romling. 2009. Quantitative determination of cyclic diguanosine monophosphate concentrations in nucleotide extracts of bacteria by matrix-assisted laser desorption/ionization-time-of-flight mass spectrometry. *Anal Biochem* 386:53-58.
115. Simm, R., U. Remminghorst, I. Ahmad, K. Zakikhany, and U. Romling. 2009. A role for the EAL-like protein STM1344 in regulation of CsgD expression and motility in *Salmonella enterica* serovar Typhimurium. *J Bacteriol* 191:3928-3937.
116. Solano, C., B. Garcia, C. Latasa, A. Toledo-Arana, V. Zorraquino, J. Valle, J. Casals, E. Pedroso, and I. Lasa. 2009. Genetic reductionist approach for dissecting individual roles of GGDEF proteins within the c-di-GMP signaling network in *Salmonella*. *Proc Natl Acad Sci U S A* 106:7997-8002.
117. Solano, C., B. Garcia, J. Valle, C. Berasain, J. M. Ghigo, C. Gamazo, and I. Lasa. 2002. Genetic analysis of *Salmonella enteritidis* biofilm formation: critical role of cellulose. *Mol Microbiol* 43:793-808.
118. Sommerfeldt, N., A. Possling, G. Becker, C. Pesavento, N. Tschowri, and R. Hengge. 2009. Gene expression patterns and differential input into curli fimbriae regulation of all GGDEF/EAL domain proteins in *Escherichia coli*. *Microbiology* 155:1318-1331.
119. Spangler, C., A. Bohm, U. Jenal, R. Seifert, and V. Kaever. 2010. A liquid chromatography-coupled tandem mass spectrometry method for quantitation of cyclic di-guanosine monophosphate. *J Microbiol Methods* 81:226-231.
120. Srivastava, D., R. C. Harris, and C. M. Waters. 2011. Integration of cyclic di-GMP and quorum sensing in the control of vpsT and aphA in *Vibrio cholerae*. *J Bacteriol* 193:6331-6341.

121. Starkey, M., J. H. Hickman, L. Ma, N. Zhang, S. De Long, A. Hinz, S. Palacios, C. Manoil, M. J. Kirisits, T. D. Starner, D. J. Wozniak, C. S. Harwood, and M. R. Parsek. 2009. *Pseudomonas aeruginosa* rugose small-colony variants have adaptations that likely promote persistence in the cystic fibrosis lung. *J Bacteriol* 191:3492-3503.
122. Stewart, M. K., L. A. Cummings, M. L. Johnson, A. B. Berezow, and B. T. Cookson. 2011. Regulation of phenotypic heterogeneity permits *Salmonella* evasion of the host caspase-1 inflammatory response. *Proc Natl Acad Sci U S A* 108:20742-20747.
123. Sudarsan, N., E. R. Lee, Z. Weinberg, R. H. Moy, J. N. Kim, K. H. Link, and R. R. Breaker. 2008. Riboswitches in eubacteria sense the second messenger cyclic di-GMP. *Science* 321:411-413.
124. Swartley, J. S., L. J. Liu, Y. K. Miller, L. E. Martin, S. Edupuganti, and D. S. Stephens. 1998. Characterization of the gene cassette required for biosynthesis of the (α 1 \rightarrow 6)-linked N-acetyl-D-mannosamine-1-phosphate capsule of serogroup A *Neisseria meningitidis*. *J Bacteriol* 180:1533-1539.
125. Tamayo, R., A. D. Tischler, and A. Camilli. 2005. The EAL domain protein VieA is a cyclic diguanylate phosphodiesterase. *J Biol Chem* 280:33324-33330.
126. Tao, F., Y. W. He, D. H. Wu, S. Swarup, and L. H. Zhang. 2010. The cyclic nucleotide monophosphate domain of *Xanthomonas campestris* global regulator Clp defines a new class of cyclic di-GMP effectors. *J Bacteriol* 192:1020-1029.
127. Tarutina, M., D. A. Ryjenkov, and M. Gomelsky. 2006. An unorthodox bacteriophytochrome from *Rhodobacter sphaeroides* involved in turnover of the second messenger c-di-GMP. *J Biol Chem* 281:34751-34758.
128. Tischler, A. D., and A. Camilli. 2005. Cyclic diguanylate regulates *Vibrio cholerae* virulence gene expression. *Infect Immun* 73:5873-5882.
129. Trimble, M. J., and L. L. McCarter. 2011. Bis-(3'-5')-cyclic dimeric GMP-linked quorum sensing controls swarming in *Vibrio parahaemolyticus*. *Proc Natl Acad Sci U S A* 108:18079-18084.
130. Truong, K., A. Sawano, H. Mizuno, H. Hama, K. I. Tong, T. K. Mal, A. Miyawaki, and M. Ikura. 2001. FRET-based in vivo Ca^{2+} imaging by a new calmodulin-GFP fusion molecule. *Nat Struct Biol* 8:1069-1073.
131. Tuckerman, J. R., G. Gonzalez, and M. A. Gilles-Gonzalez. 2011. Cyclic di-GMP Activation of Polynucleotide Phosphorylase Signal-Dependent RNA Processing. *J Mol Biol* 407:633-639.
132. Tuckerman, J. R., G. Gonzalez, E. H. Sousa, X. Wan, J. A. Saito, M. Alam, and M. A. Gilles-Gonzalez. 2009. An oxygen-sensing diguanylate cyclase and phosphodiesterase couple for c-di-GMP control. *Biochemistry* 48:9764-9774.
133. Vanderklish, P. W., L. A. Krushel, B. H. Holst, J. A. Gally, K. L. Crossin, and G. M. Edelman. 2000. Marking synaptic activity in dendritic spines with a calpain substrate exhibiting fluorescence resonance energy transfer. *Proc Natl Acad Sci U S A* 97:2253-2258.
134. Wang, J., J. Zhou, G. P. Donaldson, S. Nakayama, L. Yan, Y. F. Lam, V. T. Lee, and H. O. Sintim. 2011. Conservative change to the phosphate moiety of cyclic diguanylic monophosphate remarkably affects its polymorphism and ability to bind DGC, PDE, and PilZ proteins. *J Am Chem Soc* 133:9320-9330.

135. Wang, Q., S. Mariconda, A. Suzuki, M. McClelland, and R. M. Harshey. 2006. Uncovering a large set of genes that affect surface motility in *Salmonella enterica* serovar Typhimurium. *J Bacteriol* 188:7981-7984.
136. Wang, S., R. T. Fleming, E. M. Westbrook, P. Matsumura, and D. B. McKay. 2006. Structure of the *Escherichia coli* FlhDC complex, a prokaryotic heteromeric regulator of transcription. *J Mol Biol* 355:798-808.
137. Wassmann, P., C. Chan, R. Paul, A. Beck, H. Heerklotz, U. Jenal, and T. Schirmer. 2007. Structure of BeF(3)(-)-Modified Response Regulator PleD: Implications for Diguanylate Cyclase Activation, Catalysis, and Feedback Inhibition. *Structure* 15:915-927.
138. Weber, H., C. Pesavento, A. Possling, G. Tischendorf, and R. Hengge. 2006. Cyclic-di-GMP-mediated signalling within the sigma network of *Escherichia coli*. *Mol Microbiol* 62:1014-1034.
139. Weinhouse, H., S. Sapir, D. Amikam, Y. Shilo, G. Volman, P. Ohana, and M. Benziman. 1997. c-di-GMP-binding protein, a new factor regulating cellulose synthesis in *Acetobacter xylinum*. *FEBS Lett* 416:207-211.
140. White, A. P., D. L. Gibson, G. A. Grassl, W. W. Kay, B. B. Finlay, B. A. Vallance, and M. G. Surette. 2008. Aggregation via the red, dry, and rough morphotype is not a virulence adaptation in *Salmonella enterica* serovar Typhimurium. *Infect Immun* 76:1048-1058.
141. White, A. P., D. L. Gibson, W. Kim, W. W. Kay, and M. G. Surette. 2006. Thin aggregative fimbriae and cellulose enhance long-term survival and persistence of *Salmonella*. *J Bacteriol* 188:3219-3227.
142. Whitney, J. C., K. M. Colvin, L. S. Marmont, H. Robinson, M. R. Parsek, and P. L. Howell. 2012. Structure of the cytoplasmic region of PelD, a degenerate diguanylate cyclase receptor that regulates exopolysaccharide production in *Pseudomonas aeruginosa*. *J Biol Chem*.
143. Wong, H. C., A. L. Fear, R. D. Calhoon, G. H. Eichinger, R. Mayer, D. Amikam, M. Benziman, D. H. Gelfand, J. H. Meade, A. W. Emerick, and et al. 1990. Genetic organization of the cellulose synthase operon in *Acetobacter xylinum*. *Proc Natl Acad Sci U S A* 87:8130-8134.
144. Woodward, J. J., A. T. Iavarone, and D. A. Portnoy. 2010. c-di-AMP secreted by intracellular *Listeria monocytogenes* activates a host type I interferon response. *Science* 328:1703-1705.
145. Xia, Z., and Y. Liu. 2001. Reliable and global measurement of fluorescence resonance energy transfer using fluorescence microscopes. *Biophys J* 81:2395-2402.
146. Zacco, M., G. Di Benedetto, V. Lissandron, L. Mancuso, A. Terrin, and I. Zamparo. 2006. Restricted diffusion of a freely diffusible second messenger: mechanisms underlying compartmentalized cAMP signalling. *Biochem Soc Trans* 34:495-497.
147. Zacco, M., and T. Pozzan. 2002. Discrete microdomains with high concentration of cAMP in stimulated rat neonatal cardiac myocytes. *Science* 295:1711-1715.
148. Zakikhany, K., C. R. Harrington, M. Nimitz, J. C. Hinton, and U. Romling. 2010. Unphosphorylated CsgD controls biofilm formation in *Salmonella enterica* serovar Typhimurium. *Mol Microbiol* 77:771-786.

149. Zhang, L. H. 2010. A novel C-di-GMP effector linking intracellular virulence regulon to quorum sensing and hypoxia sensing. *Virulence* 1:391-394.
150. Zhang, Y. L., E. Arakawa, and K. Y. Leung. 2002. Novel *Aeromonas hydrophila* PPD134/91 genes involved in O-antigen and capsule biosynthesis. *Infect Immun* 70:2326-2335.
151. Zogaj, X., M. Nimtz, M. Rohde, W. Bokranz, and U. Romling. 2001. The multicellular morphotypes of *Salmonella typhimurium* and *Escherichia coli* produce cellulose as the second component of the extracellular matrix. *Mol Microbiol* 39:1452-1463.

VITAE

Ingrid Swanson Pultz, formerly Ingrid Elizabeth Swanson, received her Ph.D. degree from the University of Washington (UW) Department of Microbiology in the lab of Dr. Samuel I. Miller in 2012. Her work on the c-di-GMP network in *S. Typhimurium* resulted in a first-author manuscript that is currently under review (2012) in the journal *Molecular Microbiology*. In addition, Dr. Pultz was co-first author on a review article on c-di-GMP signaling, “The bacterial second messenger c-di-GMP: mechanisms of signaling,” that appeared in the journal *Cellular Microbiology* on June 24, 2011.

In addition to her graduate work, Dr. Pultz founded the UW International Genetically Engineered Machine (iGEM) team in 2008, and advised the UW team from 2008-2011. iGEM is an annual synthetic biology competition in which undergraduates design, build, and test a novel biological system over the course of a summer. Under the direction of Dr. Pultz, the UW experienced much success. The 2008 and 2009 UW teams were awarded bronze and gold medals, respectively, at the competition. The 2010 team earned a gold medal, and was awarded the prize for Best Health or Medicine Project. The 2011 team won the Grand Prize BioBrick and numerous other awards, including Best Food or Energy Project and Best Poster. Student projects during this time have included developing novel antibiotics, constructing a strain of bacteria that generates diesel fuel, and engineering a novel therapeutic for Celiac disease.

Before attending graduate school, Dr. Pultz worked with Dr. Tatyana Golovkina at the Jackson Laboratory from 2003-2005, which resulted in the first-author publication “Sequences within the *gag* gene of mouse mammary tumor virus needed for mammary gland cell transformation” in the *Journal of Virology* in April, 2006. She graduated from Wellesley College *cum laude* with a BA in Biology in 2003.